REGULATION OF APOPTOSIS AND DESMOSOMES BY RHOE

by

Katie Rose Ryan

A thesis submitted to

The University of Birmingham

for the degree of

DOCTOR OF PHILOSOPHY

School of Biosciences

The University of Birmingham

September 2010

ABSTRACT

The human epidermis is a self-renewing stratified epithelial tissue that forms the outermost protective layer of the skin. The epidermis is comprised of a number of cell types, the most abundant of which are keratinocytes. Normal function of the epidermis requires that keratinocyte proliferation, differentiation, and apoptosis be precisely regulated and a failure to regulate these processes is a feature of many skin diseases. Although the precise mechanism by which epidermal homeostasis is regulated is still far from clear, much progress has been made in the characterisation of signaling pathways involved in normal epidermal function. A key group of signaling proteins that have been clearly implicated in epidermal function are the Rho family of small GTP-binding proteins. This thesis focuses on one member of the family, RhoE/Rnd3, and the analysis of the role it plays in the regulation of proliferation, differentiation, apoptosis and cell-cell adhesion in the epidermis.

Use of RNA interference to specifically 'knock-down' expression of RhoE has led to the discovery of a novel role for RhoE in regulation of cell-cell adhesion and apoptosis. Loss of RhoE expression resulted in keratinocytes developing resistance to apoptosis mediated via either the intrinsic or extrinsic pathways. RhoE depletion was also associated with increased expression of desmosomal proteins and increased numbers of desmosomes. Resistance to apoptosis was shown to be a function of desmosome-mediated cell-cell adhesion and a component of demosomes – plakoglobin – was shown to play a key role in RhoE-mediated resistance to apoptosis.

ACKNOWLEDGMENTS

I would like to acknowledge the following people for all their help and support throughout my PhD.

Anne Ridley for providing the pCMV5RhoEFlag construct, Shuh Narumiya for providing both the wild type and kinase dead ROCK I constructs, Martyn Chidgey for providing antibodies against desmosomal proteins, John Heath for the use of equipment and reagents and Frances Lock for her advice and expertise. I would like to thank everyone on the 5th floor for all their help and support. Thank you for making the lab a fantastic place to work and for all the laughs you have provided and for all the friendships I was able to make. I would also like to thank my mom, dad and brother for their continued support and encouragement and Chris for proof reading my thesis and maintaining my sanity.

I would like to give special thanks to Neil for all his support, enthusiasm and advice throughout the four years of my PhD. I could not have asked for a better supervisor!

This work was funded by a BBSRC studentship and CRUK.

TABLE OF CONTENTS

TABLE OF FIGURES

TABLE OF TABLES

LIST OF ABBREVIATIONS

GTP	Guanosine triphosphate
GDP	Guanosine diphosphate
GAP	GTPase activating protein
GEF	Guanine nucleotide exchange factor
GDI	Guanine nucleotide dissociation inhibitor
MLCK	Myosin light chain kinase
MLCP	Myosin light chain phosphatase
PRK-2	Protein kinase C-related protein kinase
RBD	Rho binding domain
PH	Pleckstrin homology
CRD	Cysteine rich domain
CDK	Cyclin dependent kinase
MEK	Mitogen-activated protein kinase-kinase
ERK	Extracellular signal-related protein
pERK	Phosphorylayed extracellular signal-related protein
DP	Desmoplakin I/II
PG	Plakoglobin
Dsc	Desmocollin

Dsg	Desmoglein
PKP	Plakophilin
MOMP	Mitochondrial outer membrane permeabilisation
AIP	Apoptosis induced factor
Smac	Second mitochondria derived activator of caspase
DIABLO	Direct inhibitor of apoptosis protein ((IAP)-binding protein with low PI)
Apaf-1	Adapter protein apoptosis inducing factor 1
AIF	Apoptosis inducing factor
PIDD	p53-induced death domain protein
IAP	Inhibitor of apoptosis protein
TNF	Tumor necrosis factor
TRAIL	TNF-related apoptosis-inducing ligand
FADD	Fas-associated death domain
DISC	Death inducing signaling complex
FLIP	Fas-associated death-domain-like IL-1beta-converting enzyme-inhibitory protein
TRADD	TNF receptor associated death domain
RIP 1	Receptor interacting protein 1
TRAF 2	TNF receptor associated factor 2
NF-κB	Nuclear factor kappa B
IκB	Inhibitor of NF-κB

IKK	IκB kinases
DMF	Dimethylformamide
BrdU	Bromodeoxyuridine

CHAPTER 1 INTRODUCTION

1.1 The epidermis

1.1.1 Introduction to the epidermis

Human skin is comprised of two layers: the dermis and the epidermis, which are separated by the basement membrane (Fuchs 2007) (Figure 1). The dermis is composed largely of vascular connective tissue and the basement membrane is made up of extracellular matrix (ECM) proteins and proteoglycans and is rich in growth factors secreted by keratinocytes and dermal fibroblasts (Marinkovich et al. 1993; Fuchs 2007). The upper most layer of the skin is the epidermis and although comprises only 25% of the total thickness of the skin it is vitally important for protecting the body from the environment (Leigh et al. 1994). The role of the epidermis is to act as a mechanical barrier protecting against infection from pathogens, noxious stimuli and UV irradiation. The epidermis also prevents dehydration and re-epithelialises during wound healing (Koster et al. 2007). In order to fulfil these roles the epidermis must continually replenish and maintain itself through proliferation, differentiation and apoptosis (Gniadecki 1998; Fuchs 2007; Koster et al. 2007).

The epidermis is a stratified epithelium made up predominantly of layers of specialised epithelial cells known as keratinocytes. Other cell types found in the epidermis include Langerhans cells, which have an immunological function, and melanocytes, which absorb UV irradiation (Leigh et al. 1994). The different layers of keratinocytes that make up the

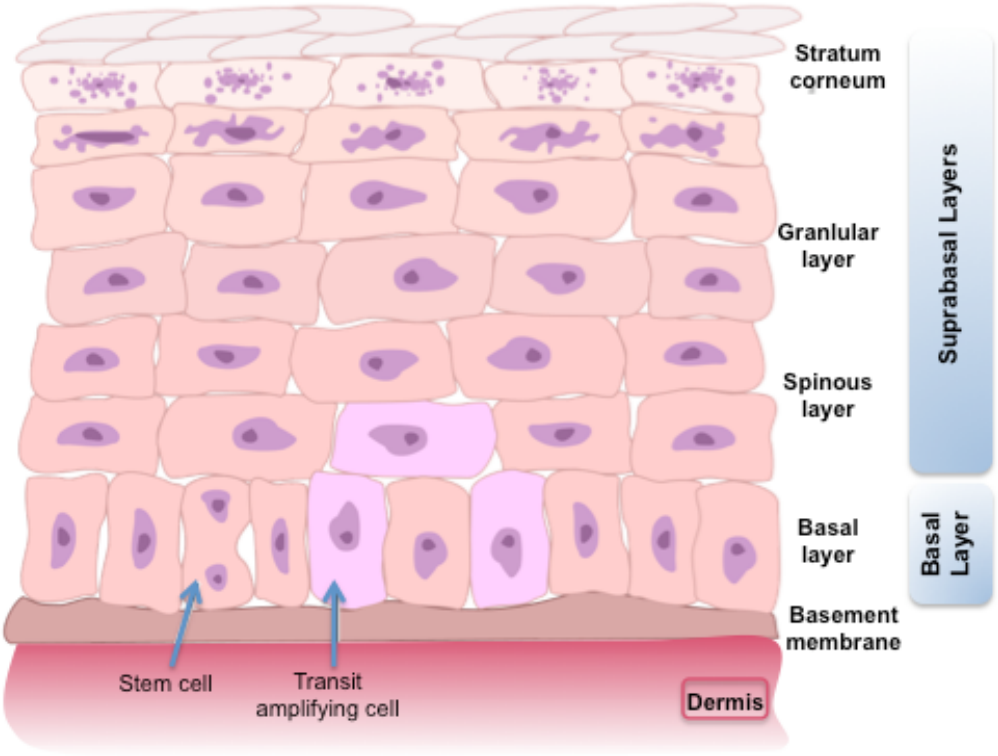

Figure 1 Organisation of the epidermis.

The epidermis is comprised of layers of keratinocytes, the basal layer houses keratinocytes with proliferative ability, stem cells and transit amplifying cells, which are anchored to the basement membrane. The suprabasal layers of the epidermis include: the spinous layer, the granular layer and the stratum corneum. These layers are comprised of differentiating keratinocytes, which are in different stages of the differentiation process.

epidermis include the basal layer, spinous layer, granular layer and the outermost stratum corneum (Koster et al. 2007) (Figure 1). Cells in the basal layer adhere to the underlying basement membrane and have the ability to undergo proliferation (Gniadecki 1998; Blanpain et al. 2004). The formation of the suprabasal layers results from the process of terminal differentiation (Koster et al. 2007). Keratinocytes that have initiated differentiation exit the cell cycle and migrate upwards with their morphology ever-changing until they become apart of the stratum corneum and are sloughed from the surface of the skin (Koster et al. 2007). Each of the suprabasal layers is composed of keratinocytes at specific points in the differentiation process and is based on gene expression, proliferation potential and adhesive properties (Fuchs 1990).

Epidermal homeostasis is vital for epidermal function and abnormalities in proliferation, differentiation, adhesion or apoptosis are a feature of many skin diseases (Fuchs 2007). A balance between cell loss and cell proliferation must be maintained as reduced proliferation results in the epidermis becoming too thin. Conversely too much proliferation results in hyperproliferative disorders such as psoriasis and cancers (Fuchs 2007). Psoriasis is common skin disease and is characterised by inflammation and hyperproliferation in the epidermis resulting in scaly patches of skin (Bata-Csorgo et al. 1995; Ilkovitch 2010). Basal cell and squamous cell carcinomas are the most common types of skin cancer (Motley et al. 2002). Both basal and squamous cell carcinoma occurs in the epidermis usually through sun exposure and are most commonly treated by surgical excision. If left untreated, invasion and metastasis can occur (Rubin et al. 2005; Lansbury et al. 2010). A less common type of skin cancer is melanoma which arises through the transformation of melanocytes, in response to UV irradiation (Diepgen

et al. 2002). Melanomas are highly malignant and responsible for the majority of deaths associated with skin cancer (Diepgen et al. 2002). For normal epidermal function, maintaining the architecture of the epidermis is vital. Disruption of adhesion, through disturbed expression of adhesion components, can also lead to uncontrolled proliferation, resulting in severe pathologies such as cancer and psoriasis (Muller et al. 2008). Pemphigus vulgaris and pemphigus foliaceus are autoimmune diseases that cause skin blistering through the production of antibodies against the desmosomal components desmoglein 1 and 3, which results in acantholysis (loss of cell–cell adhesion) (Waschke 2008). Apoptosis is important for the regulation of epidermal homeostasis and provides protection against diseases such as autoimmune disorders, cancer and infection through the removal of affected cells (Kalden 2004; Rovere-Querini et al. 2005).

1.1.2 Keratinocyte proliferation

Cell proliferation in normal epidermis is confined to keratinocytes present in the basal layer with two types of keratinocytes undergoing division (Watt 1988; Gniadecki 1998; Blanpain et al. 2004; Fuchs 2007). Stem cells have unlimited proliferative capability and transit amplifying cells undergo a finite number of rounds of division before committing to terminal differentiation (Potten 1981). Mechanisms that control the transition from stem cell to transit amplifying cell to differentiating cell are poorly understood.

Keratinocyte proliferation is mainly regulated in G1 phase (Gniadecki 1998). Progression through G1 relies on the sequential activation of cyclin dependent kinases (CDK), which is

regulated by growth factors and adhesion to the ECM (Assoian et al. 2001; Muller et al. 2008). The main CDKs involved in G1 phase are CDK4, CDK6 and CDK2 and they are activated on binding with cyclins (Klein et al. 2008). Cyclin D (D1, D2 and D3) binds to CDK4 and CDK6 whereas cyclins E and A bind to CDK2 (Gniadecki 1998; Welsh 2004). In mid-G1 phase the D-type cyclins are synthesised primarily in response to growth factor stimulation of the Ras-dependent pathway involving the sequential activation of Raf, MEK then the sustained activation of extracellular signal-related protein (ERK) (Diehl 2002). Of the three D-type cyclins only cyclin D1 is frequently over-expressed in cancer (Diehl 2002). Over-expression of cyclin D1 in mice causes hyperplasia in basal keratinocytes confirming a key role for cyclin D1 in the epidermis (Robles et al. 1996). Cyclin D1 binding to CDK4/6 is the rate-limiting step in progression through G1 phase (Klein et al. 2008). Adhesion to the ECM and growth factors present in the basement membrane induce cyclin D1 expression and promote proliferation (Assoian et al. 2008), whereas the repression of cyclin D1 expression is a hallmark of cell differentiation (Mejlvang et al. 2007) but cyclin D1 is not required in mouse keratinocytes (Robles et al. 1998).

The major targets for the activated CDK-cyclin complexes are members of the retinoblastoma (Rb) family, which includes retinoblastoma protein (pRb), protein p170 and protein p130 (Poznic 2009). In quiescent cells these proteins are hypophosphorylated and complex with the E2F transcription factor family of proteins, pRb and p170 complex with E2F1, E2F2 and E2F3, while E2F4 and E2F5 complex with p130 (Sardet et al. 1995; Berckmans et al. 2009; Poznic 2009). Binding of the Rb family members to the E2F transcription factors leads to the

transcriptional repression of E2F target genes (Berckmans et al. 2009). During G1 the Rb proteins are initially phosphorylated by the activated CDK4/6-cyclin D complexes resulting in the release of the E2F transcription factors and then the subsequent induction of E2F target genes, which includes cyclin E and A (Poznic 2009). Cyclin E then complexes with CDK2, activating it while the CDK4/6-cyclin D complex further aids the activation of CDK2 by incorporating the CDK2 inhibitor $p27^{Kip1}$ into the CDK4/6-cyclin D complex (Sherr 1993). There are two families of CDK inhibitors; the Cip/Kip family ($p21^{Cip1}$, $p27^{Kip1}$ and $p57^{Kip2}$) which bind CDK4/6-cyclin D, and CDK2-cyclinE/A, and the INK4 family ($p15^{INK4A}$, $p16^{INK4B}$ and $p18^{INK4C}$) that bind to CDK4/6-cyclin D only (Abbas et al. 2009). Activation of CDK2-cyclin E leads to the hyperphosphorylation of the Rb family proteins resulting in the release of more E2F transcription factors and the transcription of genes required for the G1 to S phase transition (Poznic 2009).

1.1.3 Terminal differentiation

A keratinocyte undergoing terminal differentiation goes through a number of phenotypic changes that include withdrawal from the cell cycle, altered protein expression, changes in adhesion, migration up through the epidermis as well as changes in morphology. Terminal differentiating keratinocytes make up the stratified suprabasal layers of the epidermis and are key for maintaining the protective function of the epidermis (Fuchs 1990; Fuchs 2007). The precise trigger for a basal keratinocyte to undergo differentiation is unclear but the process itself has been well-documented (Fuchs 2007).

One of the earliest events of terminal differentiation is the irreversible withdrawal from cell cycle that occurs in a specific subset of basal cells known as the transit amplifying cells (Albers et al. 1987). As these cells exit the basal layer they enter the spinous layers (4 to 8 layers thick) these cells are now known as spinous cells (Figure 1). Spinous cells are post mitotic but still metabolically active (Fuchs 1990). Synthesis of glutamine and lysine rich envelope proteins occurs, such has involucrin, and are deposited at the inner surface of the plasma membrane (Rice et al. 1979). The spinous cells also switch production of keratins, with the down-regulation of basal keratins, keratin 5 and 14, coupled with the up-regulation of keratin 1 and 10, which is a reliable indication of terminal differentiation (Fuchs et al. 1980; Fuchs 2007). Keratin 1 and 10 form tonofilaments and connect to desmosomes, which provide cell-cell adhesion allowing spinous cells to form connected sheets and columns, producing a 3D lattice (Fuchs 1990; Fuchs 2007). Membrane-coating granules are also made at this stage and will later fuse with the plasma membrane and release lipids into the intracellular spaces of the granular and stratum corneum cells (Swartzendruber et al. 1989). Once spinous cells reach the granular layers keratin and envelope protein synthesis is stopped and the synthesis of profilaggrin occurs. Profilaggrin is processed to produce filaggrin, which bundles the keratin tonofilaments into macrofibrillar cables (Fleckman et al. 1985; Fuchs 2007). The next stage involves permeabilisation of the cell resulting in an influx of calcium ions leading to the activation of transglutaminase, which catalyses the formation of E-(y-glutamyl) lysine bonds cross linking the envelope proteins producing a proteinaceous sack to hold the keratin macrofibrils (Rice et al. 1979; Fuchs 2007). The final stage of terminal differentiation, known as cornification, is the release of lytic enzymes, which eradicate all metabolic activity through the destruction of the

nucleus, organelles and the lipid bilayer producing dead flattened stratum corneum cells (squames) that are comprised of cornified sacs containing keratin macrofibrils. These squames are sealed together by lipids producing the impermeable stratum corneum, which is continually replenished by basal keratinocytes executing a program of terminal differentiation (Fuchs 1990; Fuchs 2007).

1.1.3.1 Markers of terminal differentiation

Several molecular markers and morphological characteristics are commonly used to assess keratinocyte terminal differentiation. A switch in the production of keratin 5 and 14 to keratin 1 and 10 (Fuchs et al. 1980; Fuchs 2007), along with the up-regulation of involucrin are commonly used markers for terminal differentiation (Watt 1983). Other molecular indicators include an up-regulation of periplakin, desmocollin 2 and transglutaminase (Rice et al. 1979; Legan et al. 1994; Nemes et al. 1999). The key morphological change associated with keratinocyte terminal differentiation is an increase in cell size with cells becoming larger and flatter (Watt 1983).

1.1.4 Cell adhesion in the epidermis

The architecture of the stratified epidermis is highly organised and requires both cell adhesion to the basement membrane and to neighbouring cells (Figure 1). The basement membrane is rich in extracellular matrix proteins as well as growth factors and keratinocytes in the basal layer adhere to these proteins through focal adhesions and hemidesmosomes (Braga 2002). Adhesion

to the basement membrane is important for these basal keratinocytes to maintain their proliferative ability as loss of adhesion to the ECM has been shown to induce differentiation (Green 1977; Muller et al. 2008). Cell-cell adhesion in the epidermis is important for maintaining epidermal architecture and mechanical strength as well as playing a role in signal transduction (Braga 2002). Tight junctions, adherens junctions and desmosomes are cell-cell adhesion complexes and like focal adhesions and hemidesmosomes they all link to the cytoskeletal network increasing the mechanical strength of the adhesion (Fuchs 2007; Waschke 2008) (Figure 2).

In addition to being required for structural integrity, adhesion complexes can serve as transducers of extracellular signals to control proliferation, differentiation and apoptosis (Muller et al. 2008). For example, integrin-mediated adhesion complexes, focal adhesions and hemidesmosomes transduce pro-proliferation signals (Muller et al. 2008). In contrast, cadherin-mediated adhesion complexes, adhesion junctions and desmosomes transduce anti-proliferative signals (Muller et al. 2008). Proliferation in the epidermis requires adhesion to the basement membrane in normal keratiocytes (Green 1977; Muller et al. 2008). Signals can be transduced by the regulation of receptor tyrosine kinases (Perrais et al. 2007) and the activation of Rho family GTPases (Noren et al. 2001).

1.1.4.1 Focal adhesions

Focal adhesions form in basal keratinocytes and aid adhesion to the basement membrane. They

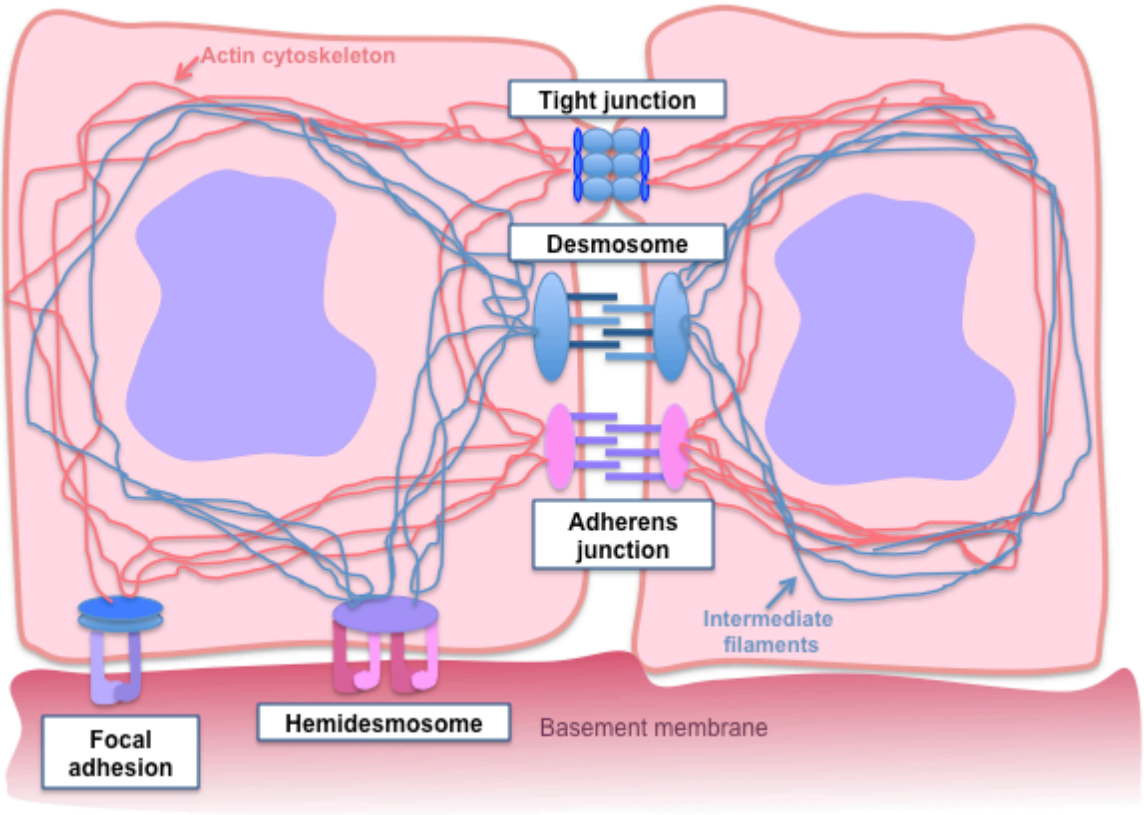

Figure 2 Cell adhesion in the epidermis.

Basal keratinocytes adhere to the basement membrane via focal adhesions and hemidesmosomes while cell-cell adhesion occurs through tight junctions, adherens junctions and desmosomes. For mechanical strength focal adhesions, tight junctions and adherens junctions are connected to the actin cytoskeleton whereas hemidesmosomes and desmosomes are connected to the intermediate filament network.

are important for maintaining tissue integrity as well as having roles in cell spreading, motility and signaling (Borradori et al. 1999; Petit et al. 2000). The adhesion receptors in focal adhesion are integrins, which are heterodimeric transmembrane glycoprotein receptors involved in adhesion to ECM components (Petit et al. 2000). Integrins found in focal adhesions include: $\alpha 2\beta 1$ integrins which binds to collagen I and $\alpha 3\beta 1$ integrins which binds to laminin 5 (Muller et al. 2008). For increased stability focal adhesions are connected to the actin cytoskeleton, this interaction is mediated through multiple proteins such as focal adhesion kinase (FAK), tensin, vinculin, paxillin, talin, α-actinin and filamin, which made up the focal adhesion complex (Petit et al. 2000).

1.1.4.2 Hemidesmosomes

Hemidesmosomes are the key molecular structures that physically attach basal keratinocytes to the basement membrane and are essential for mechanical strength, spatial organisation and tissue architecture in the epidermis (Litjens et al. 2006). Hemidesmosomes are composed of the transmembrane proteins $\alpha 6\beta 4$ integrins and the tetraspanin CD151, which connect to intermediate filaments via the plakin family members, plectin and BP230. Hemidesmosomes bind to collagen 17 and laminin 5 in the ECM (Borradori et al. 1999; Litjens et al. 2006).

1.1.4.3 Tight junctions

The role of tight junctions is to provide a barrier function that renders the epidermis impermeable to solutes and ions and to prevent apical and basolateral diffusion of membrane components (Braga 2002; Brandner et al. 2002). Tight junctions are composed of specific

transmembrane proteins, occludin and claudin, and plaque proteins, ZO-1 and symplekin. Occludin and the family of claudins play a role in cell adhesion while the plaque proteins are involved in linking the tight junction to the actin cytoskeleton (Brandner et al. 2002).

1.1.4.4 Adherens junctions

Adhesion junctions are required for mechanical strength by forming cell-cell adhesions and linking to the actin cytoskeleton. The main adhesion receptor in epidermal cells is E-cadherin, a member of the cadherin family, which forms adhesive cell–cell contacts through homotypic interactions. E-cadherin dimerises and clusters in a calcium-dependent manner, leading to recruitment of α - and β -catenin, members of the armadillo family, which mediate the association of E-cadherin with the actin cytoskeleton (Jamora et al. 2002; Niessen 2007).

1.1.5 Desmosomes

Desmosomes are intercellular junctions that provide mechanical strength to tissues such as the stratified epithelium and myocardium by adhering cells together and intracellularly linking to the intermediate filament network (Garrod et al. 2008). Termed “cellular rivets” due to their role in providing mechanical strength, they are also dynamic structures that are subject to transcriptional and post-transcriptional regulation and have roles in tissue morphogenesis, proliferation and differentiation (Yin et al. 2004; Muller et al. 2008).

Desmosomes are highly organised, electron dense, disc-shaped structures that form on closely

opposing plasma membranes of neighboaring cells. They are less than 1μm in diameter and consist of two identical cytoplasmic plaques that are associated with the intermediate filament network separated by a central core region that spans the intercellular space between the opposing cells (Garrod et al. 2008). Desmosomes are comprised of proteins from at least three distinct gene families, cadherins, armadillo proteins, and plakins (Huber 2003). The desmosomal cadherins are further divided into desmocollins (Dsc1–3) and desmogleins (Dsg1–4) and these two subfamilies mediate calcium-dependent cell–cell adhesion (Garrod et al. 2002). The armadillo proteins include plakophilins (PKP1-3) and plakoglobin/gamma-catenin (Diepgen et al.) and make up the desmosomal plaques, along with desmoplakin, linking cadherins to desmoplakin (Hatzfeld 1999). Desmoplakins I and II (DspI/II) are members of the plakin family and are integral to the desmosomal structure by linking the intermediate filaments to the to the rest of the desmosome (Yin et al. 2004).

All desmosomes contain desmoplakin, plakoglobin and at least one isoform each of plakophilin and the desmosomal cadherins desmocollin and desmoglein. There are also a number of accessory proteins that are associated with desmosomes (Garrod et al. 2008). The desmocollin and desmoglein members of the transmembrane cadherin family cooperate to form the adhesive interface of the desmosome and unlike E-cadherin in adherens junctions, the desmosomal cadherins form both homophilic and heterophilic interactions (Garrod et al. 2002; Jamora et al. 2002). The cytoplasmic tail of the desmosomal cadherins binds the armadillo proteins plakoglobin and plakophilin. They in turn bind to desmoplakin, which links the intermediate filament network to the desmosome (Schmidt et al. 2005) (Figure 3). Plakoglobin and β-catenin

are both members of the armadillo family and plakoglobin has been shown to substitute β-catenin in adherens junctions (Bierkamp et al. 1999; Green et al. 2007). Desmosomes are stabilized laterally by interactions among the proteins present in the junction and by plakophilin (Hatzfeld 2007). The interactions between these proteins are not yet fully understood (Garrod et al. 2008).

1.1.5.1 Regulation of desmosomes and adherens junctions

The formation of both adherens junctions and desmosomes is calcium dependent (Chitaev et al. 1997; Jamora et al. 2002). Calcium binding to the extracellular domain of the desmosomal cadherins induces conformational changes required to mediate the formation of desmosomes (Dusek et al. 2007). In the presence of calcium desmosomal cadherins become rigid, the change in conformation allows both homodimers and heterodimers to form in a *cis* interaction between cadherins on the same membrane. This is followed by a *trans* interaction with cadherin dimers on the opposing membrane of another cell, forming the adhesive interface (Steinberg et al. 1999). In low calcium conditions these calcium dependent desmosomes and adherens junctions break up due to the cadherins losing their ability to form dimers leading to cell separation. Calcium-independent desmosomes have been identified and maintain structural integrity in low calcium conditions. These desmosomes are hyper-adhesive and are thought to form due to the highly organised structure of the desmosome trapping calcium ions (Garrod et al. 2008).

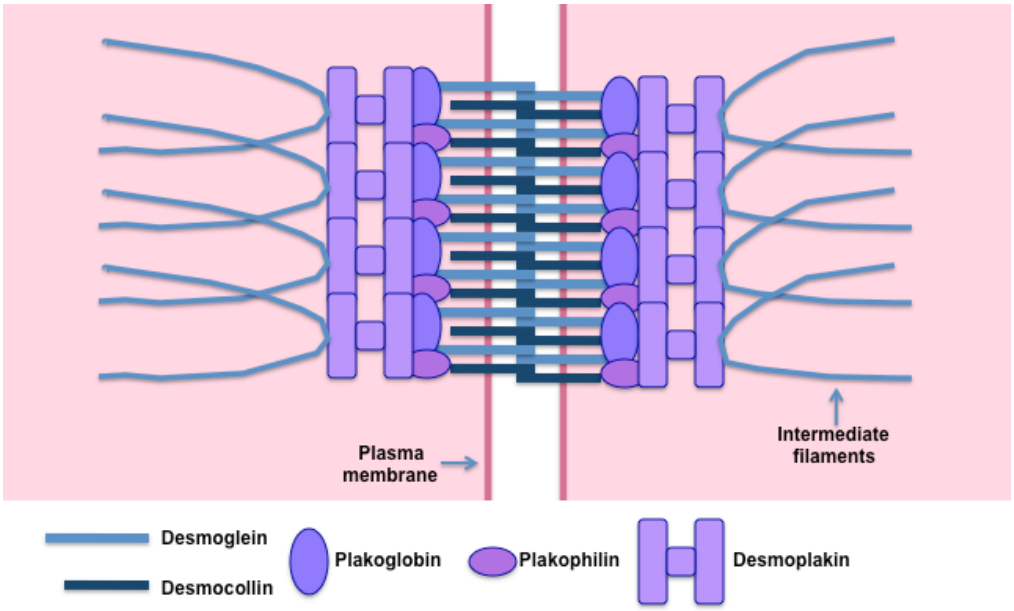

Figure 3 Desmosome structure.

Desmosomes contain desmoplakin, plakoglobin and at least one isoform each of plakophilin and the desmosomal cadherins desmocollin and desmoglein. Desmocollin and desmoglein form the adhesive interface between two neighboring cells while plakoglobin, plakophilin and desmoplakin form the intracellular plaque which links to the intermediate filament network.

1.1.5.2 Desmosomes and terminal differentiation

Electron microscopy has revealed that desmosomes vary in appearance and size in different cell types and in distinct layers of the epidermis. Desmosomes in the basal layer of the epidermis appear small and less organised when compared to those in suprabasal layers. The number of desmosomes increases as keratinocytes move up through the suprabasal layers until the final stages of terminal differentiation where desmosomes break down (Skerrow et al. 1989; Chapman et al. 1990).

Desmosomal cadherin expression is tightly regulated in a cell-type specific manner and also during terminal differentiation and stratification of the epidermis (Garrod et al. 2008). Desmocollin 2 and desmoglein 2 are ubiquitously expressed in all tissues containing desmosomes, including all epithelia, heart myocardium and in dendritic cells of lymph nodes (Nuber et al. 1995; Schafer et al. 1996). In the epidermis all seven of the desmosomal cadherins are expressed, with their expression changing depending on the cell position and differentiation state (Green et al. 2007). As well as desmosomal cadherins, plakophilins also are differentially expressed in the stratified epidermis (Garrod et al. 2008). Migration up through the epidermis is associated with an increase in desmocollin 1, desmoglein 1 and plakophilin 1 and a decrease in desmocollin 3, desmoglein 3 and plakophilin 2 (Dusek et al. 2007; Garrod et al. 2008). Plakoglobin and desmoplakin are expressed in the basal layer but their expression is up-regulated in the suprabasal layers (Klein-Szanto 1977; Arnemann et al. 1993). Desmocollin 2 is weakly expressed in the basal layer and is up-regulated in the spinous layer. However in higher

suprabasal layers desmocollin 2 expression is down-regulated (Legan et al. 1994). Desmoglein 2 is only expressed in basal cells whereas desmoglein 4 is only expressed in upper granular and stratum corneum layers (Bazzi et al. 2006; Garrod et al. 2008) (Figure 4).

The differentiation-specific expression patterns of the desmosomal cadherins as well as overlapping expression means single desmosomes can contain more than one type of desmocollin and desmoglein (North et al. 1996; Garrod et al. 2008). This differential expression of desmosomal caderins is not fully understood but evidence is emerging for its importance in the maintenance of cell relationships during morphogenesis and the regulation of terminal differentiation and proliferation (Yin et al. 2004). Sorting of luminal and myoepithelial cells in 3D mammary cultures is prevented when pairing of desmoglein 2 with desmocollin 2 or desmocollin 3 is prevented (Runswick et al. 2001). Misexpression of desmogelin 2, desmoglein 3 or desmocollin 3 in the suprabasal layers of the epidermis results in increased cell proliferation and altered differentiation (Merritt et al. 2002; Hardman et al. 2005; Brennan et al. 2007). These data indicate the importance of desmosomal cadherin expression patterns for normal terminal differentiation and morphogenesis.

1.2 Apoptosis

1.2.1 Introduction to apoptosis

Mammalian cells undergo several types of cell death, including necrosis, autophagy and apoptosis. Necrosis occurs when cells are damaged by acute cellular injury. Cells die due to

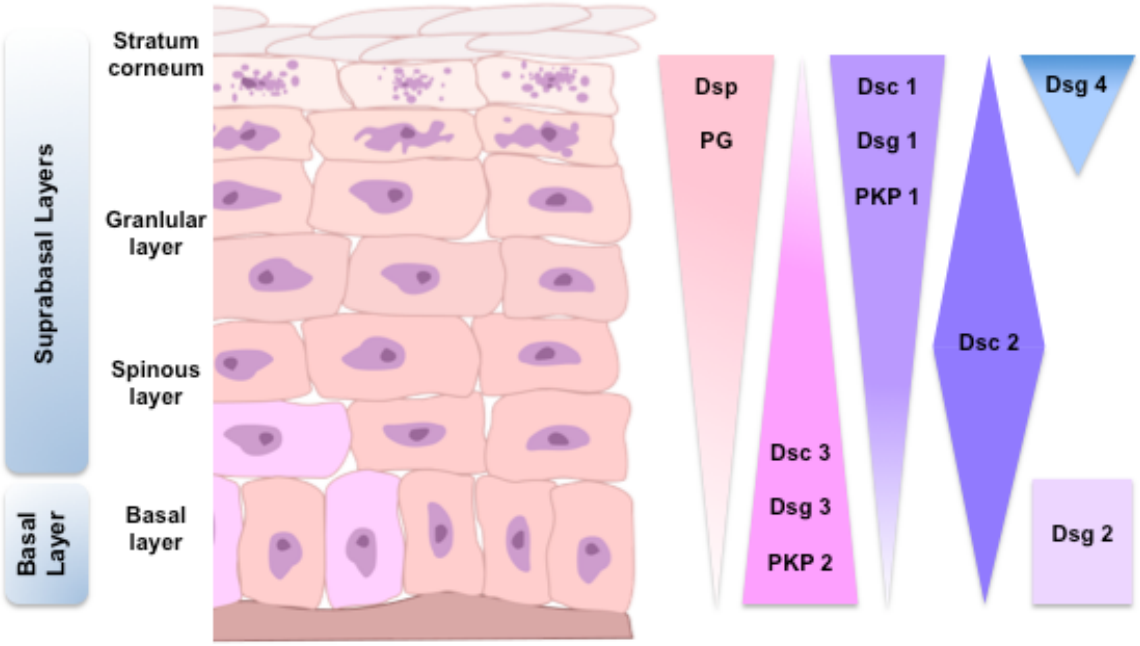

Figure 4 Differentiation-specific expression of desmosomal proteins in the epidermis.

In the epidermis desmosomal protein expression is regulated in a differentiation-specific manner. This schematic represents the relative alterations in expression levels of desmosomal proteins in the different differentiation layers of the epidermis. Dsp, Desmoplakin I/II; PG, Plakoglobin; Dsc, Desmocollin; Dsg, Desmoglein; PKP, Plakophilin

vacuolation of the cytoplasm, swelling and lysis resulting in leakage of cell contents which can be harmful to surrounding cells and can cause inflammation (Kerr et al. 1972). Necrotic cells frequently exhibit changes in nuclear morphology but organised chromatin condensation, which is characteristic of apoptosis, is not observed (Edinger et al. 2004). Autophagy has been classified as a distinct form of non-apoptotic death that is separate from necrosis. During autophagy, double membrane vesicles encapsulate cellular organelles and cytoplasm. The autophagosomes fuse with lysosomes and the contents are degraded and recycled. Autophagy is a highly regulated process and provides a mechanism for the turnover of damaged organelles and long-lived proteins (Maiuri et al. 2007). Apoptosis is critical for normal epidermal homeostasis and is required for epithelial turn over (Ziegler et al. 1994) it also plays an important role during development (Kerr et al. 1972). The function of apoptosis is the removal of unnecessary, damaged and harmful cells and the process involves a sequence of cytoplasmic and nuclear changes that result in the death of single cells (Haake et al. 1993). Apoptosis culminates in the cleavage of DNA by endonucleases and the condensation and fragmentation of the nucleus. The plasma membrane undergoes blebbing and the cell breaks up into discrete, membrane bound fragments, with the cytoplasmic organelles and plasma membrane retaining their integrity. During apoptosis there is no leakage of the cell content so no inflammatory response is initiated and the dead cells are rapidly phagocytosed by neighbouring cells or by macrophages (Gandarillas et al. 1999). The duration of apoptosis from initial cell shrinkage through to removal of apoptotic bodies requires as little as 1-3 hrs in lymphocytes, but up to 48-72 hrs in epidermal keratinocytes (Haake et al. 1993).

Apoptosis can be initiated via two major pathways, the intrinsic pathway, involving subcellular organelles, or the extrinsic/death receptor pathway, which involves the activation of death receptors in response to ligand binding (Servais et al. 2008). Typically both pathways converge to a final common pathway involving the activation of caspase cascade (Ghobrial et al. 2005). The caspase cascade involves initiator caspases (2, 8, 9, 10) becoming activated by aggregation and proteolytic cleavage induced by the intrinsic or extrinsic pathway. Once activated the initiator caspases activate executioner caspases (3, 6, 7), which are responsible for the cleavage of regulatory and structural molecules, culminating in the death of the cell (Slee et al. 2001; Ghobrial et al. 2005).

1.2.2 The intrinsic apoptosis pathway

The intrinsic pathway is most commonly centred around mitochondrial outer membrane permeabilisation (MOMP) and cytochrome c release, which is regulated by members of the Bcl-2 family (Green et al. 2004) (Figure 5). Lysosomes and the endoplasmic reticulum can also be involved in the intrinsic apoptosis pathway (Servais et al. 2008). A diverse group of apoptosis promoting stimuli such as cytotoxic drugs, radiation, heat shock, survival factor deprivation and other cellular stresses can induce apoptosis via the intrinsic pathway. Although these stimuli may damage cells in very different ways, all of these pathways engage the intrinsic apoptosis pathway by triggering MOMP (Slee et al. 1999).

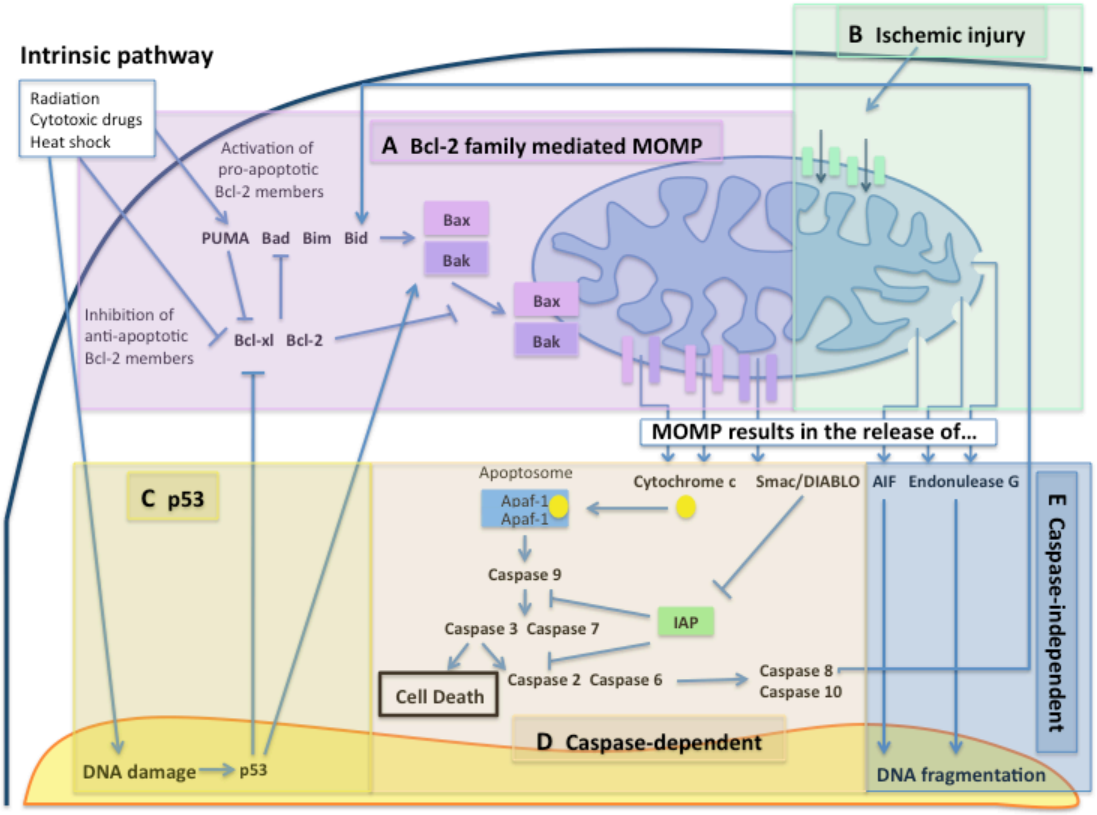

Figure 5 Intrinsic-apoptosis pathways.

The intrinsic-apoptosis pathway converges around MOMP. **A** Stimuli inducing the intrinsic-apoptosis pathways affect the anti- and pro-apoptoic members of the Bcl-2 family, which regulate the activation of Bax and Bak causing MOMP. **B** Ischemic injury can also cause MOMP by opening pores in the mitochondrial membrane. **C** Some stimuli induce DNA damage and the up-regulation of p53. p53 can interact with Bcl-2 family members inducing Bax activation. After MOMP is induced cell death can occur via two pathways: **D** Caspase-dependent cell death involves cytochrome c inducing the formation of the apoptosome and caspase 9 activation resulting in the activation of the caspase cascade and cell death. **E** Caspase-independent cell death occurs due to the release of AIF and endonuclease G from the mitochondria, which induces DNA fragmentation and cell death.

1.2.2.1 MOMP and the Bcl-2 family

MOMP can be induced through different mechanisms. Reduced oxygen conditions such as those seen in ischemic injury can induce pores present in either the outer or inner mitochondrial membranes to open, changing the membrane potential and leading to swelling and disruption of the membrane (Green et al. 2004) (Figure 5B). However MOMP is most commonly mediated by Bcl-2 family proteins which consist of both anti-apoptotic Bcl-2 members that act as repressors of apoptosis by blocking the release of cytochrome c, and pro-apoptotic members that act as promoters (Green et al. 2004). Pro-apoptotic members of the Bcl-2 family include Bax, Bak, Bad, Bcl-Xs, Bid, Bik, Bim, Puma, Nova and Hrk, and anti-apoptotic members include Bcl-2, Bcl-X_L, Bcl-W, Bfl-1 and Mcl-1 (Reed 1994). These proteins share one or more Bcl-2 homology (BH) domains and control MOMP mostly at the mitochondrial outer membrane (Kuwana et al. 2003). The pro-apoptotic multi-domain proteins Bax and Bak (containing BH-1, -2, and -3 domains) mediate MOMP when activated by inserting into the outer mitochondrial membrane, forming pore-like structures (Korsmeyer et al. 2000; Basanez et al. 2002) (Figure 5A). They can be activated by other Bcl-2 family members, the BH3-only proteins, Bad, Bim, Bid, Puma as well as non-Bcl-2 family proteins (Kuwana et al. 2003). Both Bid and Bim activate Bax directly (Kuwana et al. 2005). Following a death signal, pro-apoptotic Bcl-2 family members undergo posttranslational modifications that include dephosphorylation and cleavage resulting in their activation, oligomerisation and translocation to the mitochondria (Scorrano et al. 2003). Anti-apoptotic Bcl-2 family members, Bcl-2, Bcl-xL, Mcl-1, and others, sequester the BH3-only proteins and probably the activated Bax and Bak proteins, preventing MOMP from occurring (Kuwana et al. 2005). Other BH3-only proteins, for example Puma, Noxa, and Bad,

can antagonize the anti-apoptotic Bcl-2 family members sensitising cells for death (Letai et al. 2002; Kuwana et al. 2005) (Figure 5A).

Bax and Bak can be activated and inhibited by non-members of the Bcl-2 family. The tumour suppressor p53 promotes apoptosis by inducing expression of the BH3-only protein PUMA (Jeffers et al. 2003). p53 can also induce MOMP and apoptosis in the absence of transcription through direct activation of Bax (Chipuk et al. 2004) or Bak (Leu et al. 2004) or through binding to Bcl-2 and Bcl-xl, blocking their activity (Chipuk et al. 2004) (Figure 5C). Caspase activation can also result in the activation of Bax and Bak in the extrinsic-apoptosis pathway with caspase 8 cleaving Bid which in turn activates Bax (Yamada et al. 1999; Korsmeyer et al. 2000).

1.2.2.2 Events following MOMP

On the permeabilisation of the outer mitochondrial membrane pro-apoptotic proteins are released into the cytoplasm. These include cytochrome c, apoptosis induced factor (AIF), second mitochondria derived activator of caspase (Smac)/direct inhibitor of apoptosis protein (IAP)-binding protein with low PI (DIABLO) and endonuclease G (Figure 5). Once in the cytoplasm these proteins can initiate the activation of the executioner caspases or can act as caspase-independent death effectors (Saelens et al. 2004).

1.2.2.3 Caspase-dependent apoptosis

When cytochrome c is released from the mitochondria it binds to the adapter protein apoptosis

inducing factor 1 (Apaf-1) inducing deoxyadenosine triphosphate binding, conformational change and oligomerisation of Apaf-1 resulting in the formation of the apoptosome (Li et al. 1997; Adrain et al. 1999; Bao et al. 2005). The initiator caspase 9 is recruited to the apoptosome and activated by proteolytic cleavage (Acehan et al. 2002). Active caspase 9 initiates the caspase cascade by the simultaneous activation of the executioner caspases 3 and 7 (Slee et al. 2001). Caspase 3 plays an important role in propagating the caspase cascade in addition to its role as an executioner caspase by driving the activation of caspases 2 and 6 (Slee et al. 2001). Following caspase 2 and 6 activation the initiator caspases 8 and 10 are also activated (Slee et al. 1999). Caspase 3 appears to be the primary executioner caspase and is required for multiple proteolytic events leading to the death of the cell, while caspases 6 and 7 have either minor or highly specialised roles (Slee et al. 2001). Activated caspase 3 leads to the cleavage of nuclear lamin and the breakdown of DNA through DNAases resulting in condensation of chromatin, DNA fragmentation and finally the death of the cell (Servais et al. 2008) (Figure 5D).

Caspases can also be controlled downstream of Bcl-2 family proteins. The inhibitor of apoptosis protein (IAP) appears to directly block caspase activity and/or activation. IAP activity can in turn be blocked by other regulatory proteins such as Smac/DIABLO that can bind too IAP and block its anti-apoptotic activity (Du et al. 2000; Verhagen et al. 2000) (Figure 5D).

1.2.2.4 Caspase-independent apoptosis

MOMP can commit the cell to caspase-independent death due to irreversible loss of mitochondrial function and mitochondrial release of caspase-independent death effectors such as

AIF (Susin et al. 1999) and endonuclease G (Li et al. 2001). AIF appears to exert its effects in a caspase-independent manner by translocating to the nucleus and triggering the chromatin collapse and digestion (Susin et al. 1999). Endonuclease G induces caspase-independent DNA fragmentation and cell death (Li et al. 2001) (Figure 5E).

The targeted induction of apoptosis in recent years has been a focus for cancer therapy with many apoptosis-inducing and anti-apoptosis-inhibiting agents appearing in clinical and preclinical trials (Ghobrial et al. 2005; Green et al. 2005). Peptides and drugs that mimic the BH3-only proteins have promise as agents that can cause MOMP and apoptosis, or sensitize cells for death (Oltersdorf et al. 2005). Conventional chemotherapeutic drugs, such as cisplatin, etoposide and doxorubicin, induce MOMP in an indirect fashion by increasing pro-apoptotic signals for example by inducing p53 expression and by affecting Bcl family members (Fulda et al. 2006).

1.2.2.5 Cisplatin

The chemotheraputic drug cisplatin is commonly used to treat small lung cancer (Wang et al. 2004) and gastric cancer (Wagner et al. 2006). Cisplatin is a DNA macrochelator and blocks DNA replication and gene transcription by inducing single and double-stranded DNA breaks (Ries et al. 1986; Siddik 2003). Cisplatin-induced DNA damage results in an up-regulation of p53, which induces the expression of p53-induced death domain (PIDD) protein and PUMA (Wei et al. 2007). PIDD promotes the activation of caspase 2, which causes the release of Apoptosis-Inducing Factor (AIF) from the mitochondria (Seth et al. 2005). AIF is a caspase-

independent promotor of apoptosis (Daugas et al. 2000). PUMA antagonises Bcl-xl (Jiang et al. 2006) allowing Bax to translocate from the cytoplasm to the mitochondria and alter the integrity of mitrochodrial membrane resulting in cytochrome c release (Ott et al. 2007). Once in the cytoplasm, cytochrome c interacts with Apaf1 forming the apoptosome, which promotes caspase 9 activation. Active caspase 9 then initiates the activation of the executioner caspases, caspase 3 and 7, inducing the caspase cascade. Caspase 3 and 7 activation results in the classic morphological signs of apoptosis, membrane blebbing, cell shrinkage and DNA fragmentation all resulting in cell death (Servais et al. 2008) (Figure 6).

1.2.3 The extrinsic apoptosis pathway

The extrinsic apoptosis pathway initiates apoptosis by the ligation of cell surface death receptors. On ligand binding the death receptor propagates apoptosis by activating the caspase cascade either by the activation of the execution caspase 3 or by inducing MOMP (Sprick et al. 2004). Death receptors are members of the tumour necrosis factor (TNF) receptor family with over 20 members that are involved in a wide range of biological functions such as the regulation of apoptosis and survival, differentiation or immune regulation (Walczak et al. 2000; Ashkenazi 2002). Members of the TNF receptor family are defined by a cytoplasmic death domain, which plays a crucial role in transmitting the death signal from the plasma membrane to the intracellular signaling pathways (Walczak et al. 2000). The best-characterised death receptors include CD95 (APO-1/Fas), TNF receptor and TNF-related apoptosis-inducing ligand (TRAIL) receptors. The corresponding death receptor ligands to the TNF receptor family members

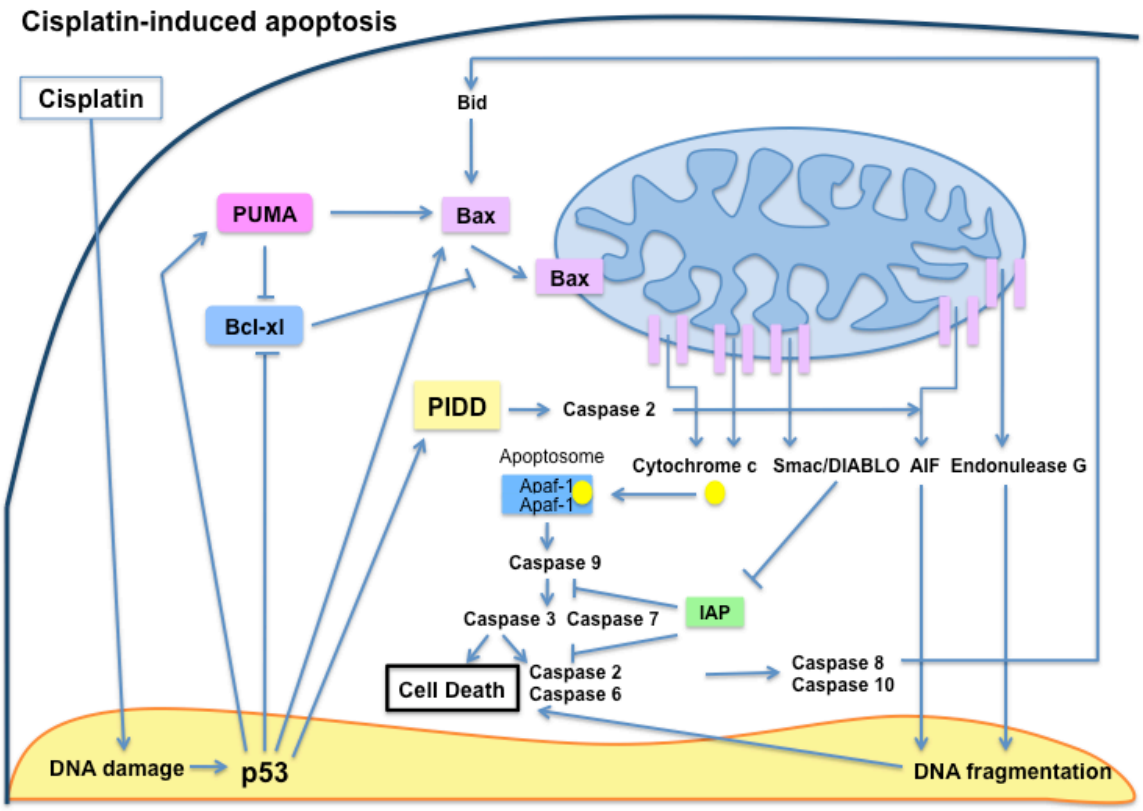

Figure 6 Cisplatin-induced apoptosis.

Cisplatin induces the intrinsic apoptosis pathway by inducing DNA damage leading to the up-regulation of p53, which induces the expression of PUMA and PIDD. PUMA and p53 inhibit Bcl-x_L and activate Bax, which translocates to the mitochondria inducing MOMP resulting in the activation of the caspase cascade and cell death. PIDD activates caspase 2, which leads to the release of AIF resulting in DNA fragmentation and cell death.

include CD95 ligand, TNF and TRAIL (Walczak et al. 2000).

1.2.3.1 CD95 and TRAIL ligation and initiation of the caspase cascade

Signaling through CD95 and TRAIL receptors occurs on ligand binding which is followed by receptor trimerisation. This leads to the clustering of the death domains on the receptors. Adaptor molecules, such as Fas-associated death domain (FADD), are recruited to the clustered death domains (Walczak et al. 2000). FADD recruits the initiator caspase, caspase 8, to the activated receptor to form the death inducing signaling complex (DISC) (Kischkel et al. 1995). Recruitment of caspase 8 to the DISC induces its activation through oligomerisation and auto-cleavage. For the CD95 and TRAIL signaling pathway, cell type specific mechanisms have been identified (Scaffidi et al. 1998; Fulda et al. 2002). In type I cells, caspase 8 is activated at the DISC to a level sufficient to directly activate the downstream executioner caspase 3 (Scaffidi et al. 1998). In type II cells, the amount of active caspase 8 generated at the DISC is insufficient to activate caspase 3 and MOMP is required for full activation of caspases (Scaffidi et al. 1998; Fulda et al. 2002). This occurs by activated caspase 8 cleaving Bid, a pro-apoptotic member of the Bcl-2 family, activated Bid in turn activates Bax resulting in MOMP (Yamada et al. 1999) (Figure 7). Type I cells include lyphoblast and lyphoma cells (Scaffidi et al. 1998; Fulda et al. 2002). Most epithelial cells including keratinocytes are type II cells and require MOMP for full initiation of the caspase cascade (Kim et al. 2004).

The cytosolic protein Fas-associated death-domain-like IL-1β-converting enzyme-inhibitory protein (FLIP) interferes with the initiation of the caspase cascade by binding to the DISC, preventing caspase 8 activation (Scaffidi et al. 1999; Krueger et al. 2001) (Figure 7A). High

levels of FLIP expression have been found in many tumour cells and has been linked with resistance to CD95L or TRAIL-induced apoptosis (Fulda et al. 2002; Longley et al. 2006).

1.2.3.2 NF-κB and apoptosis

In contrast to CD95 and TRAIL, which leads to the recruitment of FADD and caspase 8 to the activated receptor, TNF receptor activation results in the recruitment of TNF receptor associated death domain (TRADD), receptor interacting protein 1 (RIP 1) and TNF receptor associated factor 2 (TRAF 2) (Figure 7B). This leads to the activation of the nuclear factor kappa B (NF-κB) and anti-apoptotic signaling (Zhang et al. 2000; Harper et al. 2003). The NF-κB transcription factors are involved in the regulation of many biological processes, such as inflammation and apoptosis (Karin et al. 2002). In its inactive form, NF-κB is sequestered in the cytoplasm by the inhibitor of NF-κB (IκB) family proteins, which bind to NF-κB and mask its nuclear localization signal (Maldonado et al. 1997). Upon stimulation the IκB are phosphorylated by IκB kinases (IKK) targeting the IκB for degradation resulting in the nuclear localisation signal of NF-κB to be unmasked and NF-κB is translocated to the nucleus. Once in the nucleus, NF-κB binds to regulatory DNA elements affecting the gene expression of a multitude of genes (Maldonado et al. 1997). TNF receptor activated NF-κB induces the transcription of inhibitor of apoptosis proteins (IAP) (Karin et al. 2002) and other anti-apoptotic proteins (Wang et al. 1998; Diessenbacher et al. 2008). After the initial burst of anti-apoptotic signaling from NF-κB, the receptor associated signaling complex dissociates and reassembles in the cytoplasm with FADD and caspase 8, resulting in the activation of caspase 8 (Micheau et al. 2003). However the initial burst of anti-apoptotic signaling from NF-κB usually protects the cell

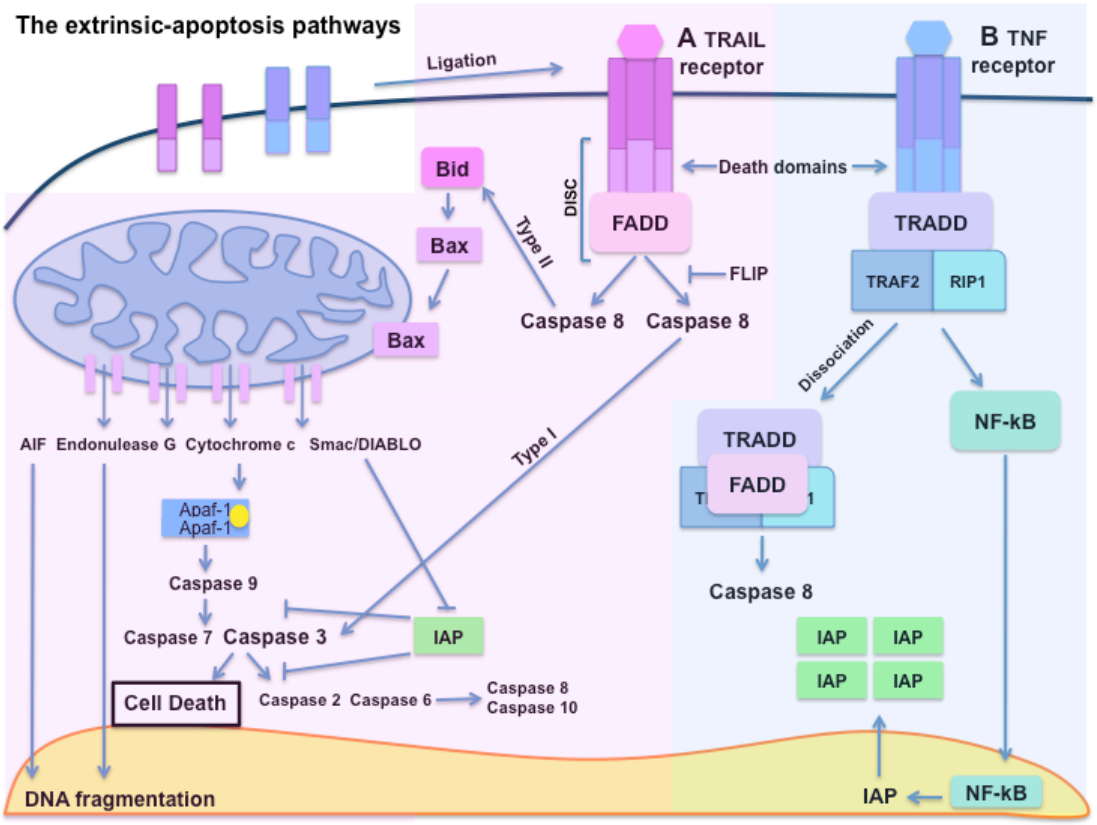

Figure 7 Extrinsic apoptosis pathways.

On ligand binding receptor trimerisation occurs leading to the clustering of the receptors death domains. **A** Ligation at the TRAIL receptor leads to the recruitment of the FADD forming the DISC resulting in the activation of caspase 8. In type I cells activated caspase 8 activates caspase 3 resulting in cells death, whereas in type II cells activated caspase 8 induces MOMP via Bid to activate the caspase cascade resulting in cell death. **B** Ligation at the TNF receptor leads to the recruitment of TRADD, RIP1, and TRAF2 resulting in the activation and translocation of NF-κB, which induces the expression of IAP inhibiting apoptosis. Dissociation of the TRADD, RIP1 and TRAF2 complex, from the receptor is followed by FADD binding and the activation of caspase 8. However the activation of caspase 8 is usually not sufficient to over come the initial anti-apoptotic signaling from NF-κB.

from caspase 8 activation, resulting in cell survival (Zhang et al. 2000). Inhibition of NF-κB activation is required to sensitise cells to TNF-induced apoptosis (Rothe et al. 1995).

The activation of NF-κB has an important role in the regulation of the extrinsic apoptosis pathway, by having both anti- and pro-apoptotic functions, determining the outcome of specific apoptotic stimuli (Kuhnel et al. 2000). The anti- and pro-apoptotic functions of NF-κB are determined by the genes NF-κB is targeted to and the level of gene transcription. An example of an anti-apoptotic function is the activation of TRAF 2 and IAP (Wang et al. 1998), while a pro-apoptotic function is the activation of p53 and caspases (Kuhnel et al. 2000).

1.2.3.3 TRAIL and NF-κB

NF-κB can be activated by numerous stimuli such as growth factors, cytokines, radiation, stress and pharmacological agents such as cisplatin and TRAIL (Walczak et al. 2000). TRAIL and TNF both activate NF-kB in human keratinocytes but only TRAIL efficiently induces apoptosis (Diessenbacher et al. 2008). When activation of NF-κB is inhibited TNF but not TRAIL-induced apoptosis is dramatically enhanced (Karin et al. 2002; Diessenbacher et al. 2008). Interfering with TRAIL-induced NF-κB activation does not alter keratinocyte sensitivity to TRAIL-induced apoptosis, indicating that TRAIL-induced NF-κB activation is an apoptosis-independent signal pathway in keratinocytes and is involved in IL-8 expression (Leverkus et al. 2003).

1.2.3.4 TRAIL and cancer

TRAIL receptors are constitutively expressed in a wide range of tissues. There are two agonistic TRAIL receptors, which contain the death domain, TRAIL-R1 and TRAIL-R2, enabling them to activate the apoptotic machinery upon ligand binding. There are also antagonistic TRAIL receptors (TRAIL-R3, R4 and R5), which bind TRAIL, but do not transmit a death signal (LeBlanc et al. 2003). Unlike TNF and CD95L, TRAIL exhibits selectivity for triggering apoptosis in tumour cells and not normal cells (Wiley et al. 1995). In addition, TRAIL exerts potent antitumour activity *in vivo* without exhibiting systemic toxicity unlike TNF and CD95L making TRAIL a potentially ideal cancer therapy (Walczak et al. 1999). TRAIL induces apoptosis in primary and transformed keratinocytes (Leverkus et al. 2000).

1.2.4 Terminal differentiation as a form of cell death

Terminal differentiation and apoptosis share some similarities but are considered distinct processes, both of which culminate in cell death (Gandarillas et al. 1999). Normal function of the epidermis requires keratinocytes to undergo terminal differentiation in order to produce the ultra-structure of the epidermis required for protection of underlying tissues. Terminal differentiation is an organised process of cell death with the final stage, known as cornification, producing the stratum corneum, which is made up of dead keratinocytes fused together forming an impermeable barrier (Fuchs 1990). By contrast, apoptosis also known as programmed cell death, is required for the removal of undesirable cells during both development and homeostasis of adult tissue (Edinger et al. 2004).

Whilst these two processes can be distinguished both morphologically and biochemically both terminal differentiation and apoptosis are metabolically active processes that induce dramatic cellular changes (Lippens et al. 2009). Initiation of terminal differentiation is associated with loss of adhesion to the basement membrane through the loss of integrins (Green 1977). This loss of adhesion in endothelial and epithelial cells can induce a form of apoptosis known as anoikis (Frisch et al. 1997). Adhesion to the ECM via intergrins prevents terminal differentiation in keratinocytes but also inhibits other cells from undergoing apoptosis (Green 1977; Adams et al. 1989; Frisch et al. 1997). Apoptosis is a rapid process taking a few hours and occurring in single cells. Cells undergoing apoptosis break up, without leaking cellular contents, and are engulfed immediately after death by phagocytes, macrophages and surrounding cells (Lippens et al. 2009). By contrast, terminal differentiation is a slow process occurring in individual cells in the suprabasal layers. The process takes up to two weeks and the dead cells are utilised for barrier function and are removed from the surface of the epidermis when they are shed (Gandarillas 2000). Terminally differentiating cells also become larger and flatter, unlike apoptotic cells that shrink during the process (Gandarillas et al. 1999; Gandarillas 2000). In both cases cellular content is eliminated and proteolysis is the major cellular event (Gandarillas 2000; Lippens et al. 2009). During apoptosis caspases 3, 6, 7, and 9 are responsible for proteolysis but the respective knockout mice show no skin abnormalities (Lippens et al. 2009). Caspase 14 is required for normal skin development and is activated during cornification. However, caspase 14 is non-apoptotic indicating that the proteolytic events important for each process are different (Lippens et al. 2000).

1.3 Rho GTPases

1.3.1 Introduction

Rho family GTPases are master regulators of many aspects of cellular behaviour including the regulation of the actin cytoskeleton, vesicular transport, gene expression, enzymatic activities, the cell cycle, cell morphogenesis, cell migration and apoptosis (Etienne-Manneville et al. 2002; Jaffe et al. 2005). Rho GTPases are a distinct family within the Ras superfamily of small GTPases with 22 mammalian genes encoding Rho GTPases identified (Jaffe et al. 2005). These small GTPases are 20-30 kDa and share 30-50% identity (Takai et al. 2001). Most Rho GTPases act as "molecular switches" cycling between two conformations; the 'active state' bound to GTP and the 'inactive state' bound to GDP (Etienne-Manneville et al. 2002; Jaffe et al. 2005) (Figure 8). The ability to hydrolyse GTP is determined by five primary sequence motifs in the GTP-binding domain, which is highly conserved among the members of the Ras superfamily (Bourne et al. 1991; Takai et al. 2001).

The switch mechanism by which Rho GTPases function enables Rho GTPases to sort and amplify transmembrane signals for the regulation of complex cellular processes. Rho GTPase activity is regulated by ancillary proteins, which facilitate the exchange of GDP and the hydrolysis of GTP, thereby regulating the switch (Schmidt et al. 2002; Bustelo et al. 2007) (Figure 8). Guanine nucleotide exchange factors (GEF) stimulate the release of GDP allowing GTP to bind, thereby activating the GTPase (Rossman et al. 2005). Once in a GTP-bound state, Rho GTPases can activate downstream effectors. GTPase activating proteins (GAP) stimulate the intrinsic GTPase activity hydrolysing GTP to GDP inactivating the switch (Bernards 2003).

This form is the resting state and guanine nucleotide dissociation inhibitors (GDI) can bind to the Rho GTPase maintaining the association with GDP. GDIs block spontaneous activation of the Rho GTPases by covering their C–terminal geranylgeranyl moiety stabilising them as cytosolic Rho-GDI complexes (Olofsson 1999; Bustelo et al. 2007). Regulation of the Rho switch is complex with over 60 GEFs and 70 GAPs identified (Etienne-Manneville et al. 2002). Rho GTPases can also be regulated through posttranslational modifications such as phosphorylation, ubiquitination and isoprenylation (Lang et al. 1996; Wang et al. 2003; Bustelo et al. 2007).

1.3.2 RhoA

RhoA is a member of the Rho GTPase family and has been implicated in many different cellular processes, including cytoskeletal organisation, gene expression, proliferation, differentiation and apoptosis (Takai et al. 2001). Known downstream effectors of RhoA include: Rho kinases (ROCK I and ROCK II), citron, the mammalian diaphanous-related formins (mDia1, 2 and 3), protein kinase C-related proteins (PRKs) and protein kinase N1 (PKN) (Schwartz 2004). ROCK I and II were the first Rho effectors to be identified and were characterised for their roles in mediating the formation of RhoA-induced actin stress fibres and focal adhesions (Ishizaki et al. 1996; Leung et al. 1996; Ishizaki et al. 1997; Riento et al. 2003). Citron is involved in cytokinesis and cell cycle progression (Madaule et al. 2000). The mammalian diaphanous-related formins stimulate actin polymerisation and stabilise microtubules during cell migration (Schwartz 2004). Protein kinase N1 is involved in endosomal trafficking (Amano et al. 1996; Schwartz 2004).

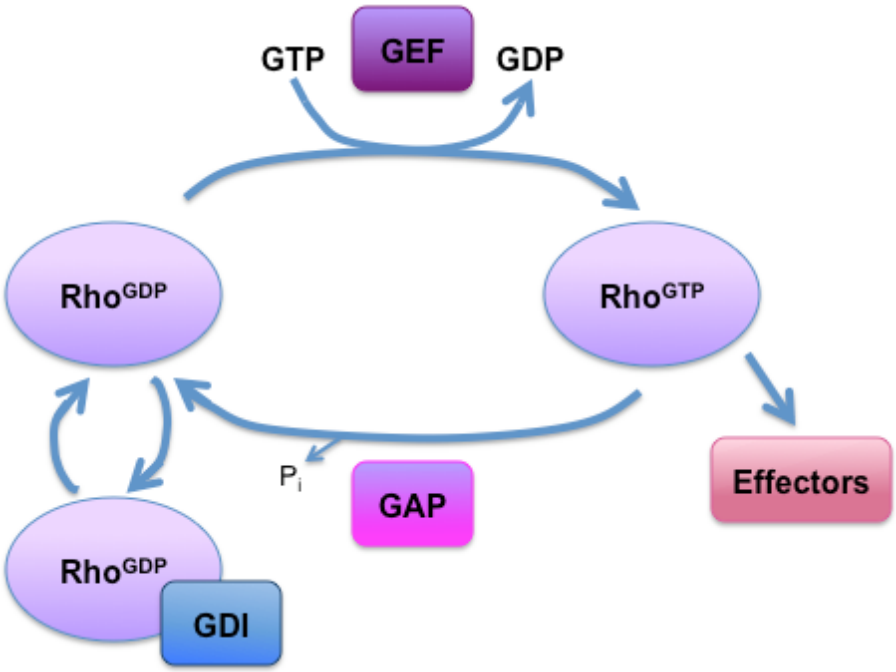

Figure 8 The Rho GTPase cycle.

Guanine nucleotide exchange factors (GEF) stimulate the release of GDP allowing GTP to bind. In a GTP-bound state Rho GTPases can activte downstream effectors. GTPase activating proteins (GAP) stimulate the intrinsic GTPase activity to hydrolyse GTP returning the Rho GTPase to an inactive state. Guanine nucleotide dissociation inhibitors (GDI) bind to the Rho GTPase maintaining the association with GDP.

1.3.3 Regulation of actin stress fibres by RhoA

RhoA regulates actomyosin-based contractility through its downstream effectors ROCK I and ROCK II, which are required for the formation of stress fibres in fibroblasts, epithelial and endothelial cells (Riento et al. 2003). Actin stress fibres are contractile fibres that and are composed of actin filaments, α-actinin, myosin II, tropomyosin and myosin light chain kinase (MLCK). They run along the cell body and terminate at focal adhesions attaching the cell to the underlying substratum generating tension, enabling cell adhesion and cell spreading (Pellegrin et al. 2007).

ROCK I and ROCK II are important for the formation of RhoA-induced actin stress fibres. Inhibition of ROCK activity results in the loss of actin stress fibres and focal adhesions whereas over-expression of ROCK induces actin stress fibre formation (Leung et al. 1996; Ishizaki et al. 1997; Uehata et al. 1997). ROCK I/II are serine/threonine kinases that are associated with actin stress fibres and phosphorylate a number of proteins involved in actin stress fibre formation (Katoh et al. 2001; Pellegrin et al. 2007). Phosphorylation of the motor protein, myosin II, induces actomyosin-based contraction and increased actin stress fibre assembly. MLC II can be phosphorylated by the calcium-dependent MLCK or by ROCK I/II (Amano et al. 1996; Katoh et al. 2001; Pellegrin et al. 2007). Myosin light chain phosphatase (MLCP) dephosphorylates myosin II inhibiting contractility, ROCK prevents this by phosphorylating and inhibiting the phosphatase (Kimura et al. 1996). To increase actin stress fibre formation ROCK phosphorylates LIM kinase I and II, which are involved in the regulation of actin dynamics (Maekawa et al. 1999; Scott et al. 2007). Phosphorylated LIM kinase I and II in turn

phosphorylates and inhibits the actin depolymerising activity of cofilin resulting in increased actin stress fibre assembly (Scott et al. 2007).

Actin stress fibres produced by the actions of calcium-dependent myosin light chain kinase are usually located to the periphery of the cell whereas RhoA-ROCK induced stress fibres are located in the cell body (Totsukawa et al. 2000). Over-expression of constitutively active ROCK induces thick actomyosin bundles with a stellate morphology that are distinct from actin stress fibres induced directly by Rho (Amano et al. 1996; Leung et al. 1996). RhoA and ROCK I/II regulate cell adhesion through the formation of these contractile actin stress fibres, which in turn induces the formation of focal adhesions (Petit et al. 2000).

1.3.4 ROCK I

The serine/threonine kinase p160ROCK/ROCKI was identified as a Rho substrate by T. Ishizaki et al. (1996) and was confirmed to be a downstream target of Rho but not Rac, and to mediate the formation of focal adhesions and stress fibres (Ishizaki et al. 1997). A homologue of ROCKI/p160ROCK/ROK_B was isolated by Leung et al. (1996) and is known as ROKa/Rho-kinase/ROCKII. ROCK I/II are serine/threonine kinases of 160kDa and consist of an amino-terminal kinase domain followed by a coiled-coil region. At the carboxyl terminal there is a Rho binding domain and a pleckstrin homology (PH) domain with an internal cysteine-rich domain (Ishizaki et al. 1997; Riento et al. 2003). The carboxyl terminal region of ROCK I/II constitutes an autoinhibitory region reducing kinase activity (Amano et al. 1999). The amino acid

sequences of the two ROCK isoforms have 65% identity with the highest identity (92%) in the kinase domains (Nakagawa et al. 1996).

1.3.5 Regulation of ROCK activity

In its GTP-bound form, RhoA enhances the activity of ROCK I/II by binding to the Rho-binding domain relieving the autoinhibition mediated by the carboxyl terminal region (Leung et al. 1995; Nakagawa et al. 1996; Fujisawa et al. 1998). The best-characterised activator of ROCK is RhoA, but other mechanisms for ROCK regulation have been identified. Lipids, such as arachidonic acid, can activate ROCK I/II (Feng et al. 1999). Protein oligomerisation might also regulate ROCK activity through amino terminal transphosphorylation (Riento et al. 2003). During apoptosis, caspase 3 cleaves the C-terminus of ROCK I resulting in a loss of autoinhibition with the active kinase responsible for membrane blebbing (Coleman et al. 2001; Sebbagh et al. 2001). Over-expression of the Rho family GTPases GEM, RhoE and Rad has been shown to inhibit ROCK function, with GEM and RhoE inhibiting ROCK I induced neurite retraction, while Rad inhibits ROCK II functions (Ward et al. 2002; Riento et al. 2003).

1.3.6 Y-27632

A number of pharmacological compounds which inhibit ROCK I/II kinase activity have been identified and used to investigate the function ROCK I/II (Darenfed et al. 2007). The most commonly used of these is a small molecule inhibitor called Y-27632 ((+)-(R)-trans-4-(1-aminoethyl)-N-(4 pyridyl)-cyclohexanecarboxamide). Y-27632 was first discovered by Yoshitomi Pharmaceutical Industries and inhibits ROCK I/II by competing for the ATP binding

site (Ishizaki et al. 2000; Darenfed et al. 2007). The use of this compound was shown to inhibit smooth muscle contractility and normalise high blood pressure in rat models by inhibiting ROCK I/II (Ishizaki et al. 2000). Y-27632 is commonly used at a concentration of 10μM where it was thought to be a specific inhibitor of ROCK I/II (Davies et al. 2000). However, further analysis revealed that at this concentration protein kinase C-related protein kinase (PRK-2) is also inhibited by Y-27632 (Davies et al. 2000). PRK-2 is an effector of both Rho and Rac and is involved in the regulation of the actin cytoskeleton (Vincent et al. 1997). Therefore studies that rely solely on the use of Y-27632 should be treated with caution.

1.3.7 ROCK substrates

The kinase domains of ROCK I and ROCK II share 92% identity and many of the proteins described as ROCK substrates have only been categorised using one isoform. However, the two ROCK isoforms have been shown to interact with and phosphorylate different substrates to different degrees. For example, ROCK I binds to and strongly phosphorylates RhoE whereas ROCK II does not bind to RhoE and only weakly phosphorylates RhoE *in vitro* (Riento et al. 2005). Studies using RNAi to specifically deplete either ROCK I or ROCK II have identified distinct substrates and distinct roles for each protein (Yoneda et al. 2005; Lock et al. 2009)

Known ROCK substrates include: MLC II, MLCP, LIM kinase I and II, the ERM family proteins (ezrin, radixin, moesin), NHE-1 and several intermediate filament proteins, such as desmin, vimentin and glial fibrillary acidic protein, are also phosphorylated by ROCK I/II to regulate intermediate filament structure assembly (Schwartz 2004). MLCP, myosin II, LIM

kinase I and II are all essential for the formation of actin stress fibres (Pellegrin et al. 2007). The ERM proteins act as linkers between actin filaments and the plasma membrane (Fehon et al. 2010). The Na/H+ antiporter NHE-1 promotes the reorganisation of actin filaments and focal adhesion assembly (Schwartz 2004). ROCK I/II can oligomerise and may regulate kinase activity through amino terminal transphosphorylation (Garg et al. 2008).

1.3.8 Role of RhoA and ROCK I/II in keratinocyte terminal differentiation

In the early stages of keratinocyte differentiation Rho signaling is activated and plays a role in the establishment of calcium-dependent cell–cell adhesion, which is important for differentiation (Braga et al. 1997). Rho activity also suppresses the expression of differentiation markers, such as keratins 1 and 10, through its effector citron kinase and for differentiation to occur citron kinase is selectively down-regulated (Grossi et al. 2005). Consistant with this the inhibition of endogenous Rho signaling induces the expression of differentiation markers (Grossi et al. 2005).

The RhoA effectors, ROCK I and ROCK II have also been implicated in regulating the switch between proliferation and terminal differentiation in keratinocytes (McMullan et al. 2003; Lock et al. 2009). ROCK I/II activity increases during suspension induced terminal differentiation and inhibiting ROCK I/II activity with treatment with Y-27632 inhibites terminal differentiation and increases cell proliferation. Expression of a constitutively-active truncated ROCK II construct induces cell cycle arrest and increases the expression of differentiation markers such as involucrin, desmocollin 1 and 2, and desmoplakin (McMullan et al. 2003). Recent data using

siRNA to analyse ROCK I and ROCK II function has revealed opposing roles for ROCK I and ROCK II in keratinocyte differentiation. ROCK I-depleted cells have an increase in keratin 10 and involucrin and a decrease in keratin 5 whereas ROCK II-depleted cells have the opposite profile with decreased keratin 10 and involucrin and increased keratin 5 protein levels. Taken together, these data suggest that loss of ROCK I expression promotes keratinocyte terminal differentiation and that loss of ROCK II expression has the opposite effect, inhibiting keratinocyte terminal differentiation (Lock et al. 2009).

1.3.9 Role of RhoA and ROCK I/II in cell proliferation

RhoA regulates G1-S phase transition with the inhibition of RhoA leading to G1 cell cycle arrest (Olson et al. 1995). RhoA inhibits the expression of the cyclin dependent kinase inhibitor, $p21_{Cip1}$ and promotes the up-regulation of cyclin D1 (Olson et al. 1998; Welsh et al. 2001). RhoA has been proposed to have a dual role in regulating cyclin D1, blocking early G1 expression of cyclin D1 and promoting sustained extracellular signal-regulated kinase (ERK) activation and mid-G1 expression of cyclin D1 (Welsh et al. 2001). The induction of type-D cyclins is the rate limiting step in the G1 to S phase transition and thus their regulation is thought to play a significant role in controlling cell cycle progression through G1 phase (Welsh et al. 2001). However inhibition of ROCK I/II activity with Y-27632 increases cell proliferation and expression of active ROCK II induces cell cycle arrest in keratinocytes (McMullan et al. 2003).

Cytokinesis is the last stage of the cell cycle and it is driven by actomyosin contractility constricting the parent cell into two daughter cells. Cycling between active and inactive forms of Rho is required for cytokinesis to occur and the Rho effectors ROCK I/II and citron are also involved (Madaule et al. 2000).

1.3.10 Role of RhoA and ROCK I in apoptosis

During apoptosis one of the first morphological changes observed is membrane blebbing, which is regulated by myosin light chain phosphoryation and actomyosin contractility (Mills et al. 1998). Once caspase 3 is activated it can in turn activate ROCK I (but not ROCK II) by cleaving the autoinhibitory C-terminus of ROCK I and induce membrane blebbing (Coleman et al. 2001; Sebbagh et al. 2001). In cells treated with an apoptotsis-inducing agent the over-expression of full-length ROCK I has no affect on apoptosis (Ongusaha et al. 2006). However, over-expression of the 130kDa fragment of ROCK I produced by caspase 3 cleavage increases apoptosis by increasing caspase 3 activation (Chang et al. 2006; Ongusaha et al. 2006). Depletion of ROCK I using RNAi or treatment with the ROCK I/II inhibitor Y-27632 protects cells from camptothecin-induced apoptosis (Ongusaha et al. 2006). Increasing evidence suggests that ROCK I/II-mediated focal adhesion and integrin activation are involved in cell survival as ROCK I/II inhibition can initiate events committing the cell to undergo apoptosis (Shi et al. 2007). As well as membrane blebbing ROCK I/II signaling is involved in the fragmentation of apoptotic cells (Shi et al. 2007). The role of ROCK I/II in the initial stages of apoptosis remains less clear with both pro-apoptotic and anti-apoptotic roles being identified (Ongusaha et al. 2006; Shi et al. 2007).

1.4 RhoE

1.4.1 Introduction

The small GTPase RhoE (also known as Rnd3) has been implicated in the regulation of many cellular processes including the organisation of the actin cytoskeleton, proliferation, differentiation and apoptosis (Guasch et al. 1998; Riento et al. 2003; Villalonga et al. 2004; Bektic et al. 2005; Liebig et al. 2009). RhoE is a member of the Rnd family, which consists of Rnd1, Rnd2 and Rnd3/RhoE. Although RhoE is most closely related to the Rho subfamily (RhoA, RhoB and RhoC), novel structural and biochemical properties have been identified (Foster et al. 1996). RhoE lacks GTPase activity, is unaffected by GAPs and has a high affinity for GTP, resulting in a constitutively active form that is not regulated by the conventional GTPase cycle (Foster et al. 1996; Guasch et al. 1998; Nobes et al. 1998) (Figure 8). Instead it is thought that gene regulation, post-translational modification and localisation contribute to RhoE's regulation (Riento et al. 2005). Up-regulation of RhoE expression has been demonstrated in response to a number of different stimuli. These include growth factor stimulation (Tanimura et al. 2002; Riento et al. 2003), B-Raf/MEK activation (Hansen et al. 2000; Klein et al. 2008), p53 induction (Ongusaha et al. 2006), cytotoxic drug treatment (Villalonga et al. 2004; Shurin et al. 2008), and UVB irradiation (Murakami et al. 2001; Boswell et al. 2007). RhoE is a substrate for ROCK I, which phosphorylates RhoE on a number of residues, regulating RhoE activity by increasing protein stability and altering the localisation of RhoE (Riento et al. 2005; Ongusaha et al. 2006). Endogenous RhoE localises both to membrane and cytosolic components (Riento et al. 2003). ROCK I-phosphorylated RhoE is localised in the

cytosol suggesting RhoE membrane association is regulated by ROCK I and PKCα phosphorylation (Riento et al. 2005; Madigan et al. 2009). In addition prenylation plays a key role in localising RhoE to the membrane (Foster et al. 1996). Phosphorylation of RhoE has been shown to correlate with actin stress fibre disruption and inhibition of Ras-induced transformation suggesting phosporylation regulates RhoE activity (Riento et al. 2005).

1.4.2 RhoE and ROCKI

Unlike active RhoA, which induces actin stress fibres and focal adhesions, over-expression of RhoE inhibits the formation of actin stress fibres in a number of different cell types (Guasch et al. 1998; Nobes et al. 1998; Riento et al. 2003). In MDCK cells expressing active RhoA, over-expression of RhoE restores actin stress fibre formation to wildtype suggesting RhoE can inhibit RhoA signaling (Guasch et al. 1998). RhoA induces actin stress fibres through the activation of ROCK I/II (Pellegrin et al. 2007). However, of the known RhoA effectors (ROCK I, mDia1, PRK1 and ROCK II) RhoE only interacts with ROCK I (Riento et al. 2003; Riento et al. 2005). A number of possible mechanisms have been suggested for the inhibition of actin stress fibre formation by RhoE. Firstly RhoE binds to and activates p190RhoGAP, which in turn catalyses the intrinsic GTPase activity of RhoA inhibiting actin stress fibre formation (Wennerberg et al. 2003). A second mechanism for RhoE inhibiting actin stress fibres involves RhoE binding to ROCK I inhibiting ROCK I-dependent phosphorylation of MLCP (Riento et al. 2003). In addition, RhoE and Rnd1 bind to a protein of unknown function called Socius (Katoh et al. 2002). RhoE appears to localise Socius to the membrane resulting in the loss of actin stress

fibres (Katoh et al. 2002).

Interestingly the interaction between RhoE and ROCK I does not occur through the Rho-binding domain of ROCK I, but through RhoE binding to the N-terminal kinase domain of ROCK I (Riento et al. 2005) (Figure 9). However, although RhoE and RhoA bind to different regions of ROCK I they cannot bind simultaneously to ROCK I (Riento et al. 2003). RhoE specifically binds to ROCK I but not ROCK II even though the kinase domains share 92% identity. However, the two regions surrounding the kinase domain, 1-76aa and 338-420aa, which are also important for RhoE binding and ROCK I dimerisation, are not conserved in ROCK II (Riento et al. 2003; Riento et al. 2005; Garg et al. 2008). An interesting feature of the interaction between ROCK I and RhoE is that the region of RhoE which binds to ROCK I is independent of its switch/effector region and involves the opposite surface of RhoE (Komander et al. 2008). This type of binding is uncommon among GTPase complexes (Vetter et al. 2001; Komander et al. 2008). Site-directed mutagenesis to disrupt the ROCK I:RhoE interaction resulted in a loss of RhoE phosphorylation but no increase in actin stress fibres (Komander et al. 2008). However, when mutations in the switch/effector region of RhoE were made no loss of actin stress fibres occur, even though the mutated RhoE was still able to bind ROCK I (Komander et al. 2008). These data suggest RhoE's effect on actin stress fibre formation is not due to antagonising ROCK I (Riento et al. 2003) but by binding to other proteins via its effector region to prevent actin stress fibre formation (Komander et al. 2008).

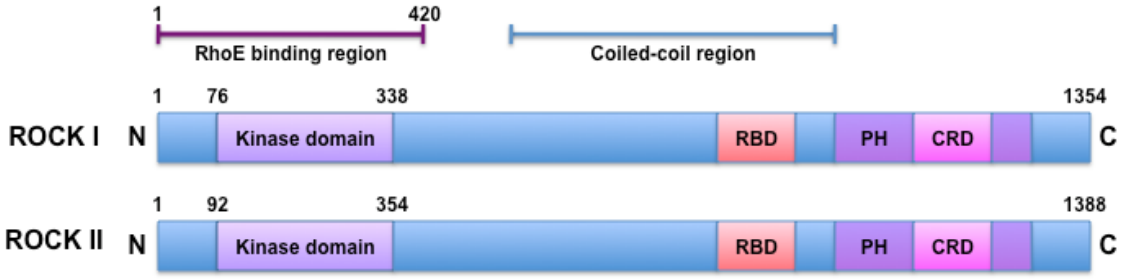

Figure 9 The structure of ROCK I and ROCK II.

Domains present in ROCK I and ROCK II include; an N-terminal kinase domain, a Rho-binding domain (RBD), and a pleckstrin homology (PH) domain with an internal cysteine-rich domain (CRD). Also indicated is the region predicted to form a coiled-coil structure, and the RhoE binding region of ROCK I (numbers indicate amino acids).

1.4.3 Role of RhoE in terminal differentiation of keratinocytes

In a recent study endogenous RhoE expression was reported to be up-regulated during keratinocyte terminal differentiation induced by calcium addition, TPA treatment or E-cadherin clustering (Liebig et al. 2009). Over-expression of RhoE results in increased cell size and localisation of RhoE over-expressing keratinocytes to the stratified layers (Liebig et al. 2009). In RhoE-depleted keratinocytes both stratification and cell size was unaffected but a delay in the up-regulation of the differentiation markers involucrin, keratin 1 and transglutaminase was observed (Liebig et al. 2009). ROCK kinase activity during the induction of keratinocyte differentiation is required for the up-regulation of RhoE expression (Liebig et al. 2009) and this would be consistant with that of ROCK being required for keratinocyte terminal differentiation (McMullan et al. 2003). These results indicate RhoE expression increases the potential of keratinocytes to undergo stratification (Liebig et al. 2009). However, *in vivo*, over-expression of RhoE in the skin of transgenic mice had no effect on epidermal histology (Boswell et al. 2007).

1.4.4 Role of RhoE in cell proliferation

A number of studies have implicated RhoE in the regulation of cell proliferation. However, the data are contradictory. Over-expression of RhoE in fibroblasts and U87 glioblastoma cells induces a G1 phase cell cycle arrest due to a decrease in cyclin D1 levels (Villalonga et al. 2004; Poch et al. 2007). ERK activation, which is important for cyclin D1 expression, was inhibited in U87 glioblastoma cells but not fibroblasts over-expressing RhoE (Villalonga et al. 2004; Poch et al. 2007). Another study in which RhoE was over-expressed in prostate cancer cell lines,

showed a G2/M phase cell cycle arrest due to a decrease in cyclin B and cyclin-dependent kinase 2 protein levels (Bektic et al. 2005). These studies suggest that RhoE over-expression inhibits cell cycle progression, although the mode of action is different in each case. Keratinocytes depleted of RhoE showed increased proliferation and enhanced levels of ERK phosphorylation (Liebig et al. 2009). However, depletion of RhoE in melanoma cells has no effect on proliferation (Klein et al. 2009).

Correlating with its ability to block cell proliferation, RhoE over-expression inhibits both Ras and Raf induced cell transformation (Villalonga et al. 2004). RhoE expression is induced by Raf activation (Hansen et al. 2000) and by mutant B-RAF expression (Klein et al. 2008). RhoE has also been implicated as a regulator of cross-talk between the B-RAF/MEK/ERK and Rho/ROCK/LIM kinase/cofilin pathways with RhoE expression correlating with the progression toward an invasive phenotype in melanoma cell lines (Klein et al. 2008). Consistent with this RhoE depletion decreased migration and invasive outgrowth (Klein et al. 2008). Collectively, these data highlight the importance of RhoE, a mutant B-RAF effector, to invasive melanoma behavior (Klein et al. 2009).

1.4.5 Role of RhoE in apoptosis

RhoE has been implicated in apoptosis by several studies. However, as with RhoE's role in cell proliferation, no firm conclusions can be drawn from the data. One study in prostate cancer cell lines found that RhoE was under-expressed when compared to normal prostate cells (Bektic et

al. 2005). When RhoE was over-expressed in the prostate cancer cell lines apoptosis was induced (Bektic et al. 2005). In a separate study, RhoE was identified as an up-regulated gene in response to NF-κB2/p52 signaling in prostate cancer cell lines. NF-κB2/p52 signaling protects prostate cancer cells from androgen deprivation-induced apoptosis (Nadiminty et al. 2010). The discrepancies in RhoE expression in these two studies may be due to the stage of the prostate cancer cell lines used. The initial stages of prostate cancer are androgen-dependent and progression to a castration-resistant stage occurs after failure to treat with androgen-deprivation therapy. Cell lines used in the Nadiminty et al. paper were early stage prostate cancer cell lines where NF-κB2/p52 signaling is critical. In the Bektic et al. paper androgen-insensitive prostate cancer cells such as PC-3 and DU145 were used. In these cells RhoE over-expression induced cell cycle arrest and apoptosis (Bektic et al. 2005; Nadiminty et al. 2010).

Another study demonstrated that the over-expression of RhoE in U87 glioblastoma cells and other tumour cell lines induced apoptosis (Poch et al. 2007). The over-expression of RhoE in the Bektic et al. (2005) and Poch et al. (2007) studies increased the basal/spontaneous rate of apoptosis (Bektic et al. 2005; Poch et al. 2007). However, apoptosis was not induced when RhoE was over-expressed in fibroblasts (Villalonga et al. 2004).

Some studies have implicated RhoE in a protective role against apoptosis. In transgenic mice RhoE over-expression in the skin increased protection from UVB irradiation (Boswell et al. 2007). In addition over-expression of RhoE in a gastric adenocarinoma cell line enhanced resistance to multiple antitumour drugs by suppressing the expression of Bax at a post-

transcriptional level (Li et al. 2009).

RhoE expression is induced by a number of apoptosis-inducing stimuli, including camptothectin (Ongusaha et al. 2006), cisplatin (Villalonga et al. 2004) and UVB irradiation (Murakami et al. 2001; Boswell et al. 2007). RhoE is also a transcriptional target of the tumour suppressor protein p53, which promotes apoptosis, and induces RhoE transcription in response to DNA damage (Jeffers et al. 2003; Ongusaha et al. 2006). Two studies, which used siRNA to inhibit RhoE induction following apoptotic stimuli, increased the levels of apoptosis (Ongusaha et al. 2006; Boswell et al. 2007). Interestingly siRNA, whilst preventing the induction of RhoE, had no affect on basal expression of RhoE (Ongusaha et al. 2006; Boswell et al. 2007). Ongusaha et al. (2006) reported that RhoE inhibits ROCK I activity during genotoxic stress (Ongusaha et al. 2006), however, Boswell et al. (2007) reported that RhoE induction was independent of p53 and ROCK I activity (Boswell et al. 2007). In a separate study depletion of RhoE in melanoma cells had no affect on apoptosis (Klein et al. 2009).

1.5 Project aims

Normal homeostasis of the epidermis requires a balance between proliferation and differentiation (Fuchs 2007). Apoptosis is also important for the removal of damaged or infected cells from the epidermis (Lippens et al. 2009). The RhoA effectors ROCK I and ROCK II have been implicated in being key regulators of the switch between proliferation to differentiation in keratinocytes, with distinct functions for each kinase (McMullan et al. 2003; Lock et al. 2009).

ROCK I has also been implicated in having a role in apoptosis (Coleman et al. 2001). Here I investigated the function of the ROCK I binding protein RhoE (Riento et al. 2003), using keratinocyte cell lines in which RhoE expression was both stably and transiently depleted, using RNAi. These cell lines were used to investigate the role of RhoE in keratinocyte proliferation, differentiation and apoptosis.

CHAPTER 2 MATERIALS AND METHODS

2.1 Materials

2.1.1 General laboratory reagents

Y-27632 (Cat. No. Y0503) and cisplatin (cis-Diammineplatinum(II) dichloride) (Cat. No. P4394) was purchased from Sigma (Poole, UK). Recombinant human TRAIL (TNF-related apoptosis-inducing ligand) (Cat. No. 375-TEC) was purchased from R&D systems (Minneapolis, MN). All other chemicals were purchased from Sigma (Poole, UK) unless otherwise stated in text.

2.1.2 Cell culture materials

Cell culture reagents were purchased from Gibco (Paisley, UK) or Sigma (Poole, UK).

2.1.3 Constructs

Over expression vectors containing wild type (wt) mouse RhoE and empty vector (EV) control, pCMV5RhoEFlag and pCMV5EVFlag, were a gift from A. Ridley (King's College London) (Riento et al. 2003), pCAG-myc-p160 (WT) wild type ROCK I and pCAG-myc-KD kinase dead ROCK I were a gift from S. Narumirya (Kyoto university Japan) (Ishizaki et al. 1997). For creating a RhoE-depleted and control cell line shRNAmir human pGIPZRhoE (Cat. No.

RHS4430-98513300) and pGIPZNSC (non-silencing control) (Cat. No. RHS4346) were purchased from Open Biosystems. For the sequence of shRNAmir human pGIPZRhoE mapped to the human RhoE sequence See Appendix 1.

See Table 1

2.1.4 Oligos

Two custom siRNA oligos against RhoE were purchased from Dharmacon, in transient RhoE depletions oligo A was predominantly used (oligo B was used for verification (stated in text)). For the sequences of RhoE oligos mapped to the human RhoE sequence See Appendix 1. On target siRNA oligos against ROCKI_6 (Cat. No. J-003536-06-0005), ROCKI_7 (Cat. No. J-003536-07-0020), Plakglobin (Diepgen et al.) (Cat. No. J-011708-10), Desmoplakin (Dsp) (Cat. No. J-019800-07) and PRMT5 (Cat. No. J-015817-06) were purchased from Dhramacon. ROCKII_5 (Cat. No. SI02223746), ROCKII_6 (Cat. No. SI02223753) and non-silencing control (Ctrl) (Cat. No. SI03650325) were purchased from Quiagen.

See Table 1

2.1.5 Antibodies

See Table 2

Table 1 Target sequences of shRNA constructs and siRNA oligos used in this study

Oligo / Construct name	Target sequence
shRNAmir pGIPZRhoE	UCUGAUAAUCUGUUGGUUUAU
RhoE_A	UAGUAGAGCUCUCCAAUCA
RhoE_B	CAAACAGAUUGGAGCAGCU
Ctrl	AAUUCUCCGAACGUGUCACGU
ROCKI_6	CUACAAGUGUUGCUAGUUU
ROCKI_7	UAGCAAUCGUAGAUACUUA
ROCKII_5	AAGCUACAUAUGGAGCUUAAA
ROCKII_6	AUGCACUUGUAUAAAGCCAUA
Dsp	GGGAUGAGUUCACCAAACA
PG	AGACAUACACCUACGACUC

Table 2 Antibodies used in this study

Antibody	Antibody Name	Supplier	Cat. No.	Species	Dilution for WB	Dilution for IF
Actin	Alexa-594-conjugated Phalloidin	Molecular Probes	A-12381	N/A	N/A	1:400
Bax	-	Cell Signaling Tec.	2774	Rabbit	1:250	1:100
BrdU	-	Boheringer Mannheim	1170376	Mouse	N/A	1:10
Caspase 9	-	Cell Signaling Tec.	9502	Rabbit	1:1000	N/A
Cyclin D1	DCS6	Cell Signaling Tec.	2926	Mouse	1:1000	N/A
Desmocollin 1	U100	Progen	65192	Mouse	1:500	N/A
Desmocollin 2	-	Progen	610120	Rabbit	1:500	1:100
Desmocollin 3	U114	Progen	65193	Mouse	1:100	1:100
Desmoglein 1 and 3	32-2B	David Garrod	-	Mouse	1:25	N/A
Desmoglein 2	33-3D	David Garrod	-	Mouse	1:25	N/A
Desmoglein 2	10G11	Progen	61059	Mouse	1:10	N/A
Desmoglein 3	G194	Progen	651112	Mouse	1:10	N/A
Desmoplakin	11-5F	David Garrod	-	Mouse	1:25	1:50
Desmoplakin	H300	Santa Cruz	sc-33555	Rabbit	1:500	N/A
Ecadherin	HECD1	Vania Braga	-	Mouse	1:500	1:100
ERK		Santa Cruz	sc-94	Rabbit	1:2000	N/A
Phospho-ERK	pERK	Santa Cruz	sc-7383	Mouse	1:1000	N/A
Involucrin	SY-5	ICRF	-	Mouse	1:1000	N/A
Keratin 1	KRT1	Abnova	H000038	Mouse	1:1000	N/A

			48-M01			
Keratin 5	EP1601Y	Abcam	ab52635	Rabbit	1:20,000	1:100
Keratin 14	-	Thermo-scientific	MS-115-PO	Mouse	1:500	N/A
Pan-keratin	-	Invirogen	18-0059	Rabbit	N/A	1:100
Mitotracker	CMXRos	Molecular Probes	M-7512	N/A	N/A	
Myc-tag	9B11	Cell Signaling	2276	Mouse	1:1000	1:100
Plakoglobin	VB3	Vania Braga	-	Rabbit	1:500	1:100
Plakoglobin		BD Trans. Labs.	610253	Mouse	1:1000	-
Periplakin	AE11	Santa Cruz	sc-80605	Mouse	1:100	N/A
RhoE		Upstate	05-723	Mouse	1:500	1:100
ROCKI	H-85	Santa Cruz	sc-5560	Rabbit	1:250	N/A
ROCKII	-	BD Trans. Labs.	610623	Mouse	1:500	N/A
α-Tubulin	DM1A	Sigma	T6199	Mouse	1:10,000	1:100
Hoechst 33342	-	Invitrogen	H21492	N/A	N/A	1:400
Anti-mouse FTIC	-	Jackson Labs	115-095-146	Goat	N/A	1:100
Anti-mouse Texas Red	-	Jackson Labs	115-075-146	Goat	N/A	1:100
Anti-rabbit FTIC	-	Jackson Labs	111-095-144	Goat	N/A	1:100
Anti-rabbit Texas Red	-	Jackson Labs	111-075-144	Goat	N/A	1:100
IRDye Anti-mouse 800cw	-	Odyssey	926-32210	Goat	1:15,000	N/A
IRDye Anti-mouse 680cw	-	Odyssey	926-32220	Goat	1:15,000	N/A
IRDye Anti-rabbit 800cw	-	Odyssey	926-32211	Goat	1:15,000	N/A
IRDye Anti-rabbit 680cw	-	Odyssey	926-32221	Goat	1:15,000	N/A
Anti-mouse HRP	-	Amersham Life Sci.	NA931	Sheep	1:5000	N/A
Anti-rabbit HRP	-	Pierce	31460	Goat	1:5000	N/A

2.2 Methods

2.2.1 Culture of HaCaT cells

HaCaT cells are a human keratinocyte cell line (Boukamp et al. 1988) non-transfected HaCaT cells and those expressing pGIPZRhoE or pGIPZNSC were cultured in Dulbecco's modified Eagles medium (DMEM) (Gibco Cat. No. 41966) supplemented with 50 units/ml penicillin, 50 ng/ml streptomycin (Gibco) and 5% (v/v) foetal calf serum (FBS) (Sigma). SCC12F cells are a primary keratinocyte cell line and were cultured in defined keratinocyte-SFM serum-free medium (Gibco Cat. No. 10744-019). Cells were maintained at 37°C in a humidified 5% CO_2 atmosphere. Cells were passaged when they reached approximately 80% confluence and low passage stocks were stored in liquid nitrogen in 90% (v/v) (FBS) and 10% (v/v) dimethylsulphoxide.

2.2.2 Generation of a RhoE-depleted keratinocyte cell line

To generate a stable RhoE-depleted (shRhoE) and control (shNSC) keratinocyte cell line HaCaT cells were transfected with the shRNA constructs pGIPZ-RhoE and pGIPZ-NSC (Section 2.1.3) by nucleofection, based on electroporation, using the Amaxa Nucleofector kit V (Amaxa Biosystems Inc.). For each transfection $3x10^6$ cells/ml and 3 ug of DNA were used and transfections were performed according to the manufacturer's instructions. shRhoE and shNSC stable cell lines were maintained in a selection of 0.5 μg/ml puromycin (Sigma Cat. No. P7522) diluted in complete growth medium.

2.2.3 Reconstitution of RhoE

To rescue the levels of RhoE in the RhoE-depleted keratinocyte cell line (Section 2.2.2) RhoE was reconstituted using wild type mouse RhoE. shRhoE HaCaT cells were transiently transfected with pCVM5FlagRhoE (wild type mouse) or pCMV5EVFlag while shNSC HaCaT cells were transfected with pCMV5EVFlag by lipid transfection using Lipofectamine 2000 (Invitrogen Cat. No. 11668-019). Forward transfections were performed in p6 well plates when cells were 60% confluent with each transfection using a total of 500 μl of Opti-mem (Invitrogen Cat. No. 11058-021) as diluting medium, 6 μl of Lipofectamine 2000, 3 μg of DNA and a total plating volume of 2.5 ml made up by normal growth medium minus penicillin and streptomycin. Transfections were performed according to the manufacturer's instructions.

2.2.4 Reverse transfection of siRNA in HaCaT cells

A number of siRNA oligos were used in this study to deplete keratinocytes of proteins of interest (Section 2.1.4). HaCaT cells were transiently transfected with either a specific oligo or combination of oligos by lipid transfection using Lipofectamine RNAiMAX (Invitrogen Cat. No. 13778). Reverse transfections were performed in p6 well plates with each transfection using 500 μl of Opti-mem (Invitrogen Cat. No. 11058-021) as diluting medium, 5 μl of Lipofectamine RNAiMAX and a total plating volume of 2.5 ml made up by normal growth medium minus penicillin and streptomycin. Concentrations of oligo used in each transfection were as follows siRhoE A and B oligos were 9 pmol while siPG and siDsp oligos were 18 pmol, the siCtrl oligo

concentration corresponded to the highest concentration in each experiment. Transfections were performed according to the manufacturers instructions. For each experiment three reverse transfections were performed resulting in a 144-168 hrs knockdown. Treatments were performed during 24 hrs prior to lysis/fixation unless stated (Figure 10).

2.2.5 Y-27632 Treatments

Y-27632 is a pharmacological inhibitor of ROCKI/II and PRK-2 when used at 5 μM (Darenfed et al. 2007). All experiments in this study used Y-27632 at 5 μM. Y-27632 was diluted in normal growth medium and incubated with cells for varying time points (specified in text). The half-life of Y-27632 is 12-16 hrs so when a time point extending this time occurred fresh medium containing Y-27632 would be applied every 12 hrs.

2.2.6 Induction of apoptosis

In this study cisplatin was used to induce the intrinsic apoptosis pathway while TRAIL was used to induce the extrinsic apoptosis pathway (Walczak et al. 2000). Both stably and transiently RhoE-depleted cells were seeded at least 24hrs before being treated with either cisplatin or TRAIL (concentrations specified in text). Cells were treated with cisplatin or TRAIL, diluted in normal growth medium, for 24 hrs in normal growth conditions before being fixed (Section 2.2.17) and lysed (Section 2.2.9). Cisplatin is made up in N, N-dimethylformamide (DMF) and

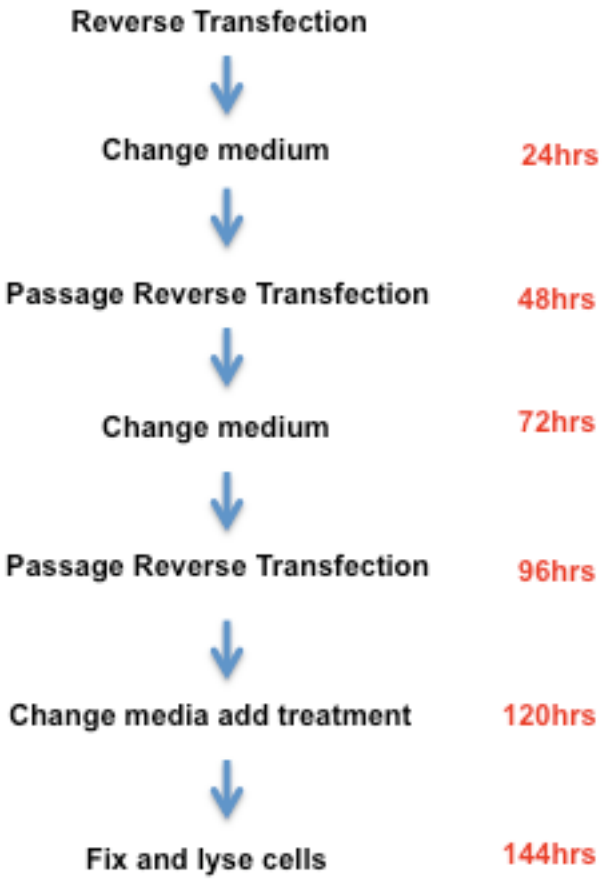

Figure 10 Flow chart and time course of siRNA oligo transfection protocol.

For each experiment in which siRNA was used to depleted RhoE levels HaCaT cells were transfected three times resulting in a 144-168 hours knock-down. Reverse transfections were performed enabling cell passage during the experiment. Treatments were performed 24 hours prior to lysis and/or fixation unless otherwise noted.

control experiments were performed using equal volumes of DMF added to the normal growth media.

2.2.7 Rescue treatments

shRhoE and shNSC cells (non-transfected (NT)) were seeded, onto cover slips, along side shRhoE with reconstituted RhoE (RhoE wt), shRhoE and shNSC cells transfected with empty vector (EV) (Section 2.2.3) in p6 well plates. 48 hrs after initial seeding and 24 hrs after transfection the cells were treated with cisplatin 60μM or TRAIL 25 ng/ml, diluted in normal growth medium, for 24 hrs before cover slips were fixed and cells were lysed.

2.2.8 Calcium depletion

Prior to calcium depletion shRhoE and shNSC cells were seeded on cover slips 48hrs and siRhoE and siNSC cells were transfected for 96-144 hrs. Calcium depletion was carried out as described previously (Leigh et al. 1994). Normal growth medium was removed and cells were washed twice in versene (0.02% (v/v) EDTA pH8.2 in PBS) before low calcium medium (DMEM-high glucose low calcium (Gibco Cat. No. 21068-028), 0.1 mM $CaCl_2$, 5% calcium depleted FSB) was added back to cells and incubated for 24 hrs. Calcium depletion commenced for 24 hrs before phase microscopy, fixation and lysis or cisplatin addition (concentration specified in text) for 24 hrs or re-addition of calcium for 24 hrs before phase microscopy, fixation and lysis.

2.2.9 Cell lysis

Adherent HaCaT cells were lysed by scrape lysis. Media was removed from adherent cells followed by 2 washes in PBS (phosphate-buffered saline). Cells were incubated with a small amount of 3xLaemelli buffer (125 mM tris-HCL pH6.8, 3% (w/v) SDS (sodium dodecyl sulfate), 1.735% (w/v) DTT (dithiothreitol), 15% glycerol, 0.1% (v/v) bromophenol blue) for 4min before being scrape lysed and boiled at 100°C for 5 min followed by 15 sec sonication. Lysates were centrifuged at 14000 rpm for 1min and stored at -20°C. In experiments were cisplatin or TRAIL treatment was used the media taken off the adherent cells was retained and centrifuged at 14000 rpm for 1 min to pellet cells that had detached from the adherent layer. These pellets were added back to the cell lysate prior to boiling.

2.2.10 SDS-PAGE

SDS-PAGE was carried out as described previously (Laemmli 1970). 10-30 µl of cell lysate (Section 2.2.9) equalling ~15-25 µg of protein were loaded onto 7.5, 10 or 12.5% SDS-PAGE gel (4% stack) depending on the molecular weight of the protein being analysed. Gels were run in tris-glycine running buffer (0.2 M glycine, 0.02 M tris, 0.1 M SDS) at 250V/25mA until the dye front reached the bottom. Molecular weight markers from New England Biolabs (Cat. No. P7708G) were run on each gel. Proteins were transferred onto a PVDF-FL membrane (Section 2.2.11).

2.2.11 Immunoblotting

Western blotting was carried out as described previously (Towbin et al. 1979). Following SDS-PAGE (Section 2.2.10) proteins were transferred electrophoretically onto PVDF-FL membrane (Millpore Cat. No. IPFL00010) in tris-glycine transfer buffer (0.2 M glycine, 0.02 M tris, 20% (v/v) methanol) for 75 min at 100V/400mA at 4°C. None specific binding was blocked by incubating the membrane with 5% (w/v) milk in tris-buffered saline containing tween 20 (TBST) (20 mM tris pH7.5, 150 mM NaCl, 0.05% (v/v) tween 20) for 1hr at room temperature or dried in methanol if using Odyssey developing method. The membrane was then incubated with the primary antibody, diluted in 5% (w/v) milk in TBST, overnight at 4°C and washed 4 times for 10 min in TBST. Following this the membrane was then incubated with either horseradish-peroxidase (HRP)-conjugated secondary diluted in TBST or Odyssey secondary antibody diluted in 5% (w/v) milk in TBST for 1hr at room temperature and washed again (Odyssey secondary and second set of washes to be kept in the dark). Bound antibody was detected using a chemiluminescent kit (Pierce) and the signal was visualised by exposure to medical X-ray film (Scientific Lab Suppliers Ltd), which was processed using an X-ograph. Odyssey antibody detection was visualised by scanning the membrane onto an Odyssey infrared imaging system (LI-COR Biosciences).

2.2.12 Purification of plasmid DNA

Constructs used in this study (Section 2.1.5) were purified using a maxiprep kit (Quiagen Cat. No. 12262). 5 ml of LB (Lurai Bertani broth) containing the appropriate selection was inoculated with *E. coil* transformed with the plasmid of interest and grown for 8 hrs at 37°C. This culture was then diluted into 500 ml of LB, again containing appropriate selection, and grown overnight at 37°C. Bacteria were harvested by centrifugation at 2350g for 15 min at 4°C and maxipreps were performed according to the manufacturers instructions. Purified DNA was stored at -20°C.

2.2.13 Quantification of DNA concentration

The concentration of DNA purified by maxipreps (Section 2.2.12) was determined by measuring the absorbance of the DNA solution diluted in dH_2O at 260 nm. One optical density unit represents 50 μg/ml DNA.

2.2.14 Preparation of competent cells

To prepare *E. coli* for transformation with plasmid DNA, competent cells were prepared using calcium chloride method (Cohen et al. 1972). 5 ml of LB was inoculated with *E. coli* and grown overnight at 37°C. 500 μl of this culture was used to inoculate 50 ml of LB and this was grown on until an absorbance of 0.5 at 650 nm was measured. Cell were harvested by centrifugation at 2350g for 5min and then resuspended in 10 ml of cold 100 mM calcium chloride. Cells were left

on ice for 20 min then harvested as before. Cells were resuspended in 5 ml of freeze thaw buffer (100 mM calcium chloride, 15% (v/v) glycerol) then aliquoted and stored at -70°C.

2.2.15 Transformation of competent *E. coli*

Competent cells were prepared as describe in (Section 2.2.14) and 50 ng of plasmid DNA was added to 100 µl of these cells. Cells were left on ice for 40 min then heat shocked at 42°C for 2 min before being returned to ice for 5 min. 1 ml of LB without selection was added and cells were grown at 37°C for 90 min. Bacteria were pelleted by centrifugation at 14000 rpm for 2 min and resuspended in 100 µl of LB. Cells were plated onto agar plates containing the appropriate selection and grown overnight at 37°C.

2.2.16 Preparation of glass cover slips for cell culture

13 mm glass cover slips where treated for 5 min in concentrated nitric acid at room temperature. The nitric acid was then diluted into water and the cover slips were washed in water for 30 min. Following washing cover slips were washed in methanol that was left to evaporate at room temperature overnight. Cover slips were autoclaved before use.

2.2.17 Immunofluorescence staining

Indirect immunofluorescence staining was performed as described previously (Akhtar et al. 2000). Cells grown on pre-prepared glass cover slips (Section 2.2.16) were washed three times in PBS and fixed in PBS containing 4% (w/v) paraformaldehyde for 10min at room temperature. Following fixation and washing in PBS cells were permeabilised with 0.2% (v/v) Triton X100 in PBS for 5 min. Cells were washed three times in PBS and the cover slips were incubated with primary antibody, diluted in PBS, for 1 hr at room temperature. Cover slips were wash three times in PBS and incubated with the appropriate FITC or Texas Red-conjugated secondary antibodies, diluted in PBS, for 1 hr at room temperature. Cover slips were wash extensively and mounted using Mowiol and immunostained cells were visualised using a Leica DMRB microscope equipped with a Hamamatsu ORCA camera. The images were captured and processed using OpenLab software (Improvision, UK).

2.2.18 Immunofluorescence staining for Flag

For Flag immunofluorescence staining blocks were used in the immunofluorescence staining protocol (Section 2.2.17) to reduce non-specific antibody binding. After fixation cells were incubated with 50 mM NH_4Cl diluted in PBS for 10 min at room temperature before being permeabilised. Following permeabilsation cells were washed three times in PBS and cover slips were incubated in 20% (v/v) Heat-inactivated normal goat serum (HINGS) (Jackson Labs Cat. No. 005-000-121) in PBS for 30 min. Anti-Flag primary antibody was diluted in 20% (v/v) HINGS for 1 hr, the rest of the protocol is as described above.

2.2.19 MitoTracker incorporation and Bax immunofluorescence staining

MitoTracker Red CMTRos was used to stain mitochondria. MitoTracker passively diffuses through the plasma membrane and accumulates in the mitochondria (Molecular Probes Cat. No. M-7512). MitoTracker was added to normal growth medium at 250 nM for 45 min prior to fixation. Fixation and permeabilised were carried out as described above in (Section 2.2.17). To reduce non-specific antibody binding cover slips were incubated in 4% (w/v) bovine serum albumin (BSA) in PBS for 10 min, the rest of the protocol is as described in (Section 2.2.17).

2.2.20 Bax translocation

HaCaT cells transfected with the shRNA constructs were seeded on cover slips 2 days prior to treatment of 25 ng of TRAIL for 6 hrs. Cover slips were incubated with MitoTracker (Section 2.2.19) and then fixed and stained with anti-Bax and Hoechst 33342. Both the total number of nuclei and cells with punctate Bax staining were counted, with approximately 200 cells counted per condition. The condition of the cell and nuclei was also taken into account and if the cell had become rounded or the nuclei fragmented these cells were not included in the counts contributing to punctate Bax staining.

2.2.21 BrdU labelling of cells

Entry into S-phase was analysed by incorporation of BrdU (Bromodeoxyuridine) using a BrdU labelling and detection kit from Boehringer Mannheim (Cat. No. 1296732). Cells were grown on glass cover slips and were incubated with BrdU, diluted in normal growth medium, for 1 hr in normal cell culture conditions. Cells were fixed in 70% ethanol in 50 mM glycine pH2 for 20min at -20°C and BrdU incorporation was accessed by indirect immunofluorescence using monoclonal antibody against BrdU. Hoechst 33342 was used to label all nuclei. Cells were visualised on a Leica DMRB microscope equipped with a Hamamatsu ORCA camera, images were taken of both BrdU positive cells and Hoechst then combined for each field of view, with four fields of view for each condition. The number of BrdU positive cells was expressed as a percentage of the total number of cells and statistical analysis was carried out using Microsoft Excel.

2.2.22 Preparation of Mowiol

Mowiol, for use in mounting cover slips for immunofluorescence, was prepared by rotating 2.4g Mowiol-4-88 (Calbiochem) in dH_2O with 0.42 mM glycerol for 2hrs at room temperature then adding Tris-HCL pH8.5 to give a final concentration of 0.13 M. This was allowed to dissolve at 50°C and then centrifuged at 5000g for 5 min at 4°C. A small O-phenyldiamine crystal was allowed to dissolve at 4°C in the dark and the Mowiol was aliquoted and stored at -70°C.

2.2.23 Microinjection

HaCaT cells were seeded on to cover slips 24 hrs prior to microinjection with 50 μg/ml pCAG-myc-p160 (WT) (pCAGmycROCK I (wt)) wild type ROCK I or pCAG-myc-KD (pCAGmycROCK I (KD)) kinase dead ROCK I a gift from S. Narumirya (Kyoto university Japan) (Ishizaki et al. 1997). 6 hrs post injection, cover slips were fixed and stained with anti-Myc, to visualise transfected cells, and Phalloidin, to visualise F-actin (Section 2.2.17). A Leica DMIRB microscope equipped with an Eppendorf micromanipulator 5171 (Eppendorf), using Femtotip II needles (Eppendorf).

2.2.24 Confocal microscopy

Cells were visualised on a Nikon A1R confocal microscope (Nikon) using a 60x oil lens. For each 3D image a Z series of 1μm stacks were taken by manually setting the gain and laser intensity as well as the bottom and top Z stack and allowing NIS-Elements to take both the Z series and channel series. The bottom and top Z series stacks were set at the cover slips surface and the last layer to contain evidence of cells. Gains and laser intensities were set and remained constant throughout. The images were captured and processed using NIS-Elements (Nikon).

2.2.25 Phase contrast microscopy

Cells were seeded onto plastic 48hrs prior to live phase microscopy. Cells were visualised on an Axiovert 135TV microscope (Zeiss) equipped with a QCam FAST1394 camera (Qimaging)

using a 32x phase one air lens. The images were captured and processed using QCapture (Qimaging).

2.2.26 Transmission electron microscopy (TEM)

TEM was used to visualise desmosomes in transiently RhoE-depleted cells. siRhoE and siCtrl HaCaT cells were plated onto plastic cover slips 48hrs prior to fixation. For fixation remove media and incubate with 2.5% (v/v) Gluteraldehyde in 0.1 M Cacodylate buffer solution pH 7.4, with 3% (w/v) sucrose and 0.1% (w/v) CaCl diluted in dH_2O, for 1 hr at 4°C. Cover slips were embedded and sections were taken orthogonally to the plane of the cover slip and stained using negative staining (Work carried out by Theresa Morris, Centre for Electron Microscopy, University of Birmingham). Images were taken on a Jeol 1200EX microscope.

2.2.27 Colony forming efficiency assay

The efficiency of keratinocytes to form colonies was analysis by experiments previously described elsewhere (Jones et al. 1993). Cells were seeded at a density of $1x10^3$ cells/ml into a 75 cm^2 tissue culture flask and cultured for 12 days in normal growth medium. After 12 days cells were washed twice in PBS and fixed in PBS containing 4% (w/v) paraformaldehyde for 10 min at room temperature and stained with 1% (w/v) rhodanile blue (Rheinwald et al. 1975). The number of colonies were counted and average colony area was determined using Photoshop. Each flask was scanned into Photoshop and saved under the same dimensions and the numbers

of colonies were counted. The differences in colony size were accessed by grouping numbers of colonies in the same size range into different classes. The approximate sizes of the colonies were established using Photoshop brush paint tools with pixel sizes 17, 27, 35, 45, 65 and over were classed as >65 (Figure 11). Colony size was expressed as a percentage of the total number of colonies and statistical analysis was carried out using Microsoft Excel.

2.2.28 Cell cycle analysis by flow cytometry

To analyse the cell cycle of transiently RhoE-depleted keratinocytes siRhoE and siCtrl HaCaT cells were seeded into cell culture flasks 24 hrs prior to analysis. Cells were removed from the flask by washing twice with versene (0.02% (v/v) EDTA pH8.2 in PBS) and treating with trypsin for 5 min at 37°C, cells were remove by strong agitation, normal growth medium was added and cells were pelleted at 1100 rpm. 1 x 10^5 cells were resuspended in 1:1 PBS and cell cycle buffer (10 μg/ml propidium iodide, 0.1 mM (w/v) sodium chloride, 1% (v/v) Triton X100) and incubated for 4 hrs at 4°C prior to analysis by flow cytometry. Staining was analysed using a FACS Calibur (Becton Dickinson) and the data evaluated using Cell Quest Pro software (Becton Dickinson).

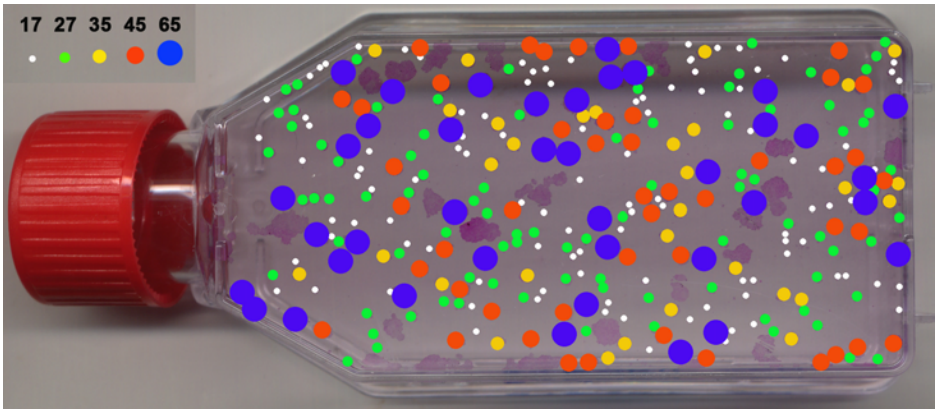

Figure 11 Colony forming efficiency assay counting and sizing method.

Flasks were scanned into Photoshop and saved under the same dimensions, the total number of colonies were counted. The differences in colony size were accessed by grouping numbers of colonies in the same size range into different classes. The approximate sizes of the colonies were established using Photoshop brush paint tools with pixel sizes 17, 27, 35, 45, 65 and over were classed as >65.

CHAPTER 3 RHOE AND THE CELL CYCLE

3.1 Introduction

Regulation of proliferation is essential for the normal homeostasis of the epidermis. Proliferation in the epidermis is confined to the basal layer and is carried out by stem cell and transit amplifying keratinocytes (Watt 1988; Gniadecki 1998; Fuchs 2007). Keratinocyte proliferation is mainly regulated in G1 phase of the cell cycle, progression through which is regulated by Rho GTPase activity (Olson et al. 1995; Gniadecki 1998). Progression from G1-S phase requires Cylin D1 expression but it is not essential as cyclin D1 knockout mice are viable (Robles et al. 1998). Rho inhibits the expression of the cyclin dependent kinase inhibitor, $p21_{Cip1}$ and promotes the up-regulation of cyclin D1 (Olson et al. 1998; Welsh et al. 2001). RhoE has been implicated in the regulation of cell proliferation by a number of studies, however a clear role for RhoE in proliferation has yet to be established (Villalonga et al. 2004; Bektic et al. 2005; Poch et al. 2007; Klein et al. 2008).

In this chapter the role of RhoE in keratinocyte proliferation is investigated by knocking down the level of endogenous RhoE in keratinocyte cells, using both stable and transient depletion. An increase in ROCK I-induced actin stress fibres was observed in RhoE-depleted keratinocytes along with altered colony morphology. Transient depletion of RhoE resulted in decreased levels of active ERK and cyclin D1 and a G1 phase cell cycle arrest. This was shown to be independent of ROCK I activity.

3.2 Results

3.2.1 RhoE depletion induces stellate actin stress fibres

To analyse RhoE function a stable RhoE-depleted keratinocyte cell line was generated using shRNAmir constructs against human RhoE (pGIPZ-RhoE) and a non-silencing control (pGIPZ-NSC). HaCaT cells were transfected with the shRNA constructs using the Amaxa nucleofection system and were maintained in medium containing puromycin ensuring selection of transfected cells. Whole cell lysates were prepared and analysed using immunoblotting to assess the level of RhoE protein depletion (Figure 12). On SDS-PAGE RhoE runs as a doublet at ~ 29 kDa (Riento et al. 2005). Significant depletion of RhoE was observed and the depletion was stable during continued culture (Figure 12).

It is well documented that RhoE over-expression inhibits actin stress fibre formation (Guasch et al. 1998; Nobes et al. 1998; Riento et al. 2003) by inhibiting both RhoA and ROCK I (Riento et al. 2003; Wennerberg et al. 2003). The effect of RhoE depletion on the actin cytoskeleton was analysed in the stably RhoE-depleted cell line. Stable RhoE-depleted (shRhoE) and control (shNSC) cells were seeded on to cover slips, fixed and stained with Phalloidin to visualise filamentous actin (F-actin). In controls cells actin stress fibres were located to the periphery of the cell whereas in RhoE-depleted keratinocytes stellate actin stress fibres, which radiate from the cell body, were induced (Figure 13A). The stellate actin stress fibres in RhoE-depleted cells

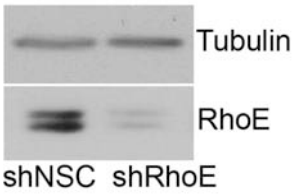

Figure 12 Knock-down of RhoE expression using shRNA.

To generate RhoE-depleted (shRhoE) and control (shNSC) keratinocyte cell lines, HaCaT cells were stably transfected with the shRNA constructs pGIPZ-RhoE and pGIPZ-NSC. Whole cell lysates were prepared and analysed by immunoblotting using antibodies against RhoE and tubulin (loading control). Data presented are representative immunoblots of three separate experiments. A decrease in the expression of RhoE was detected in shRhoE cells when compared to shNSC cells.

are similar to those produced when ROCK I is over-expressed (Figure 13B). When RhoE-depleted and control cells were treated for 12 hours with the ROCK inhibitor, Y-27632, actin stress fibres were lost (Figure 14). These data indicate an increase in endogenous ROCK I activity in RhoE-depleted cells.

RhoE was also transiently depleted in keratinocytes using siRNA oligos as a means to verify data generated by the stable RhoE-depleted cell line. Two siRNA oligos targeting different sequences of RhoE were used. For most experiments oligo A was used and results were verified using oligo B (stated in text). HaCaT cells were transiently transfected with siRNA oligos against RhoE and with a non-silencing control oligo using Lipofectamine RNAi max (Invitrogen). 144 hours after RhoE-depletion whole cell lysates were prepared from HaCaT cells transfected with either siRNA oligo A or oligo B and analysed using immunoblotting to assess the level of RhoE protein depletion. In RhoE-depleted HaCaT cells the expression of RhoE was significant depleted by oligo A and oligo B (Figure 15). The actin cytoskeleton of transiently RhoE-depleted cells treated with Y-27632 and stained with Phalloidin was analysed by immunofluorescent microscopy. The same stellate actin stress fibres seen in shRhoE cells were observed in siRhoE cells. These actin structures were lost following Y-27632 treatment (Figure 16).

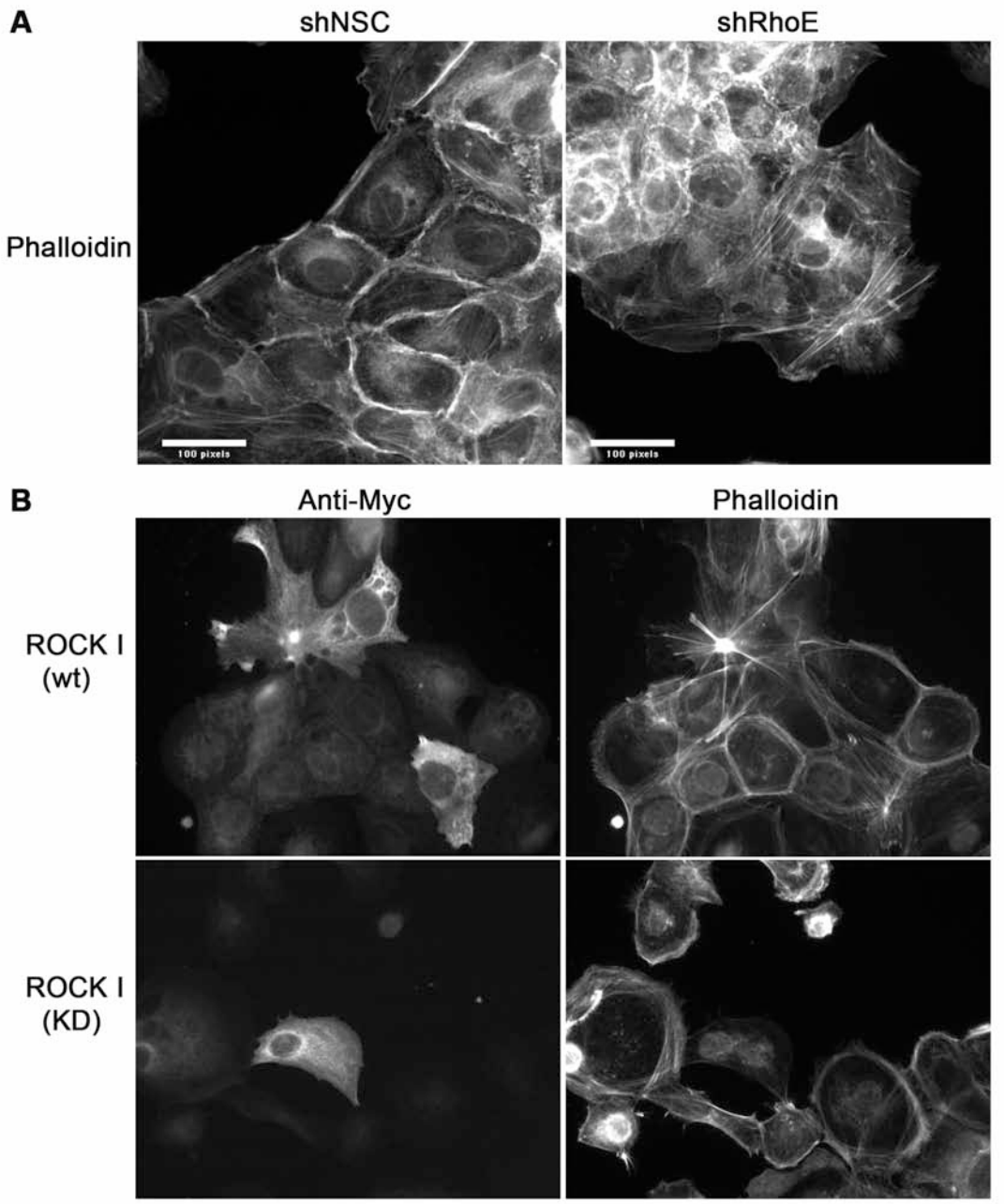
A
shNSC
shRhoE
Phalloidin
100 pixels
100 pixels
B
Anti-Myc
Phalloidin
ROCK I
(wt)
ROCK I
(KD)

Figure 13 Depletion of RhoE induces the formation of stellate actin stress fibres.

A HaCaT cells stably depleted of RhoE (shRhoE) and control cells (shNSC), were seeded onto cover slips 24 hours prior to fixation. Cover slips were then stained with Phalloidin to visualise F-actin. shRhoE cells have stellate actin stress fibres whereas in shNSC cells actin stress fibres are located to the periphery of the cell. **B** HaCaT cells were seeded onto cover slips 24 hours prior to microinjection with pCAGmycROCK I (wt) wild type or pCAGmycROCK I (KD) kinase dead. 6 hours post injection, cover slips were fixed and stained with anti-Myc to visualise transfected cells and Phalloidin. ROCK I (wt) transfected cells have increased stellate actin stress fibres compared to non-transfected cells and ROCK I (KD) cells. Data presented are representative immunofluorescence images of three separate experiments, taken using a 40x lens with the gain and exposure time remaining constant (scale bar 30 μm).

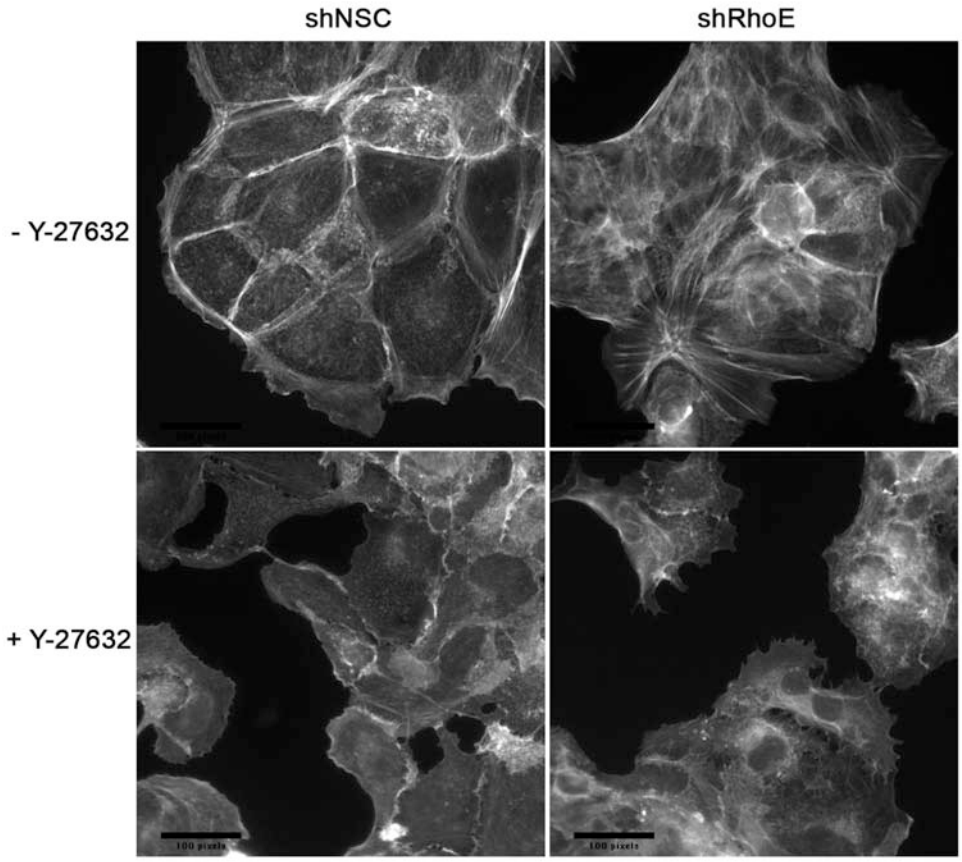

Figure 14 Keratinocytes depleted of RhoE lose actin stress fibres following treatment with Y-27632.

HaCaT cells stably depleted of RhoE (shRhoE) and control cells (shNSC), were seeded onto cover slips for 24 hours before being treated with 5 μM of Y-27632 for 12 hours prior to fixation. Cover slips were then stained with Phalloidin to visualise F-actin and images were taken using a 40x lens. Data presented are representative immunofluroescent images of three separate experiments, with the gain and exposure time remaining constant (scale bar 30 μm). In the absence of Y-27632 shRhoE cells have stellate actin stress fibres whereas in shNSC cells actin stress fibres are located to the periphery of the cell. In the presence of Y-27632 both shNSC and shRhoE cells lose actin stress fibres.

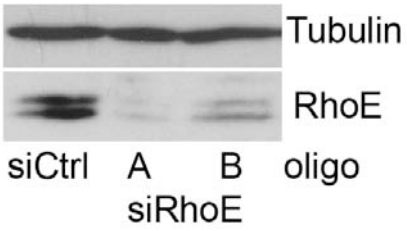

Figure 15 Transient knock-down of RhoE expression using siRNA.

To deplete RhoE expression in keratinocytes, HaCaT cells were transiently transfected three times with siRNA oligos against RhoE (siRhoE) (oligo A or B) and non-silencing control (siCtrl) for a total of 144 hours prior to lysis. Whole cell lysates were prepared and analysed by immunoblotting using antibodies against RhoE and tubulin (loading control). Data presented are representative immunoblots of three separate experiments.

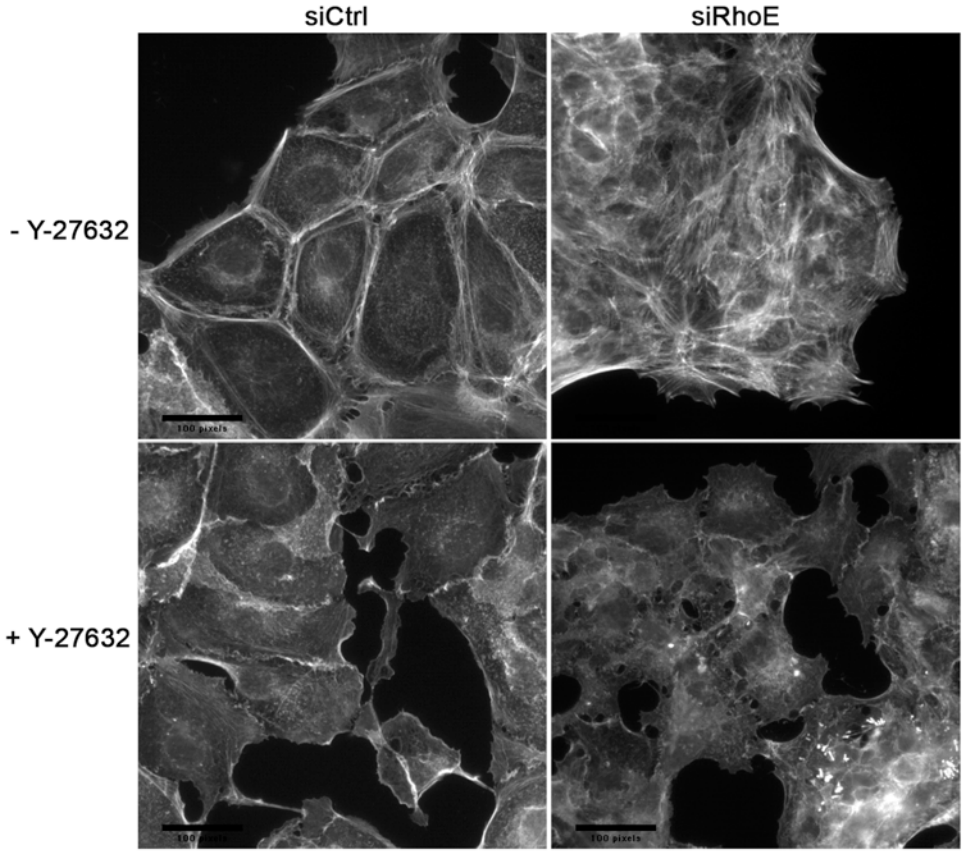

Figure 16 Keratinocytes transiently depleted of RhoE lose actin stress fibres following treatment with Y-27632.

HaCaT cells transiently transfected with siRNA to depleted RhoE (siRhoE) and control cells (siCtrl) were seeded onto cover slips for 24 hours before being treated with 5 μM of Y-27632 for 12 hours prior to fixation. Cover slips were then stained with Phalloidin to visualise F-actin and images were taken using a 40x lens. Data presented are representative immunofluroescent images of three separate experiments, with the gain and exposure time remaining constant (scale bar 30 μm). In the absence of Y-27632 siRhoE cells have stellate actin stress fibres whereas in siCtrl cells actin stress fibres are located to the periphery of the cell. In the presence of Y-27632 both siCtrl and siRhoE cells lose actin stress fibres.

3.2.2 Keratinocytes depleted of RhoE form small colonies

Colony forming efficiency assays were performed to assess the ability of RhoE-depleted cells to form colonies. Stably RhoE-depleted (shRhoE) and control (shNSC) HaCaT cells were seeded at $1x10^3$ cells/ml into cell culture flask and incubated for 12 days prior to fixation and rhodanile blue staining to visualise keratinocyte colonies. A significant decrease in colony size was observed in colonies formed by RhoE-depleted cells (Figure 17A). Statistical analysis confirmed that RhoE-depleted cells form a significantly larger percentage of small colonies (<17 pixels) and fewer large colonies (>45 pixels) compared to controls cells (Figure 17B). The mean total number of colonies formed by both RhoE-depleted and control cells showed no significant difference (Figure 17C). These data indicate that RhoE-depleted cells have the ability to adhere and proliferate to form colonies but expansion of the colony is inhibited.

3.2.3 Transiently RhoE-depleted but not stably RhoE-depleted keratinocytes undergo cell cycle arrest

BrdU incorporation and flow cytometry were used to analyse the cell cycle in RhoE-depleted cells. BrdU is a nucleoside analogue and is incorporated into DNA during S-phase, this can be used to assess the percentage of cells going through S-phase at a fixed time point. shRhoE and control shNSC HaCaT cells were seeded on to cover slips for 24 hours before incubating with BrdU for one hour. After fixation cells were stained with an antibody against BrdU and the nuclei stain Hoechst 33342. Both BrdU positive and the total number of cells were counted and the percentage of cells with BrdU incorporation was analysed. Representative

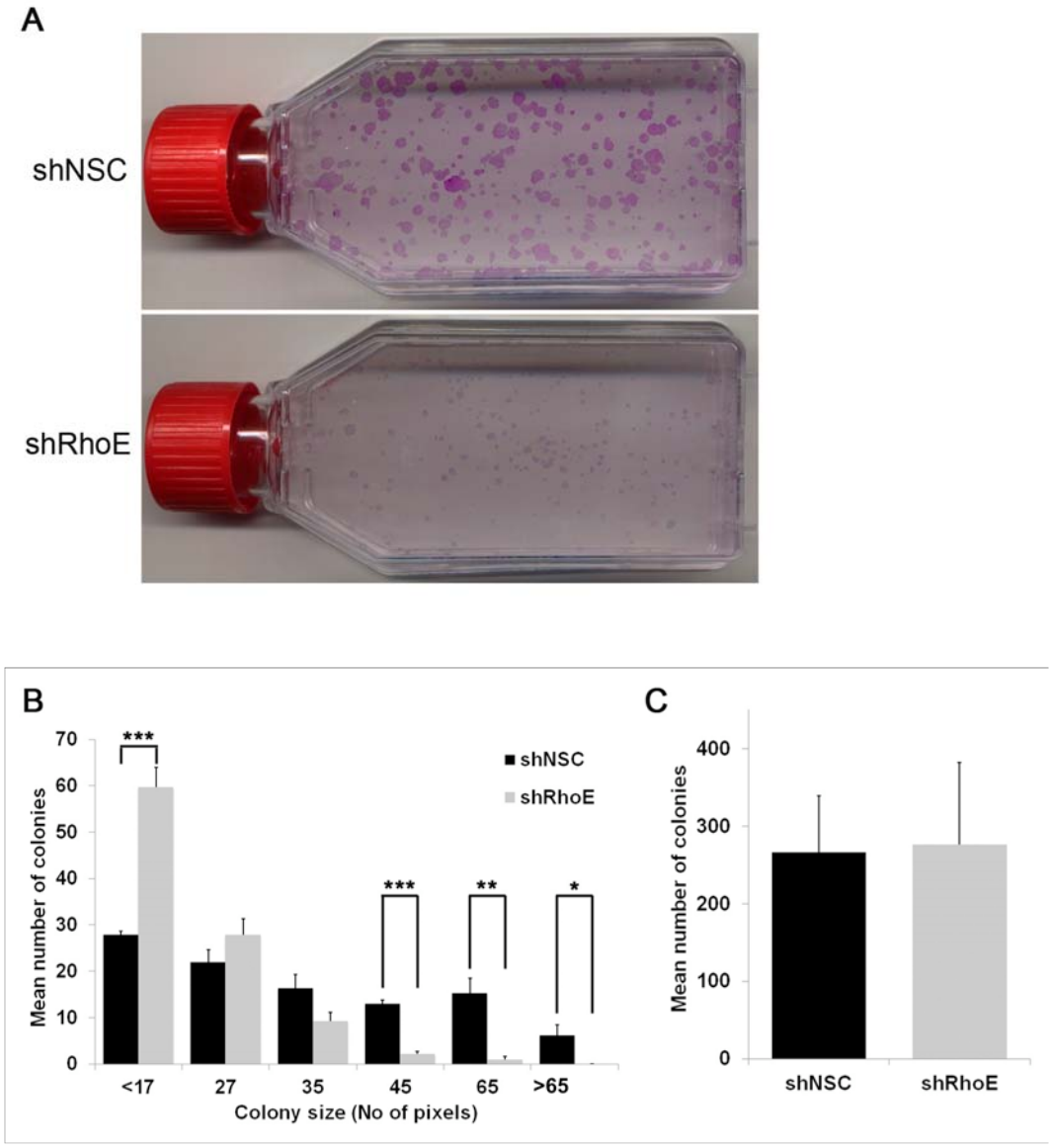
A
shNSC
shRhoE
B
Mean number of colonies
70
60
50
40
30
20
10
0
***
***
**
*
shNSC
shRhoE
<17
27
35
45
65
>65
Colony size (No of pixels)
C
Mean number of colonies
400
300
200
100
0
shNSC
shRhoE

Figure 17 Keratinocytes stably depleted of RhoE exhibited a decrease in colony size.

HaCaT cells stably depleted of RhoE (shRhoE) and control (shNSC) cells, were seeded at $1x10^3$ cell/ml into cell culture flask and incubated for 12 days prior to fixation and rhodanile blue staining to visualise colonies. **A** Scans of flask containing rhodanile blue stained colonies of shNSC and shRhoE cells. **B** Colony size was analysed as described in section 2.2.27 (Figure 11). The mean colony size of shRhoE colonies is significantly smaller than shNSC colonies. **C** The mean total number of colonies shows no significant difference between shNSC and shRhoE cells. Data presented are representative images and the mean, standard error and t-test of three separate experiments (* $P<0.05$, ** $P<0.01$ and *** $P<0.001$). **B** and **C** data generated from three separate experiments. In each experiment three flasks were counted per condition with approximately 300 colonies per flask.

immunofluorescent images of BrdU incorporation in both shRhoE and shCtrl cells show similar levels of incorporation (Figure 18A). This was confirmed by statistical analysis, which revealed no significant difference between shRhoE and shNSC cells in the percentage of BrdU incorporation (Figure 18B).

BrdU incorporation was also analysed in transiently RhoE-depleted keratinocytes. These data revealed a significant decrease in BrdU incorporation in siRhoE cells, with ~35% of siCtrl cells incorporation BrdU compared to ~10% in siRhoE cells (Figure 19). These data were confirmed using a separate siRNA oligo (oligo B) (Figure 20). As an alternative method for analysing cell proliferation, the cell cycle profile of siRhoE and siCtrl cells was analysed by flow cytometery using propidium iodide staining. Transient RhoE-depletion resulted in a significant accumulation of cells in G1 phase (~80% compared to siCtrl ~60%) and a reduction of cells in G2/M phase (~5% compared to siCtrl ~10%) and a significant reduction of cells in S phase (~10% compared to siCtrl ~30%) (Figure 21B). These data indicate transient RhoE depletion induces G1 phase cell cycle arrest.

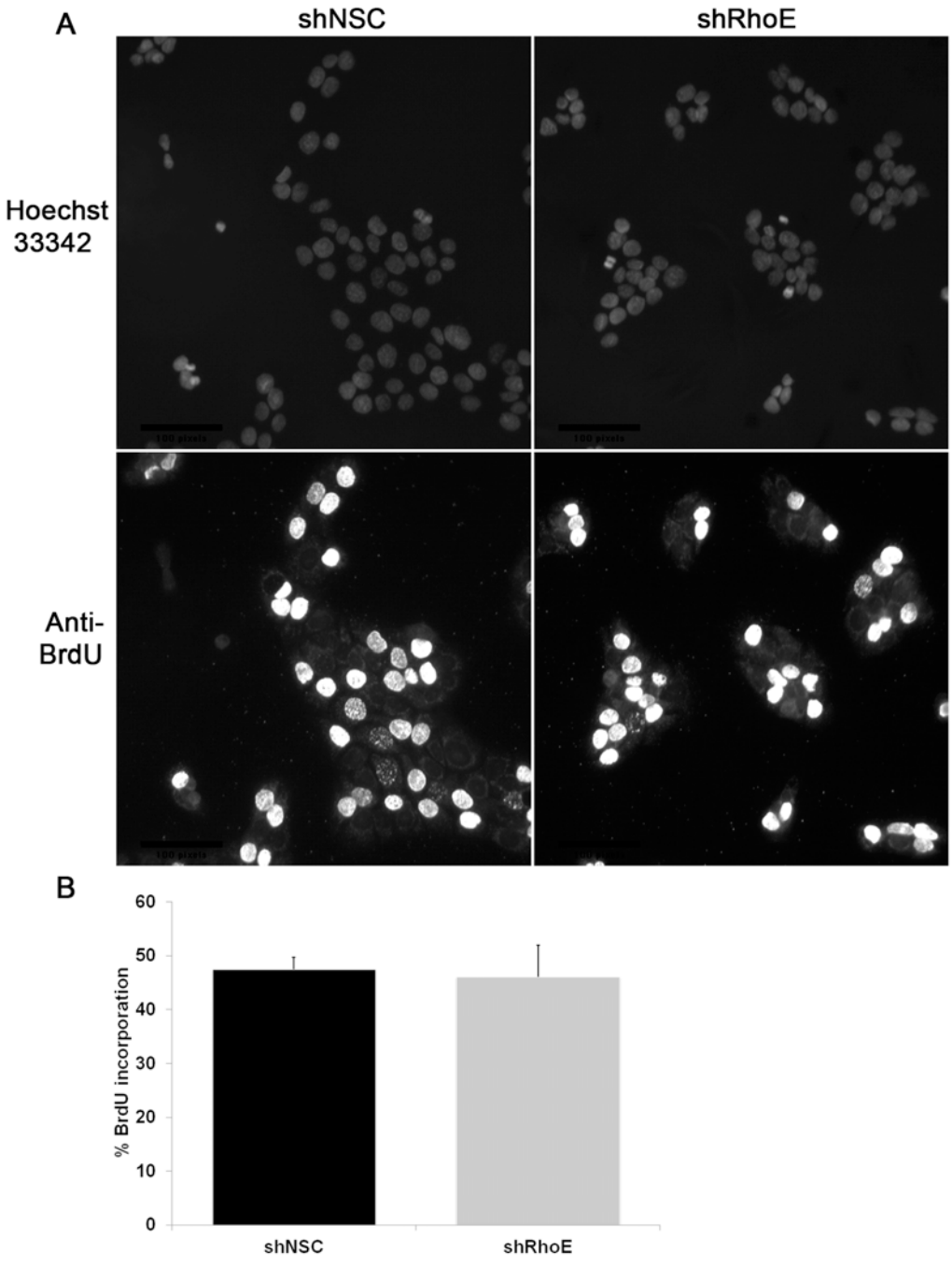
A
shNSC
shRhoE
Hoechst 33342
Anti-BrdU
B
% BrdU incorporation
60
50
40
30
20
10
0
shNSC
shRhoE

Figure 18 Stable depletion of RhoE expression in keratinocytes had no effect cell cycle progression.

HaCaT cells stably depleted of RhoE (shRhoE) and control cells (shNSC) were seeded onto cover slips for 24 hours before incubating with BrdU for one hour prior to fixation. Cover slips were then stained with Hoechst 33342, to visualise the nuclei, and anti-BrdU. Both the total number of nuclei and BrdU positive cells were counted, with approximately 400 cells counted per condition. **A** Representative immunofluorescence images of shRhoE and shNSC cells stained with Hoechst 33342 and anti-BrdU (scale bar 60 μm). **B** The percentage of cells with BrdU incorporation was analysed and the data presented are the mean, standard error and t-test of three separate experiments.

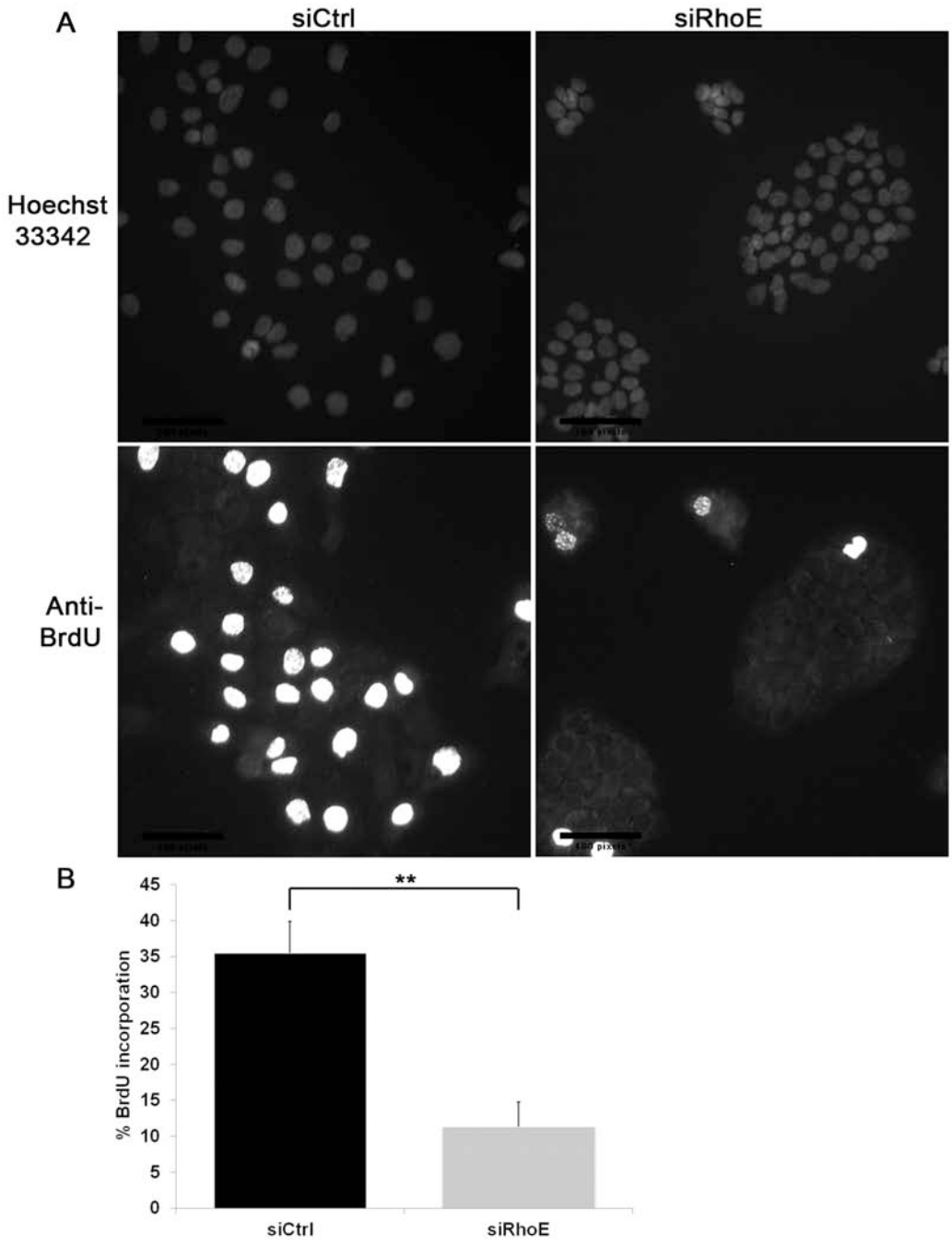
A
siCtrl
siRhoE
Hoechst 33342
Anti-BrdU
B
**
% BrdU incorporation
45
40
35
30
25
20
15
10
5
0
siCtrl
siRhoE

Figure 19 Transient depletion of RhoE expression in keratinocytes inhibited cell cycle progression.

HaCaT cells transiently transfected with siRNA oligo A to deplete RhoE (siRhoE) and control cells (siCtrl) were seeded onto cover slips for 24 hours before incubating with BrdU for one hour prior to fixation. Cover slips were then stained with Hoechst 33342, to visualise the nuclei, and anti-BrdU. Both the total number of nuclei and BrdU positive cells were counted, with approximately 400 cells counted per condition. **A** Representative immunofluroescent images of siRhoE and siCtrl cells stained with Hoechst 33342 and anti-BrdU (scale bar 60 μm). **B** The percentage of cells with BrdU incorporation was analysed and the data presented are the mean, standard error and t-test of three separate experiments (** $P<0.01$).

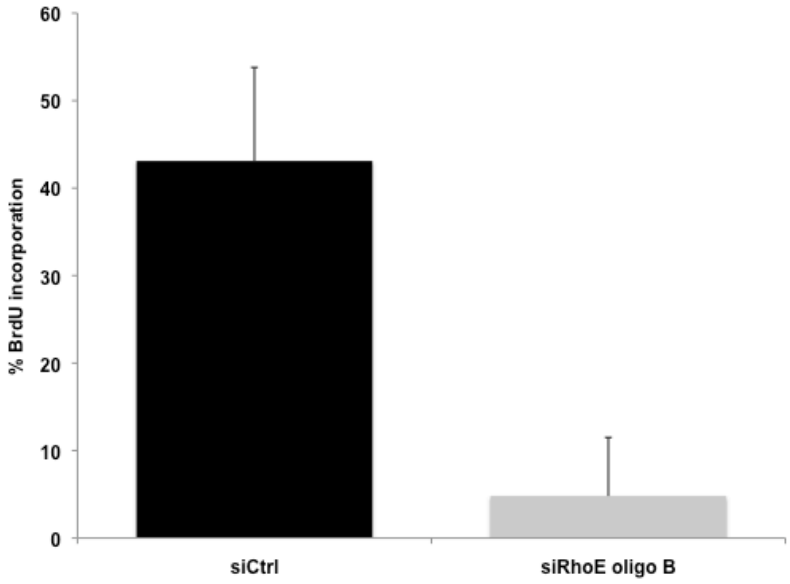

Figure 20 Transient depletion of RhoE expression in keratinocytes inhibited cell cycle progression.

HaCaT cells transiently transfected with siRNA oligo B to depleted RhoE (siRhoE oligo B) and control cells (siCtrl) were seeded onto cover slips for 24 hours before incubating with BrdU for one hour prior to fixation. Cover slips were then stained with Hoechst 33342, to visualise the nuclei, and anti-BrdU. Both the total number of nuclei and BrdU positive cells were counted, with approximately 400 cells counted per condition. The percentage of cells with BrdU incorporation was analysed and the data presented are the mean and standard deviation from one experiment.

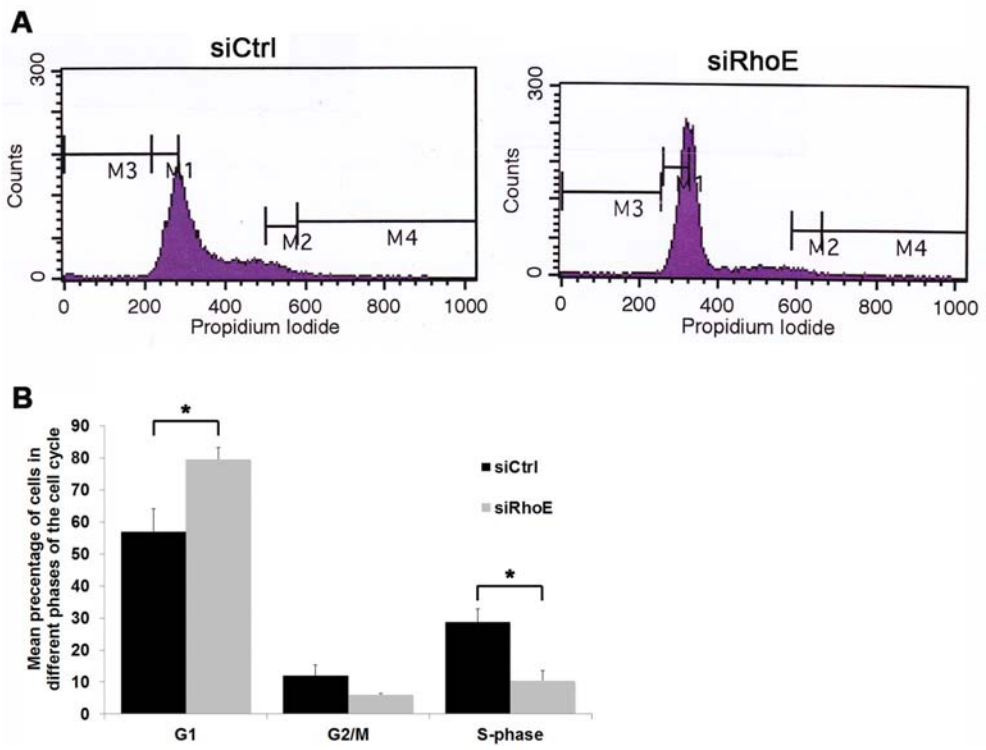

Figure 21 Keratinocytes transiently depleted of RhoE arrest in G1 phase.

The cell cycle profile of transiently RhoE-depleted (siRhoE) (oligo A) and control (siCtrl) keratinocytes was analysed using propidium iodide staining and flow cytometry. **A** Representative images of siCtrl and siRhoE cell cycle profiles. **B** The mean percentage of cells in each phase of the cell cycle. Data presented are the mean, standard error and t-test of three separate experiments (* $P<0.05$).

3.2.4 pERK and cyclin D1 expression is decreased in keratinocytes transiently depleted of RhoE

In mid-G1 phase growth factors and adhesion to the basement membrane stimulates the mitogen-activated protein kinase signaling pathways resulting in the phosphorylation and activation of ERK (Lansbury et al.), which induces cyclin D1 expression (Welsh et al. 2001; Diehl 2002; Assoian et al. 2008). Cyclin D1 expression enables cells to undergo G1-S phase transition (Klein et al. 2008). Both pERK and cyclin D1 protein levels in transiently RhoE-depleted keratinocytes were analysed by immunoblotting. A decrease in both pERK and cyclin D1 protein levels was observed in siRhoE cells (Figure 22).

3.2.5 Cell cycle arrest induced by transient depletion of RhoE was not rescued by ROCK I/II inhibition

Data generated from the analysis of the actin cytoskeleton in RhoE-depleted cells (Section 3.2.1) suggested an increase in endogenous ROCK activity in RhoE-depleted cells. I investigated whether the inhibition of ROCK activity would rescue the cell cycle arrest observed in transiently RhoE-depleted cells. siRhoE and control siCtrl cells were incubated with Y-27632 for 12 hours before a BrdU assay was performed. No appreciable effect on the percentage of BrdU incorporation was observed in the presence of Y-27632 treatment (Figure 23). These data indicate that increased ROCK I activity in RhoE-depleted cells is not responsible for cell cycle arrest.

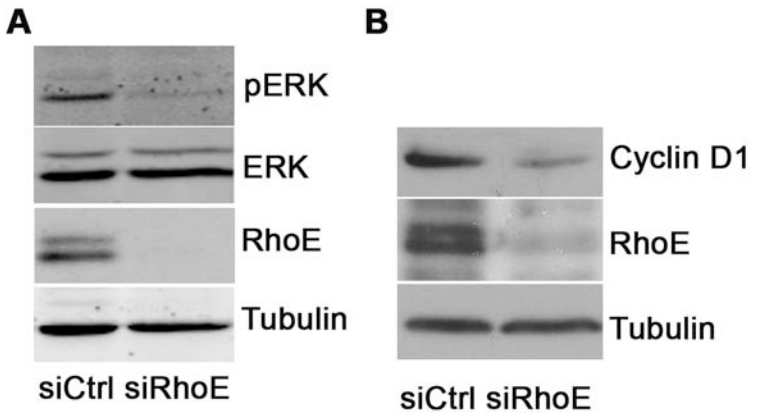

Figure 22 Phosphorylated ERK and cyclin D1 expression is decreased in keratinocytes depleted of RhoE.

HaCaT cells transiently depleted of RhoE (siRhoE) (oligo A) and control (siCtrl) cells were incubated in normal growth conditions prior to lysis. Immunoblotting was used to detect the protein levels of ERK, pERK, cyclin D1, RhoE and tubulin (loading control). Data presented are representative immunoblots of three separate experiments. **A** ERK and pERK levels in siRhoE cells. **B** Cyclin D1 expression in siRhoE cells.

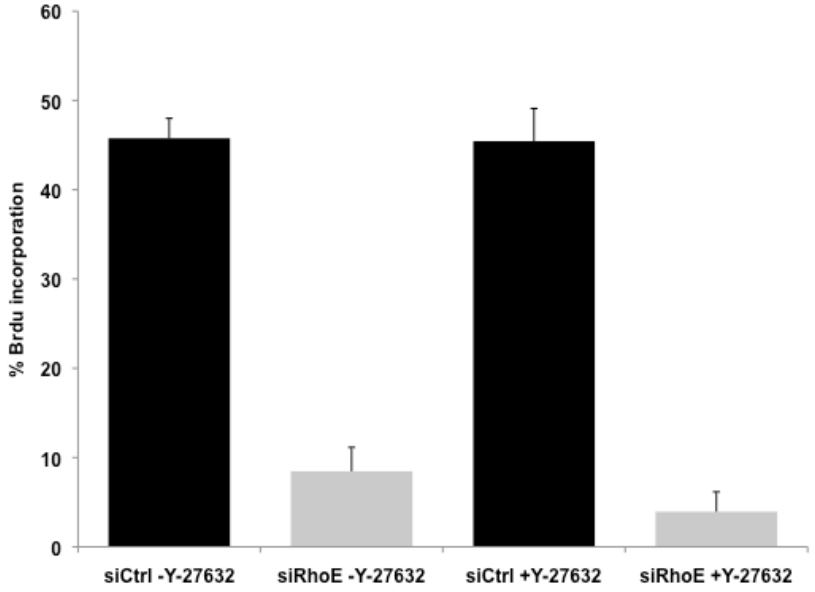

Figure 23 Cell cycle arrest induced by transient depletion of RhoE was not rescued by ROCK I/II inhibition.

HaCaT cells transiently depleted of RhoE (siRhoE) and control (siCtrl) cells were seeded onto cover slips for 24 hours before incubating with Y-27632 for 12 hours and BrdU for one hour prior to fixation. Cover slips were then stained with Hoechst 33342, to visualise the nuclei, and anti-BrdU. Both the total number of nuclei and BrdU positive cells were counted, with approximately 400 cells counted per condition. The percentage of cells with BrdU incorporation was analysed and the data presented are the mean, standard error and t-tests of three separate experiments.

3.3 Discussion

A number of studies have shown that RhoE over-expression inhibits actin stress fibre formation (Guasch et al. 1998; Nobes et al. 1998; Riento et al. 2003) through the inhibition of both RhoA and ROCK I (Riento et al. 2003; Wennerberg et al. 2003). In experiments where RhoE protein levels have been depleted the data are less clear. Transient depletion of RhoE levels in melanoma cells induces the formation of actin stress fibres that run in parallel bundles across the cell body, due to increased endogenous ROCK I activity (Klein et al. 2008). Ongusaha et al. (2006) and Boswell et al. (2007) transiently inhibited DNA damage regulated induction of RhoE expression, using siRNA. In both studies no increase in actin stress fibres was observed in RhoE "depleted" (induction of RhoE inhibited) cells (Ongusaha et al. 2006; Boswell et al. 2007). However, in both studies the basal level of RhoE was unchanged (Ongusaha et al. 2006; Boswell et al. 2007). The data generated in this study show that both stable and transient depletion of RhoE basal levels induced the formation of stellate actin stress fibres, which bore a close resemblance to the stress fibres produced when wild type ROCK I was over-expressed (Figure 13). The induction of actin stress fibres induced in both siRhoE and shRhoE keratinocytes was prevented when the cells were treated with the ROCK inhibitor Y-27632. RhoE is known to inhibit ROCK I (Riento et al. 2003). This, taken together with my data, suggests increased endogenous ROCK activity in RhoE-depleted keratinocytes.

Keratinocytes stably depleted of RhoE formed smaller colonies in comparison to control cells. Possible causes for decreased colony size include: cell cycle arrest, induced apoptosis or

terminal differentiation. Other aspects of colony morphology and the role RhoE plays in producing this phenotype are discussed in detail in chapter 4 whereas this chapter focuses on cell proliferation. Analysis of colony forming efficiency assays revealed no significant difference in the number of colonies produced (Figure 17) and BrdU incorporation (Figure 18) was not altered in the stably RhoE-depleted cells ruling out proliferation defects decreasing colony size. Changes in cell cycle progression were observed in cells transiently depleted of RhoE (Figure 19). The differences observed in the data from stable and transient RhoE-depletion are most likely explained by the selection process when creating a stable cell line which favours proliferative cells. In contrast, the transiently transfected cell lines are not subjected to the same selective pressure.

Previous studies have shown that RhoE over-expression induces G1 phase cell cycle arrest due to a decrease in the level of cyclin D1, which is required for the G1-S phase transition (Villalonga et al. 2004; Poch et al. 2007). Cyclin D1 expression requires ERK activation, which was reported to be decreased in cells over-expressing RhoE and responsible for loss of cyclin D1 expression (Poch et al. 2007). However, Villalonga et al. (2004) show that cyclin D1 expression was decreased in RhoE over-expressing cells but no alteration in ERK activation was observed (Villalonga et al. 2004). RhoE over-expression has also been shown to increase the levels of ERK activation (Guasch et al. 2007). My analysis of active ERK and cyclin D1 expression in keratinocytes transiently depleted of RhoE revealed both were decreased (Figure 22). Studies have reported that RhoE over-expression inhibits cell cycle progression (Villalonga et al. 2004:Bektic, 2005 #495; Poch et al. 2007), however I report that RhoE depletion also

inhibits cell cycle progression. One possible explanation for the apparent differences observed in these studies maybe that RhoE expression is regulated during G1 phase and cell type specificity.

A recent study in keratinocytes depleted of RhoE showed increased proliferation and enhanced levels of ERK phosphorylation (Liebig et al. 2009). My data contradicts these findings. However, both the BrdU assays and analysis of ERK activation in Liebig et al. (2009) were performed in cells 24 hours after they were induced to terminally differentiate (Liebig et al. 2009). My analysis was performed on cells cultured in normal growth conditions and this may explain the differences observed.

RhoE is a known antagonist of RhoA/ROCK I signaling (Wennerberg et al. 2003; Riento et al. 2005). Inhibition of ROCK I/II activity with Y-27632 has been shown to increase cell proliferation in keratinocytes (McMullan et al. 2003). My data shows that both stable and transient depletion of RhoE expression increased endogenous ROCK I activity (Section 3.2.1). I investigated whether the inhibition of cell cycle progression was due to the increased ROCK I activity observed in the transiently RhoE-depleted cells. Following ROCK inhibition, using Y-27632 treatment, no effect on cell proliferation was observed (Figure 23). These data indicate that the cell cycle arrest observed in the transiently RhoE-depleted cells is not dependent on ROCK activity.

In summary, both stable and transient depletion of RhoE in keratinocytes induces the formation of ROCK-dependent stellate actin stress fibres. A decrease in colony size was observed in stably RhoE-depleted keratinocytes, however cell cycle progression was unaffected in these cells. Whereas transient depletion of RhoE in keratinocytes resulted in decreased expression of active ERK and cyclin D1, and a G1 phase cell cycle arrest, which was shown to be independent of ROCK I activity.

CHAPTER 4 RHOE AND REGULATION OF DESMOSOMES

4.1 Introduction

The architecture of the epidermis is important for the protection of the underlying dermis. The epidermis is a stratified epithelium made up predominantly of layers of differentiating keratinocytes (Fuchs 1990). Cells in the basal layer adhere to the underlying basement membrane, via hemidesomosomes and focal adhesions and have the ability to undergo proliferation (Gniadecki 1998). Adhesion to the basement membrane maintains the ability of normal basal keratinocytes to proliferate and loss of adhesion has been shown to induce differentiation (Green 1977; Muller et al. 2008). Cell-cell adhesion in the epidermis, through desmosomes and adherens junctions, is important for stratification, maintaining epidermal architecture, mechanical strength and signal transduction (Braga 2002).

Keratinocyte terminal differentiation involves cell cycle arrest followed by a number of biochemical and morphological changes, such as changes in protein expression, altered adhesion and an increase in cell size (Watt 1983; Fuchs 1990). Alterations in adhesion include loss of attachment to the basement membrane and an increase in cell-cell adhesion coupled with alterations in the expression of different desmosomal proteins (Garrod et al. 2008). The process of terminal differentiation transforms a metabolically active proliferating keratinocyte into a dead enucleated stratum corneum cell (squame), which is comprised of a cornified sack containing keratin macrofibrils (Fuchs 1990; Fuchs 2007).

Keratinocytes over-expressing RhoE have been shown to increase in cell size and locate to stratified layers in cultures induced to terminally differentiate, implicating RhoE in playing a role in terminal differentiation (Liebig et al. 2009). This chapter addresses the altered morphology of RhoE-depleted keratinocytes (first reported in Section 3.2.2) by investigating the role of RhoE in keratinocyte differentiation. For the investigation both stable and transient depletion of endogenous RhoE levels in keratinocyte cells was used. Differentiation was not induced by RhoE depletion. However, there was an up-regulation of desomosomal proteins and increased numbers of desmosomes, which is responsible for the altered colony morphology observed in RhoE-depleted cells.

4.2 Results

4.2.1 RhoE depletion alters keratinocyte colony morphology

Previous data (Section 3.2.2) generated from colony forming efficiency assays of stably RhoE-depleted cells revealed a significant decrease in colony size when compared to control colonies. The reduction in colony size was not due to alterations in proliferation or apoptosis, as proliferation was unaffected in the stably RhoE-depleted cells (Section 3.2.3) and apoptosis was not induced (Section 5.2.3). Colony morphology was analysed using phase contrast microscopy. Both stably and transiently RhoE-depleted cell lines (shRhoE and siRhoE HaCaT cells) were analysed to verify that changes in colony morphology was not due to off target effects of either siRNA or shRNA. shRhoE and siRhoE HaCaT cells and controls (shNSC and siCtrl) were

plated into cell culture flasks 48 hours prior to live phase contrast microscopy. Control cells formed monolayer colonies in which cells appeared large and spread (Figure 24). In contrast shRhoE and siRhoE cells formed colonies with a much more compacted 3D organisation in which individual cells appeared small (Figure 24). When comparing colony morphology of shNSC against siCtrl or shRhoE against siRhoE HaCaT cells no differences were observed (Figure 24).

Colony morphology was also analysed using confocal microscopy by taking Z series images and producing a 3D reconstruction of colonies. Stably RhoE-depleted (shRhoE) and control (shNSC) HaCaT cells (Figure 25) as well as transiently RhoE-depleted (siRhoE) and control (siCtrl) HaCaT cells (Figure 26) were seeded onto glass cover slips 48 hours prior to fixation. Cover slips were stained with antibodies against E-cadherin to visualise cell-cell boundaries and Hoechst 33342 to visualise nuclei. Both the 3D reconstruction and single Z series imaging of control colonies revealed a 2D spread monolayer with nuclei spread evenly throughout the colony, with clear spaces between and no overlap from neighbouring nuclei. Individual control cells, identified by E-cadherin staining, appeared large and spread. In contrast, both the 3D reconstruction and single Z series imaging of RhoE-depleted colonies revealed a 3D compacted phenotype with limited stratification. Neighbouring nuclei, in RhoE-depleted colonies, were in close proximity to each other and in some cases overlap of nuclei occurred (indicated by arrows). Individual cells, identified by E-cadherin staining, appeared small and compacted. The nuclei of control cells appeared larger than those in the RhoE-depleted cells. When comparing colony morphology of siNSC against siCtrl or shRhoE against siRhoE HaCaT cells no

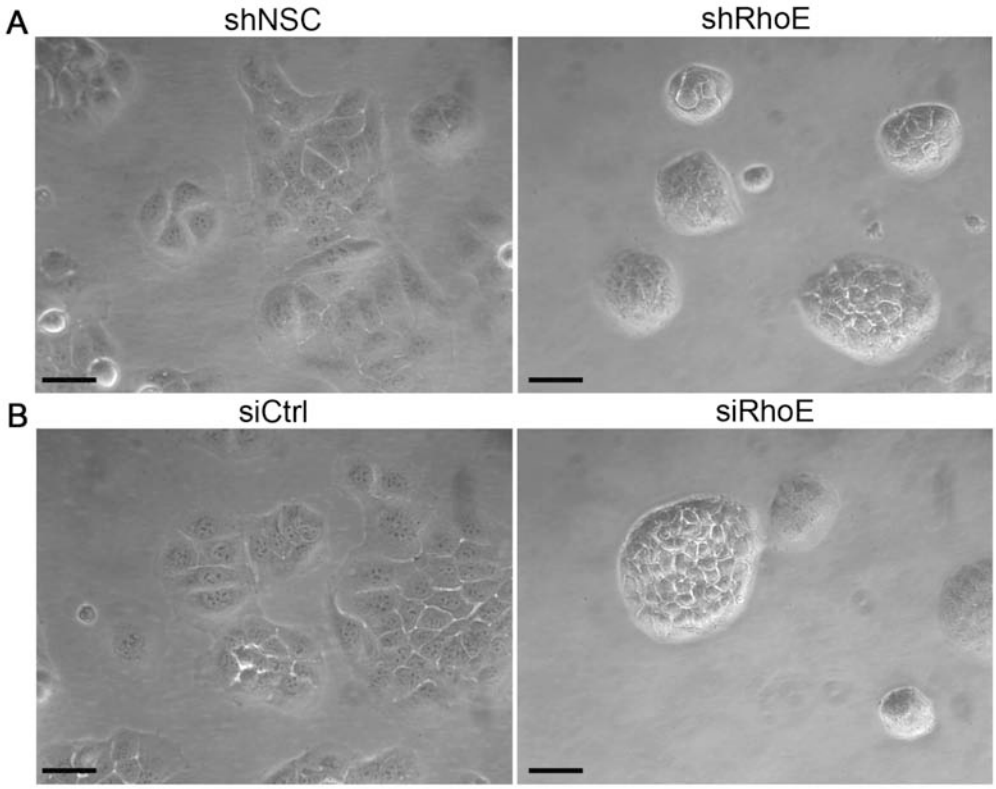

Figure 24 RhoE depletion alters keratinocyte colony morphology.

Keratinocytes depleted of RhoE were seeded into cell culture flasks 48 hours prior to live phase contrast microscopy using a 32x lens. **A** Phase contrast images of stably RhoE-depleted (shRhoE) and control (shNSC) HaCaT cells. **B** Phase contrast images of transiently RhoE-depleted (siRhoE) HaCaT cells and control (siCtrl) cells. Data presented are representative images of three separate experiments (scale bar 30 μm).

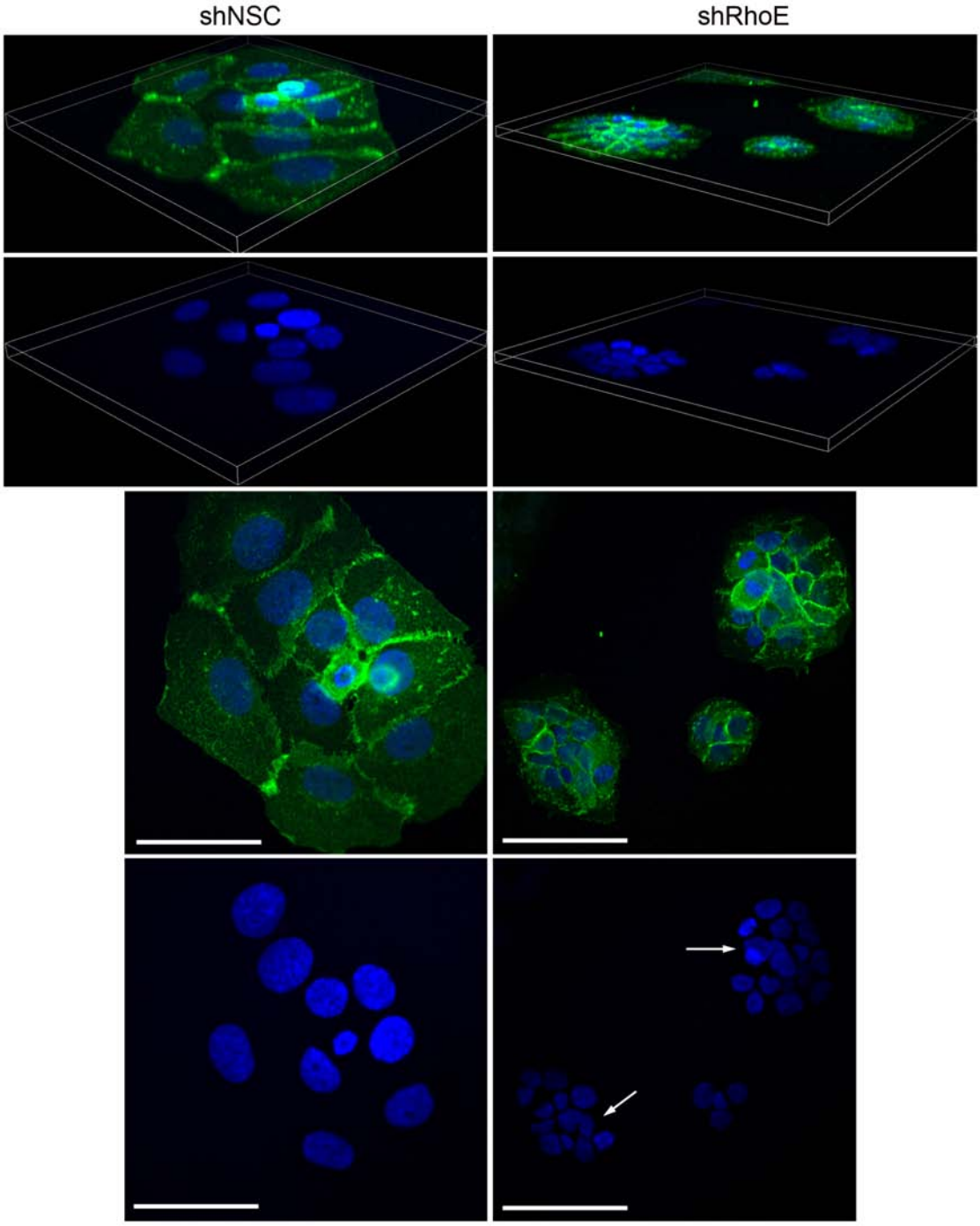
shNSC
shRhoE

Figure 25 Stable depletion of RhoE expression alters keratinocyte colony morphology.

HaCaT cells stably depleted of RhoE (shRhoE) and control (shNSC) cells were seeded onto glass cover slips 48 hours prior to fixation. Cover slips were stained with antibodies against E-cadherin (green) to visualise cell-cell boundaries and Hoechst 33342 (blue) to visualise nuclei. Z series images were taken through the colony using confocal microscopy using a 60x lens. The first 4 panels are of the 3D reconstruction of confocal layers. The lower four panels are of a single 1 μm Z series stack corresponding to the middle layer of the 3D image. Data are representative images of two separate experiments with the gain and exposure times remaining constant (scale bar 30 μm). Arrows indicate overlapping nuclei.

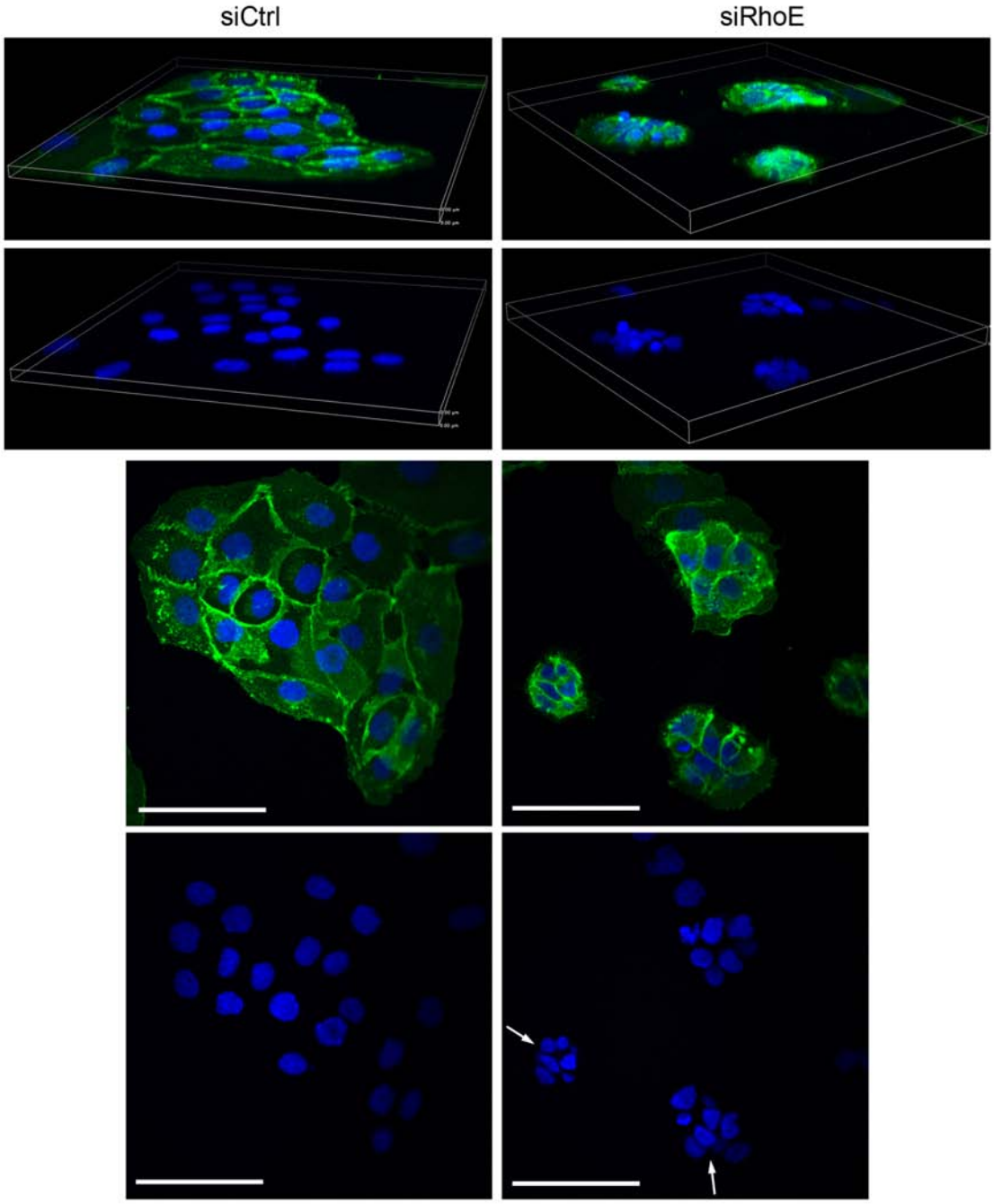
siCtrl
siRhoE

Figure 26 Transient depletion of RhoE expression alters keratinocyte colony morphology.

HaCaT cells transiently depleted of RhoE (siRhoE) and control (siCtrl) cells were seeded onto glass cover slips 48 hours prior to fixation. Cover slips were stained with antibodies against E-cadherin (green) to visualise cell-cell boundaries and Hoechst 33342 (blue) to visualise nuclei. Z series images through the colony were taken using confocal microscopy using a 60x lens. The first 4 panels are of the 3D reconstruction of confocal layers. The lower four panels are of a single 1 μm Z series stack corresponding to the middle layer of the 3D image. Data are representative images of two separate experiments with the gain and exposure times remaining constant (scale bar 30 μm). Arrows indicate overlapping nuclei.

differences were observed (Figure 25 & 26). These data indicate that RhoE depletion resulted in altered colony morphology from a 2D spread monolayer to a 3D compacted limited stratified phenotype.

4.2.2 Differentiation is not induced in RhoE-depleted keratinocytes

Keratinocytes depleted of RhoE appeared to stratify with colonies containing overlapping nuclei and RhoE has been implicated in the regulation of keratinocyte differentiation and stratification (Liebig et al. 2009). To assess whether RhoE-depleted cells were undergoing terminal differentiation whole cell lysates were prepared from transiently RhoE-depleted keratinocytes and were analysed using immunoblotting with antibodies against known differentiation markers. The markers included involucrin, periplakin, keratin 1 and desmocollin 2, which are up-regulated during differentiation and keratin 5 and 14, which are down-regulated during differentiation (Rice et al. 1979; Fuchs et al. 1980; Watt 1983; Legan et al. 1994). No change in expression was detected for involucrin, periplakin or keratin 14 in siRhoE cells when compared to siCtrl cells. Interestingly a decrease in keratin 1 expression and an increase in keratin 5 and desmocollin 2 expression were detected in siRhoE cells when compared to siCtrl cells (Figure 27). These data suggest that despite evidence for stratification RhoE-depleted cells are not undergoing differentiation.

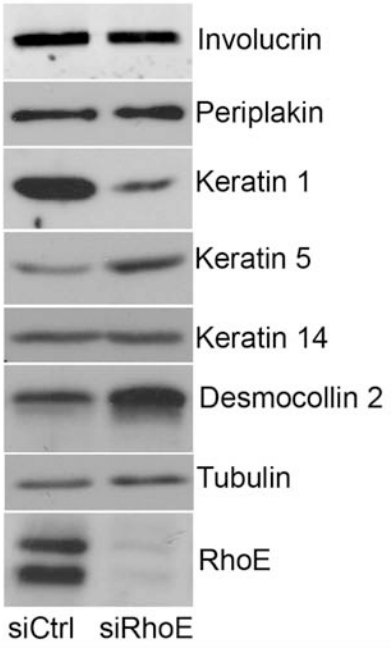

Figure 27 Differentiation marker profile in keratinocytes depleted of RhoE.

HaCaT cells transiently depleted of RhoE (siRhoE) and control (siCtrl) cells were incubated in normal growth conditions prior to lysis. Immunoblotting using antibodies against known differentiation markers such as involucrin, periplakin, keratin 1, 5, 14, and desmocollin 2, as well as RhoE and tubulin were used to detect the expression of the proteins of interest and as a loading control respectively. Data presented are representative immunoblots of three separate experiments.

4.2.3 RhoE depletion increased expression of desmosomal proteins

Having observed an increase in desmocollin 2 expression in RhoE-depleted cells (Figure 27) immunoblotting was used to analyse the expression of other adhesion proteins. Antibodies against E-cadherin, desmocollin 1, 2 and 3, desmoglein 2 and 3, desmoplakin I/II and plakoglobin were used to analyse expression of adherens junction proteins and desmosomal proteins. No change in E-cadherin expression, a component of adherens junctions, was observed (Figure 28A). Increased expression of desmocollin 2 and 3, desmoglein 3 and desmoplakin I/II was observed in RhoE-depleted cells whereas no change in expression was detected in desmocollin 1, desmoglein 2 or plakoglobin when compared to control cells (Figure 28B-D).

4.2.4 RhoE depletion increased the number of desmosomes

Transmission electron microscopy (TEM) was used to visualise desmosomes in transiently RhoE-depleted cells. siRhoE and siCtrl HaCaT cells were plated onto plastic cover slips 48 hours prior to fixation. Cover slips were embedded and sections were taken orthogonally to the plane of the cover slip and stained using negative staining (work carried out by Theresa Morris, Centre for Electron Microscopy, University of Birmingham). Desmosomes were detected in both siRhoE and siCtrl cells (indicated by arrows) with no apparent difference in size (Figure 29A). Desmosomal frequency was analysed by counting the number of desmosomes present along each cell-cell boundary. Although these are very preliminary data an apparent increase in the number of desmosomes was observed in RhoE-depleted cells (Figure 29B).

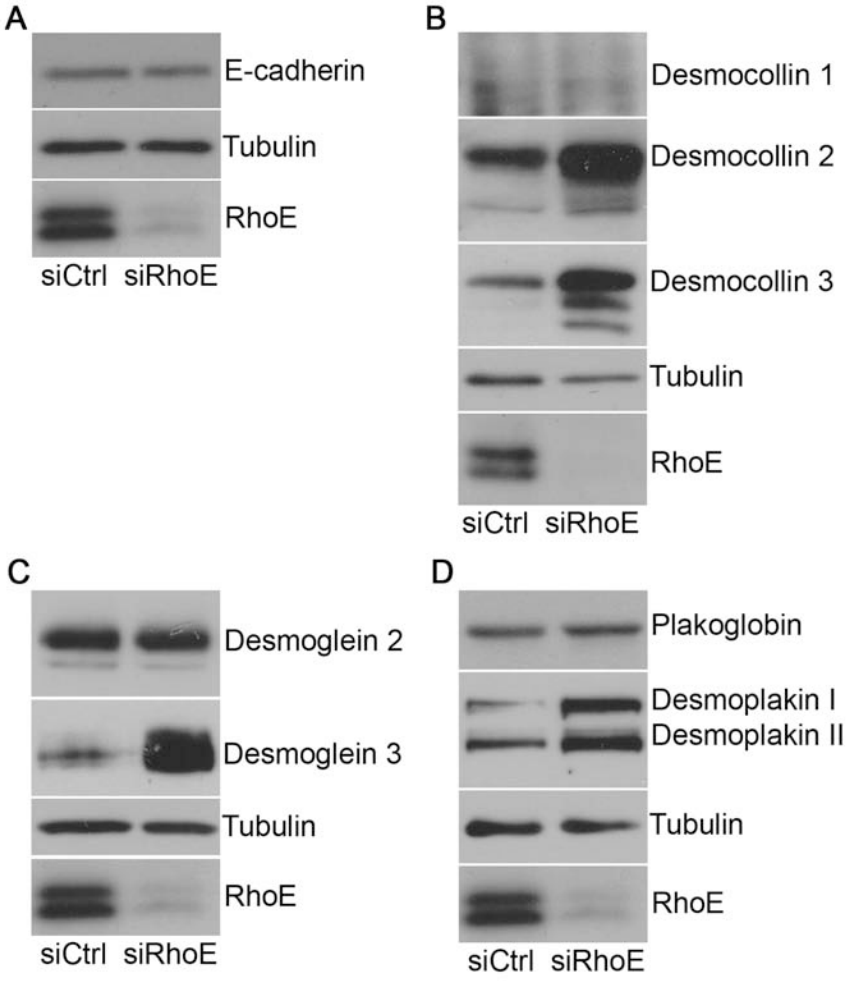

Figure 28 Expression of desomsomal proteins is increased in keratinocytes depleted of RhoE.

HaCaT cells transiently depleted of RhoE (siRhoE) and control (siCtrl) cells were incubated in normal growth conditions prior to whole cell lysis. Immunoblotting using antibodies against E-cadherin, desmocollin 1, 2 and 3, desmoglein 2 and 3, desmoplakin I/II and plakogobin were used to analyse the expression of adherens junction and desmosomal proteins. Data presented are representative immunoblots of three separate experiments. **A** E-cadherin expression. **B** Desmocollin 1, 2 and 3 expression. **C** Desmoglein 2 and 3 expression. **D** Desmoplakin and plakoglobin expression.

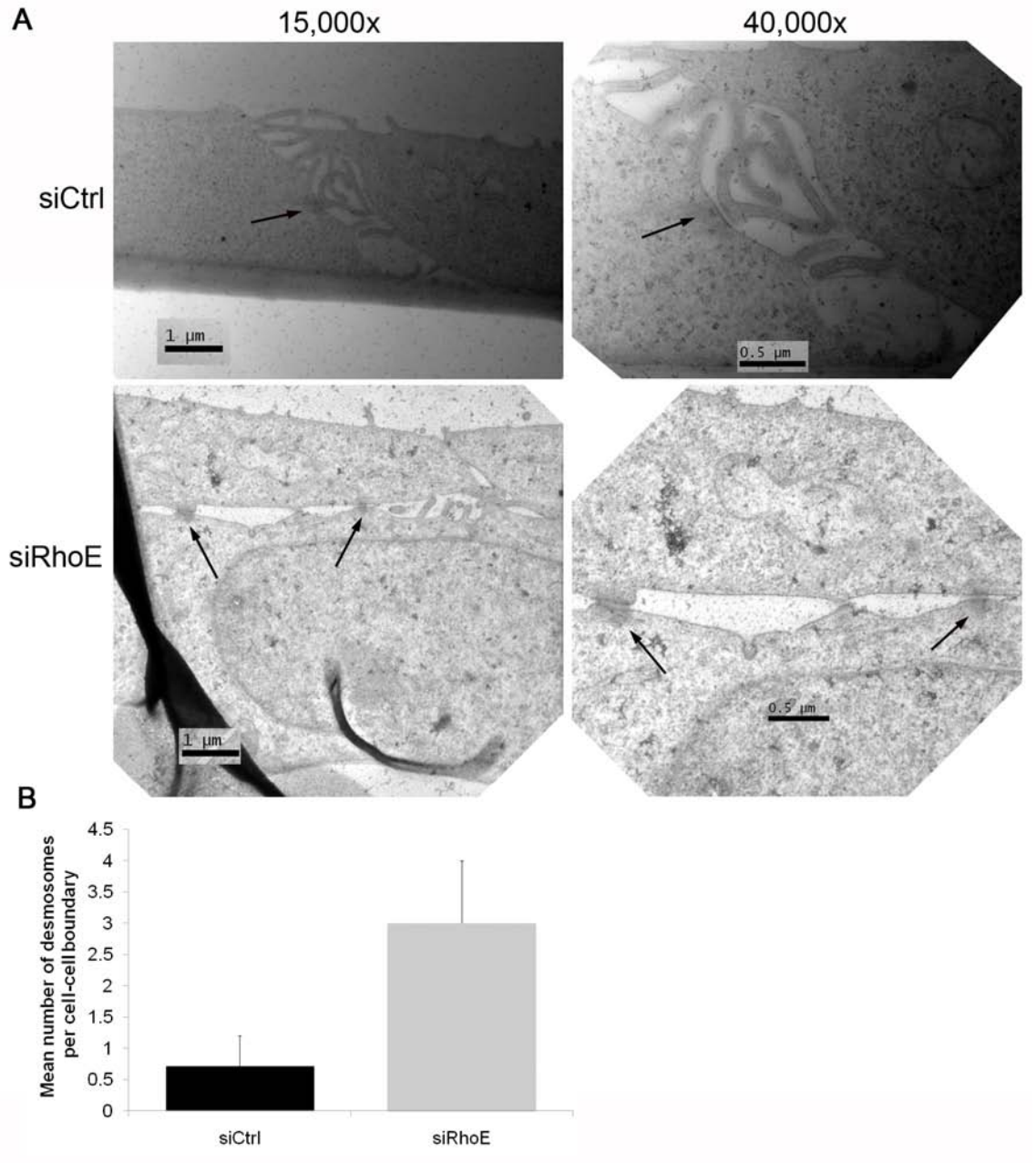
A
15,000x
40,000x
siCtrl
siRhoE
1 µm
0.5 µm
1 µm
0.5 µm
B
Mean number of desmosomes per cell-cell boundary
4.5
4
3.5
3
2.5
2
1.5
1
0.5
0
siCtrl
siRhoE

Figure 29 Transmission electron microscopy in keratinocytes depleted of RhoE.

HaCaT cells transiently depleted of RhoE (siRhoE) and control (siCtrl) cells were plated onto plastic cover slips 48 hours prior to fixation. Cover slips were embedded and sections were taken orthogonally to the plane of the cover slip and stained using negative staining (work carried out by Theresa Morris, Centre for Electron Microscopy, University of Birmingham). Images were taken on a Jeol 1200EX microscope using 15,000x and 40,000x magnification. **A** Desmosomes were detected in both siRhoE and siCtrl cells (indicated by arrows). Data presented are representative images from one experiment. **B** Desmosomal frequency was analysed by counting the number of desmosomes present along each cell-cell boundary and the data presented are the mean and standard deviation of 7 cell-cell boundaries in one experiment.

To analyse the localisation of desmosomal proteins, cells were stained with antibodies against desmocollin 3, desmoplakin I/II and plakoglobin. Cells were also stained with Hoechst 33342 to visualise nuclei. In both siCtrl and siRhoE cells desmocollin 3 and desmoplakin I/II staining appeared as a punctate pattern along cell-cell boundaries, in siRhoE cells this punctate staining is increased (Figure 30 & 31). Punctate desmoplakin I/II staining also occured in the cytoplasm, which is increased in siRhoE cells (Figure 31). Plakoglobin staining localised to the cell-cell boundaries, like E-cadherin staining, in both siCtrl and siRhoE cells but unlike E-cadherin plakoglobin staining was brighter at cell-cell boundaries in siRhoE cells (Figure 32). Taken together these data suggest that loss of RhoE expression resulted in an increase in the number of desmosomes in keratinocytes.

4.2.5 Colony morphology and desmosomal protein expression is disrupted in low calcium conditions

Both desmosomes and adherens junctions require extra cellular calcium for cell-cell adhesion to occur (Chitaev et al. 1997; Jamora et al. 2002). As a preliminary experiment to analyse whether colony morphology in RhoE-depleted cells would revert to a normal morphology when cell-cell adhesion is disrupted, cells were cultured in reduced calcium conditions. Stably RhoE-depleted (shRhoE) and control (shNSC) HaCaT cells were seeded into cell culture flasks and incubated in normal growth media for 48 hours (+ calcium). Cells were then incubated in low calcium medium for 24 hours (- calcium). Following calcium depletion cells were incubated in normal medium for 24 hours (-+ calcium 24hrs) and 48 hours (-+ calcium 48hrs). At each stage colony

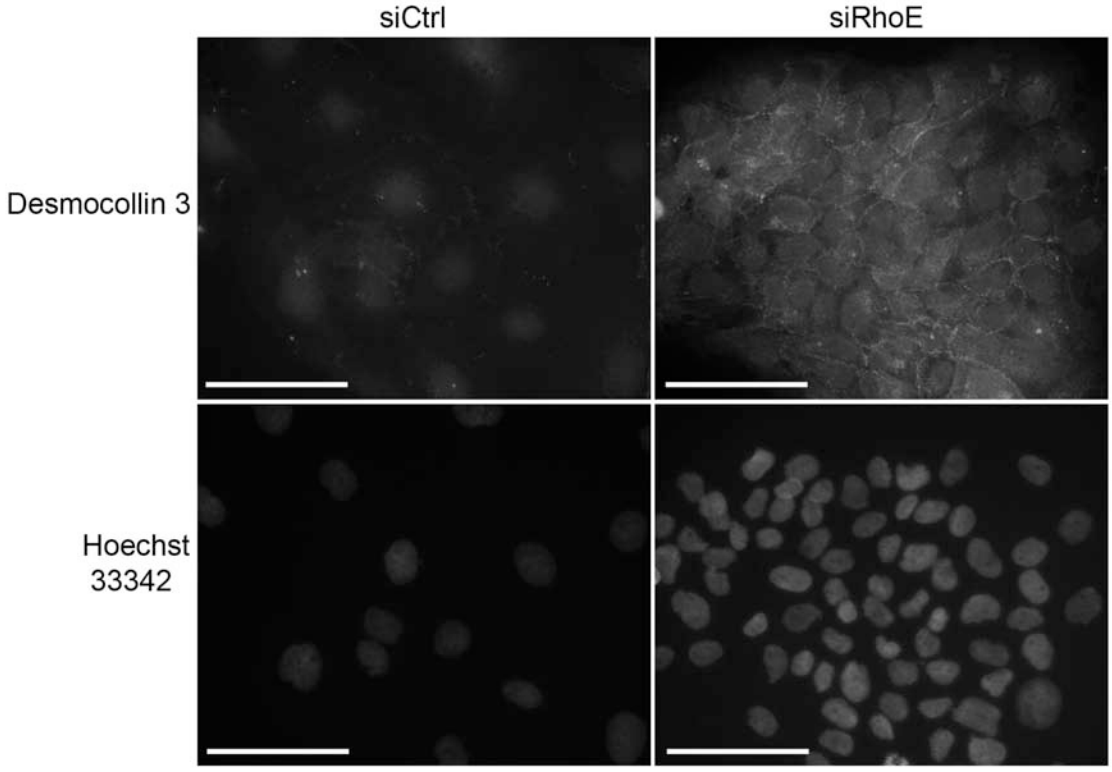

Figure 30 Desmocollin 3 staining is increased at cell-cell boundaries in keratinocytes depleted of RhoE.

HaCaT cells transiently depleted of RhoE (siRhoE) and control (siCtrl) cells were plated onto glass cover slips 48 hours prior to fixation. Cover slips were stained with antibodies against desmocollin 3 and with Hoechst 33342 to visualise nuclei. Images were taken on an epifluorescence microscope using a 40x lens. Data presented are representative images of three separate experiments, with the gain and exposure time remaining constant (scale bar 30 μm).

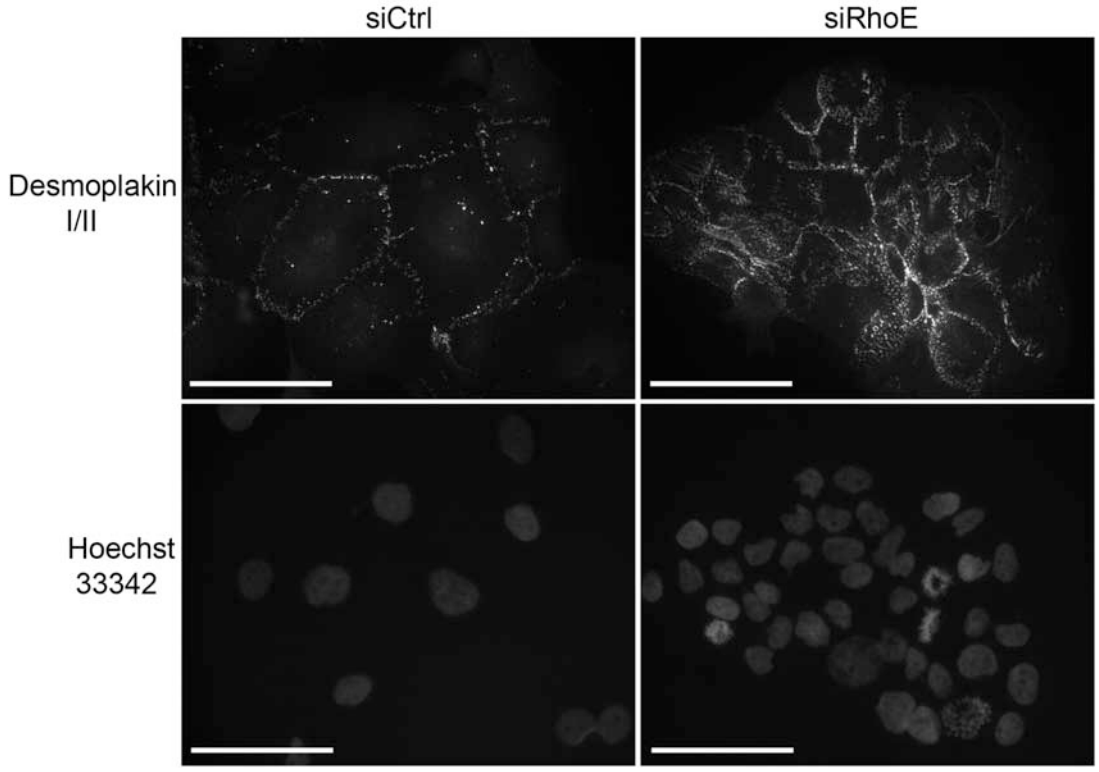

Figure 31 Desmoplakin I/II staining is increased at cell-cell boundaries in keratinocytes depleted of RhoE.

HaCaT cells transiently depleted of RhoE (siRhoE) and control (siCtrl) cells were plated onto glass cover slips 48 hours prior to fixation. Cover slips were stained with antibodies against desmoplakin I/II and with Hoechst 33342 to visualise nuclei. Images were taken on an epifluorescence microscope using a 40x lens. Data presented are representative images of three separate experiments, with the gain and exposure time remaining constant (scale bar 30 μm).

Figure 32 Plakoglobin staining is increased at cell-cell boundaries in keratinocytes depleted of RhoE.

HaCaT cells transiently depleted of RhoE (siRhoE) and control (siCtrl) cells were plated onto glass cover slips 48 hours prior to fixation. Cover slips were stained with antibodies against plakoglobin, E-cadherin to visualise cell-cell boundaries, and Hoechst 33342 to visualise nuclei. Images were taken on an epifluorescence microscope using a 40x lens. Data presented are representative images of three separate experiments, with the gain and exposure time remaining constant (scale bar 30μm).

morphology was documented using live phase contrast microscopy. Following calcium depletion shRhoE HaCaT cells appeared more rounded with gaps between neighbouring cells and colony morphology had lost the compacted stratified phenotype (- calcium). Following re-addition of calcium for 24 hours (-+ calcium 24hrs) and 48 hours (-+ calcium 48hrs) shRhoE colonies reverted back to the original compacted stratified morphology (+ calcium) (Figure 33). The experiment was repeated using transiently RhoE-depleted siRhoE and siCtrl HaCaT cells and similar results were observed (Figure 34).

The effect of low calcium conditions on desmosomal protein expression was analysed in control and RhoE-depleted cells. Transiently RhoE-depleted (siRhoE) and control (siCtrl) cells were incubated in either low calcium or normal growth medium 24 hours prior to lysis. Whole cell lysates were analysed by immunoblotting using antibodies against the desmosomal proteins desmoglein 3, desmocollin 2 and desmocollin 3. An increase in the expression of desmoglein 3, desmocollin 2 and 3 was detected in siRhoE cells compared to siCtrl cells in normal growth conditions (+ calcium). In both cells lines calcium depletion resulted in a loss of expression for desmoglein 3, desmocollin 2 and desmocollin 3 (Figure 35). These data indicate that in low calcium conditions cell-cell adhesion is lost along with the expression of desmosomal proteins, which restored the colony morphology of RhoE-depleted cells from a stratified phenotype to a monolayer.

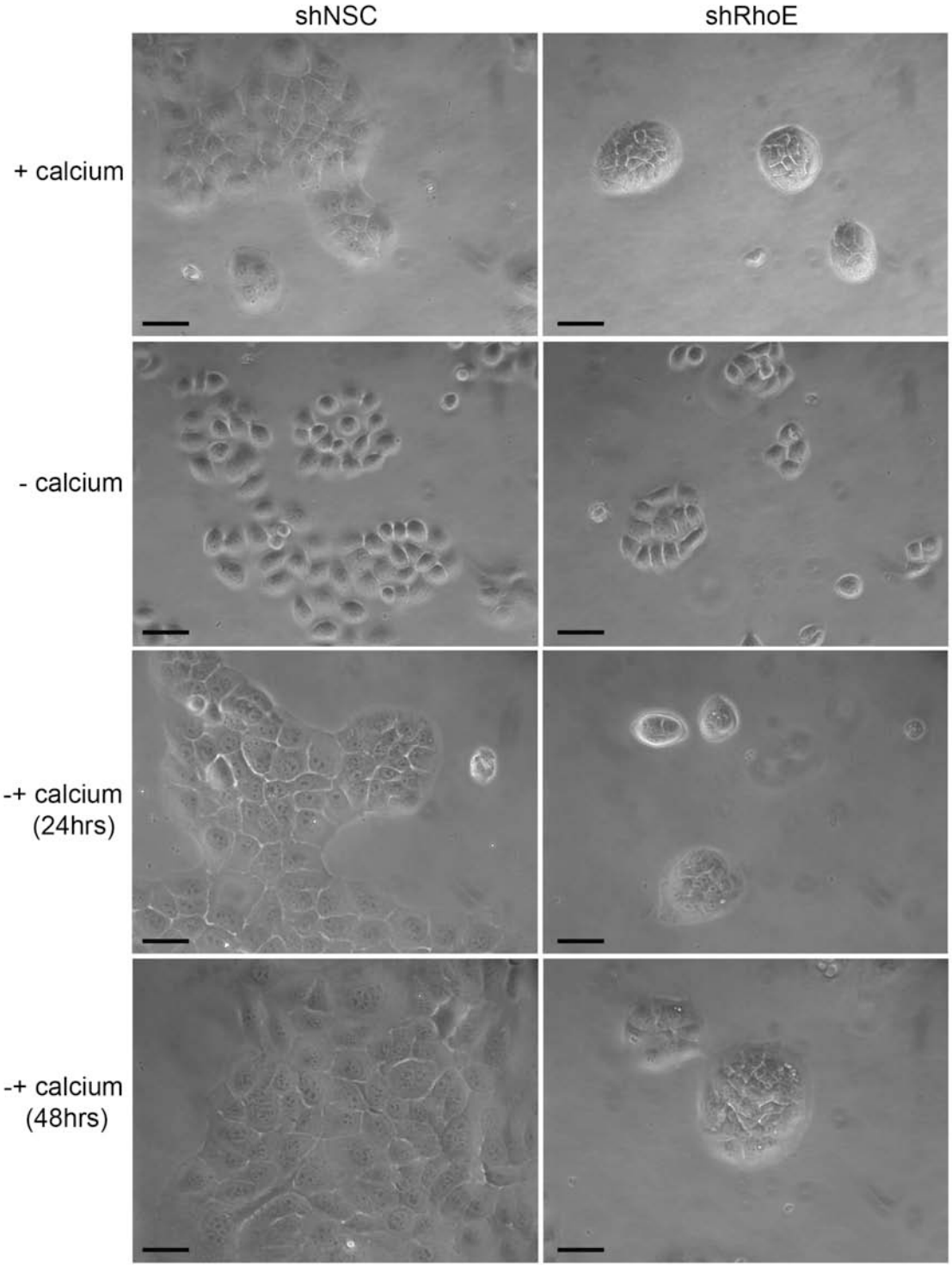
shNSC
shRhoE
+ calcium
- calcium
-+ calcium
(24hrs)
-+ calcium
(48hrs)

Figure 33 Colonies formed from keratinocytes stably depleted of RhoE lose the stratified morphology when cultured in low calcium medium.

HaCaT cells stably depleted of RhoE (siRhoE) and control (siCtrl) cells were seeded into cell culture flasks and incubated in normal growth medium for 48 hours (+ calcium). Cells were then incubated in low calcium medium for 24 hours (- calcium), followed by re-addition of normal medium for 24 hours (-+ calcium 24hrs) and 48 hours (-+ calcium 48hrs). At each stage live phase microscopy images were taken using a 32x lens. Data presented are representative images of three separate experiments (scale bar 30 μm).

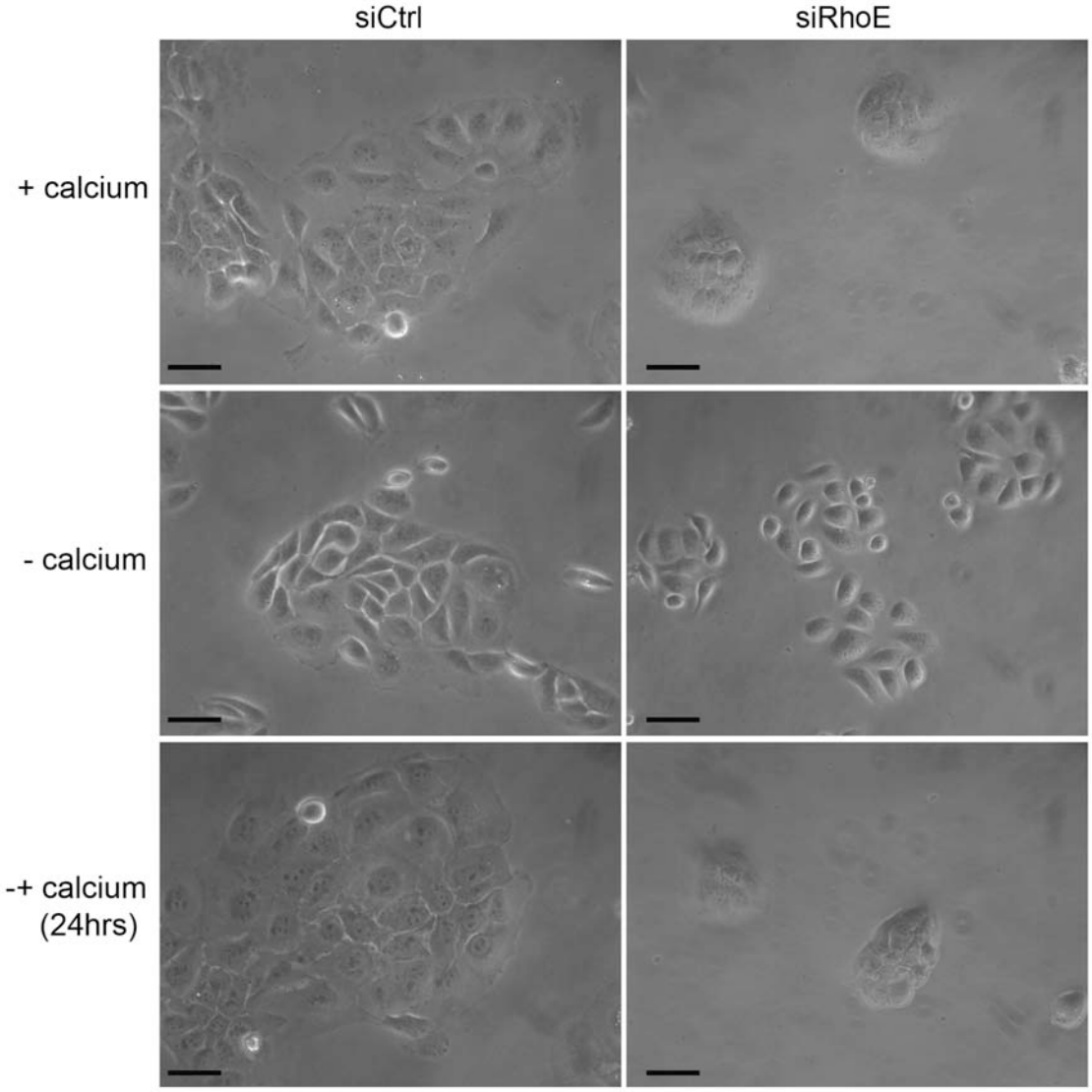
siCtrl
siRhoE
+ calcium
- calcium
-+ calcium
(24hrs)

Figure 34 Colonies formed from keratinocytes transiently depleted of RhoE lose the stratified morphology when cultured in low calcium medium.

HaCaT cells transiently depleted of RhoE (siRhoE) and control (siCtrl) cells were seeded into cell culture flasks and incubated in normal growth medium for 48 hours (+ calcium). Cells were then incubated in low calcium medium for 24 hours (- calcium), followed by re-addition of normal medium for 24 hours (-+ calcium 24hrs). At each stage live phase contrast microscopy images were taken using a 32x lens. Data presented are representative images from three separate experiments (scale bar 30 μm).

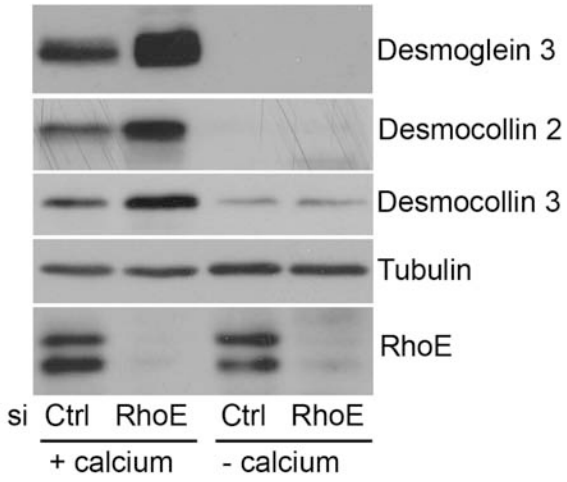

Figure 35 Expression of desmosomal proteins is increased in keratinocytes depleted of RhoE in normal growth medium but expression is lost when cells are cultured in low calcium medium.

HaCaT cells transiently depleted of RhoE (siRhoE) and control (siCtrl) cells were incubated in either low calcium or normal growth medium 24 hours prior to whole cell lysis. Immunoblotting using antibodies against desmoglein 3, desmocollin 2, desmocollin 3, RhoE and tubulin were used to detect expression of desmosomal proteins, RhoE protein and as a loading control respectively. Data presented are representative immunoblots of three separate experiments.

4.2.6 Disruption of desmosomes rescues the colony morphology of keratinocytes depleted of RhoE

To analyse whether the up-regulation of desmosomal proteins and increased number of desmosomes was responsible for the alteration in colony morphology seen in RhoE-depleted cells siRNA oligos were used to disrupt desmosomes. Depletion of major desmosomal proteins, desmoplakin I/II or plakoglobin, disrupts desmosomes (Gallicano et al. 1998; Bierkamp et al. 1999; Vasioukhin et al. 2001; Acehan et al. 2008). I analysed whether this would revert colony morphology back to a normal phenotype in HaCaT cells depleted of RhoE. Transient single knock-downs of desmoplakin I/II (siDSP), plakoglobin (siPG) and RhoE (siRhoE) as wells as in combination decreased expression of target proteins, detected by immunoblotting (Figure 36). These cells were plated into cell culture flasks 48 hours prior to phase contrast microscopy and lysis. Phase contrast microscopy of siCtrl, siDsp and siPG cells revealed monolayer colonies in which individual cells appeared large and spread. In contrast, siRhoE colonies had a 3D compacted phenotype in which individual cells appeared small. Both siRhoE:Dsp and siRhoE:PG colonies had a control colony phenotype, with monolayer colonies in which individual cells appeared larger and more spread when compared to siRhoE cells (Figure 37). Taken together these data indicate that RhoE-depletion increases the number of desmosomes which leads to altered colony morphology.

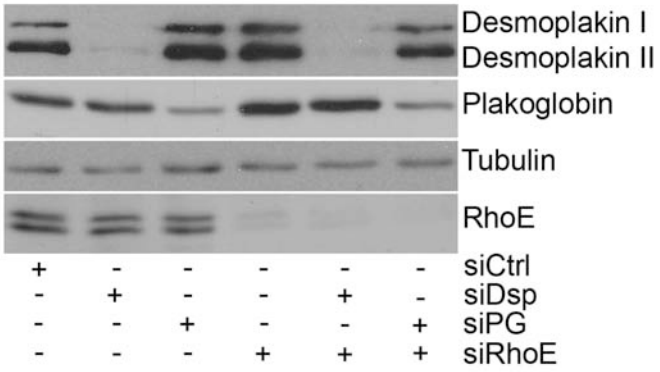

Figure 36 Transient knock-down of desmoplakin I/II, plakoglobin and RhoE expression in keratinocytes, using siRNA oligos.

Individual and combined depletion of desmoplakin I/II (Dsp), plakoglobin (Diepgen et al.) and RhoE (siRhoE) in HaCaT cells were achieved by transiently transfecting cells with siRNA oligos to depleted proteins of interest for 144 hours prior to whole cell lysis. Immunoblotting using antibodies against desmoplakin I/II, plakoglobin, RhoE and tubulin were used to detect the level of the proteins of interest and as a loading control respectively. Data presented are representative immunoblots of three separate experiments.

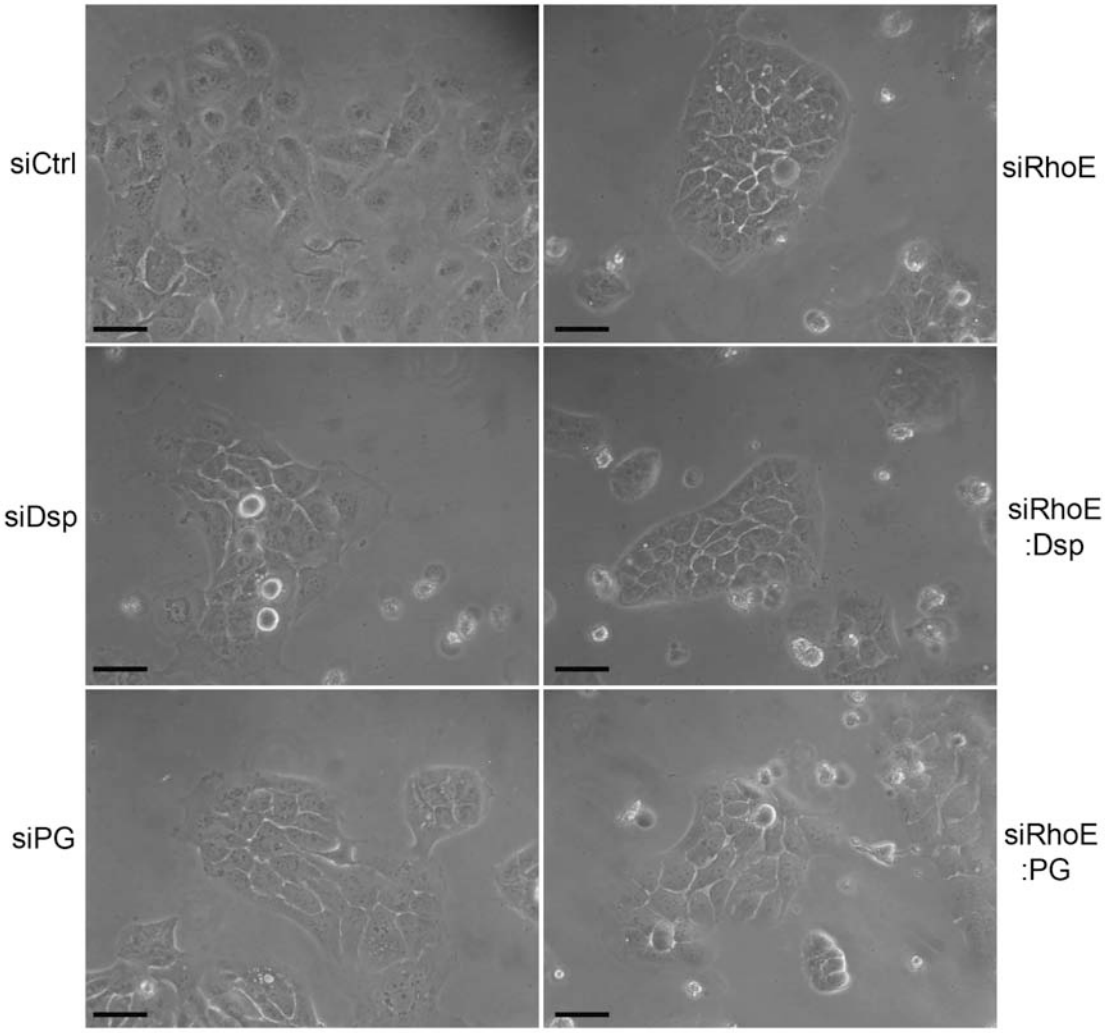

Figure 37 Disruption of desmosomes rescues colony morphology of keratinocytes depleted of RhoE.

Transient single knock-downs, of desmoplakin I/II (siDsp), plakoglobin (siPG) and RhoE (siRhoE), and combined knock-downs, siRhoE:Dsp and siRhoE:PG HaCaT cells, were seeded onto plastic 48 hours prior to live phase microscopy using a 32x lens. Data presented are representative images from three separate experiments (scale bar 30 μm).

4.3 Discussion

A recent study reported that, in keratinocytes over-expressing RhoE, cell size was increased and stratification was promoted whereas depletion of RhoE using siRNA had no effect on either cell size or stratification (Liebig et al. 2009). Using phase contrast and confocal microscopy my data revealed that depletion of RhoE altered colony morphology in keratinocytes. RhoE-depleted cells formed smaller more compact colonies compared to control cells and cells within the RhoE-depleted colonies were less spread and appeared smaller than control cells (Section 4.2.1). In addition, in RhoE-depleted colonies there is evidence for increased stratification with neighbouring nuclei overlapping each other. A key difference between my study and that of Liebig et al. are the culture conditions used and cell type. In Liebig et al. keratinocytes depleted of RhoE were cultured in low calcium conditions both prior to, and post, transient transfection with siRNA to deplete RhoE expression (Liebig et al. 2009). These RhoE-depleted cells were cultured in low calcium medium until a monolayer was formed and then the cells were induced to stratify by culturing in medium containing an increased calcium concentration (1.8mM) for 8 hours (Liebig et al. 2009). In most of my experiments RhoE-depleted cells were cultured at sub-confluency in normal growth medium containing physiological levels of calcium (1.8mM) (Section 4.2.5). However, in experiments where I cultured RhoE-depleted cells in low calcium medium no stratification or cell size change was observed (Figure 33 & 34). A second issue is the length of time during which cells were cultured in normal medium. In Liebig et al. medium containing 1.8mM calcium was only added for 8 hours, whereas in my experiment RhoE-depleted cells were cultured for 24 hours in this medium (Section 4.2.5). I have shown that the altered colony morphology in RhoE-depleted cells is due to an increase in desmosomal protein

expression and an increase in desmosome number (Section 4.2.3 & 4.2.4). In low calcium conditions cell-cell adhesion through desmosomes and adherens junctions are lost (Chitaev et al. 1997; Jamora et al. 2002) as is the increase in desomosomal proteins seen in RhoE-depleted cells (Section 4.2.5 Figure 35).

The observation that RhoE-depleted cells were forming partically stratified colonies lead me to analyse differentiation markers in these cells to assess whether differentiation was being induced following RhoE depletion. Commonly used markers for differentiation include an increase in involucrin expression and a switch in keratin expression from keratin 5 and 14 to keratin 1 and 10 (Fuchs et al. 1980; Watt 1983; Fuchs 2007). Other markers that indicate keratinocytes are undergoing differentiation include the up-regulation of certain desmosomal proteins, such as desmocollin 2, and increased periplakin expression (Rice et al. 1979; Legan et al. 1994; Nemes et al. 1999). The expression levels of many of these markers were analysed in RhoE-depleted cells (Figure 27). Evidence suggesting RhoE-depleted cells might be undergoing differentiation included limited stratification and increased desmocollin 2 expression. However, no other change in the expression of differentiation markers was observed, strongly arguing against a differentiation phenotype. Furthermore, during differentiation cell size increases (Watt 1983). RhoE-depleted cells did not increase in size and appeared smaller than control cells (Section 4.2.1). Taken together these data indicate that terminal differentiation is not occurring in RhoE-depleted cells. Consistent with this, Liebig et al. (2009) also looked at differentiation markers (involucrin, keratin 1 and transglutaminase) in their RhoE-depleted keratinocytes and observed no change in expression. When differentiation was artificially induced they also observed a

delay in the up-regulation of these markers in RhoE-depleted cells (Liebig et al. 2009). These data suggest that RhoE depletion in keratinocytes does not induce terminal differentiation.

Of all the differentiation markers analysed only desmocollin 2 was up-regulated in RhoE-depleted keratinocytes. Desomocollin 2 is a desmosomal cadherin and a component of desmosomes (Garrod et al. 2008). Analysis of the expression levels and localisation of other desmosomal proteins revealed major changes in RhoE-depleted cells (Section 4.2.3 & 4.2.4). Of the desmosomal proteins analysed, an increase in the expression of desmocollin 2, desmocollin 3, desmoglein 3 and desmoplakin I/II was observed in RhoE-depleted cells. Thus RhoE-depleted cells show increased expression for most of the components required for desmosomal assembly and ectopic expression of these components in fibroblasts can result in the formation of desmosomes (Kowalczyk et al. 1997). Transmission electron microscopy was used to investigate the structure and number of desmosomes present in RhoE-depleted cells. No obvious changes in desmosomal structure were observed. However, preliminary data indicated an increase in the number of desmosomes in RhoE-depleted cells (Figure 29). This was also suggested by epifluorescent imaging of RhoE-depleted cells where, consistent with the immunoblotting data, I observed increased cell-cell staining of desmoplakin I/II, desmocollin 3 and plakoglobin (Figure 30, 31 & 32). Punctate cytoplasmic desmoplakin I/II staining was observed in both cell lines but was increased in RhoE-depleted cells (Figure 31). This type of desmoplakin I/II staining is indicative of the formation of non-membrane bound desmoplakin I/II-containing particles that subsequently translocate to cell–cell borders and incorporate into maturing desmosomes (Godsel et al. 2005). These data indicate that RhoE-depletion in

keratinocytes increases the expression of desmosomal proteins and the number of desmosomes.

Plakoglobin localises to several different locations in the cell: These include desmosomes and adherens junctions where it is involved in cell-cell adhesion and the nucleus where it can act as a transcription factor (Hu et al. 2003; Garcia-Gras et al. 2006; Dusek et al. 2007; Acehan et al. 2008). Immunoblotting revealed no change in total plakoglobin expression (Figure 28) but epifluorescent imaging revealed a marked increase in plakoglobin staining in RhoE-depleted cells at the cell-cell boundary (Figure 32). This indicates a relocalisation of plakoglobin to cell-cell boundaries in RhoE-depleted cells. RhoE-depletion appears to have no effect on adherens junctions as the expression and localisation of E-cadherin is unchanged in RhoE-depleted cells (Figure 28 & 32). This suggests that RhoE is regulating a desmosome-specific pathway and not having a global effect on cell-cell adhesion.

Cell-cell adhesion maintained by desmosomes and adherens junctions is dependent on the presence of extracellular calcium (Chitaev et al. 1997; Braga 2002; Garrod et al. 2008). In low calcium conditions adherens junctions and desmosomes disassemble due to the cadherins losing their ability to form dimers (Garrod et al. 2008). This results in a disruption of cell-cell adhesion and prevents stratification (Watt et al. 1984; O'Keefe et al. 1987; Garrod et al. 2008). Keratinoncytes depleted of RhoE when cultured in low calcium conditions lose the stratification phenotype (Figure 33 & 34). Loss of desmocollin 2, desmocollin 3 and desmoglein 3 expression was also observed in RhoE-depleted cells cultured in low calcium medium (Figure 35). Thus, the altered colony formation seen in RhoE-depleted keratinocytes is most likely a function of

increased desmosome-mediated cell-cell adhesion. Consistent with this, depletion of desmoplakin I/II in keratinocytes, using siRNA, disrupted desmosomes and also resulted in reduced expression of other desmosomal proteins including desmocollin 2, 3 and desmoglein 1 and 2 as well as all three plakophilin members (Wan et al. 2007).

A number of studies have demonstrated that depletion of either desmoplakin I/II or plakoglobin leads to a loss of desmosomes and decreased cell-cell adhesion (Gallicano et al. 1998; Bierkamp et al. 1999; Vasioukhin et al. 2001; Wan et al. 2007; Acehan et al. 2008). I used siRNA to deplete expression of desmoplakin I/II or plakoglobin in RhoE-depleted cells and in both cases a reversion to control colony phenotype was observed (Figure 36 & 37). Knocking-out plakoglobin, or depleting desmoplakin I/II expression, has no apparent affect on adherens junctions as E-cadherin staining and expression was unaffected in these cells (Wan et al. 2007; Acehan et al. 2008) and I also observed no change in E-cadherin expression or localisation in RhoE-depleted cells (Figure 28 & 32). This is an important observation as plakoglobin has been reported to localise to adherens junctions (Hu et al. 2003). These data show that depletion of either desmoplakin I/II or plakoglobin affects the formation of desmosomes without affecting adherens junctions. Taken together these data indicate increased cell compaction and stratification observed in RhoE-depleted keratinocytes is a consequence of increased desmosome expression and function.

Cell-cell adhesion maintained by desmosomes and adherens junctions is vital for keratinocyte differentiation and stratification (Braga 2002). Desmosomes are the principal junctions of the

epidermis and are essential for its function (Vasioukhin et al. 2001; Jonkman et al. 2005). Low calcium conditions prevent keratinocytes from stratifying even when terminal differentiation has been initiated, due to the prevention of cell-cell adhesion (Chitaev et al. 1997; Jamora et al. 2002). In RhoE-depleted keratinocytes no increase in differentiation markers was observed but the numbers of desmosomes was significantly increased (Figure 27 & 28). Thus I hypothesise that RhoE-depletion results in increased expression of desmosomal components and the formation desmosomes, and that this induces a stratification phenotype without initiating differentiation.

RhoE-depleted keratinocytes cultured in normal growth conditions appear smaller, and have smaller nuclei than control cells. However, no difference in cell size was observed when RhoE-depleted keratinocytes were cultured in low calcium conditions (Section 4.2.5). Targeted misexpression of desmoglein 2, to the suprabasal layers of the epidermis in mice, increases both the size of keratinocytes in the upper suprabasal layers and also the size of the nuclei (Brennan et al. 2007). Whilst we see a decrease in cell size, the expression levels of desmoglein 2 are unchanged in RhoE-depleted cells. However, other desmosomal components are up-regulated in RhoE-depleted cells opening up the possibility that different desmosomal proteins or desmosomes could regulate cell growth.

4.3.1 How might RhoE regulate desmosome formation?

The formation of desmosomes involves desmoplakin I/II being rapidly accumulated at the

contacting cell boundary after the initial cell-cell contact is made (Godsel et al. 2005). This is followed by the formation of non-membrane bound desmoplakin I/II- and plakophilin 2-containing particles in the cortical region of the cell. These desmosomal particles translocate to cell–cell borders and incorporate into maturing desmosomes (Godsel et al. 2005). The translocation of these desmosomal particles requires both intermediate filaments and actin microfilament interactions (Godsel et al. 2005). Connection to the intermediate filaments is regulated by protein kinase A, through the phosphorylation of desmoplakin I/II (Godsel et al. 2005). Plakophilin 2 also recruits protein kinase C α to desmoplakin I/II, which attenuates desmoplakin I/II interactions with intermediate filaments (Bass-Zubek et al. 2008). The formation of desmosomes also requires an intact actin cytoskeleton (Pasdar et al. 1993) and if the actin cytoskeleton is disrupted translocation of desmosomal particles to maturing desmosomes is prevented (Godsel et al. 2005). These data suggest that both intermediate filaments and the actin cytoskeleton are involved in regulating desmosomal assembly.

How RhoE-depletion induces the expression of desmosomal proteins and an increase in desmosomes is not known. Unlike desmosomal protein-protein interactions, which are well-documented, little is known about desmosomal protein expression and assembly (Green et al. 2007). One possible mechanism whereby RhoE might regulate desmosomes is regulation of the actin cytoskeleton through either RhoA-dependent or independent mechanisms. RhoE is known to regulate RhoA activity through the p190RhoGAP (Wennerberg et al. 2003) and the RhoA GEF Syx (Goh et al. 2010). Constitutively active RhoA was reported to disrupt tight junction formation, which was inhibited by RhoE expression (Rubenstein et al. 2005). RhoE over-

expression also induces the localisation of β-catenin and ZO-1 to adherens junctions and tight junctions as well as inducing tight junction sealing (Rubenstein et al. 2005). Inhibition of RhoA induces keratinocyte dissociation through the loss of desmosomes (Waschke et al. 2006). Activation of RhoA accelerates the initial translocation of desmoplakin I/II to desmosomes but sustained RhoA activity compromised desmosomal maturation (Godsel et al. 2010). RhoA activity during the redistribution of desmoplakin I/II to desmosomes is not affected by p190RhoGAP (Godsel et al. 2010) but this still leaves the possibility that RhoE is regulating RhoA through Syx or through some unknown RhoE effector. RhoE is also known to regulate the actin cytoskeleton through ROCK I and through ROCK I independent pathways including Socius (Katoh et al. 2002; Riento et al. 2003; Komander et al. 2008). Further characterisation of the mechanism that regulate desmosomal assembly and disassembly will be important for understanding how these systems are disrupted in human disease.

In summary, I have shown that depletion of RhoE expression in keratinocytes results in alatered colony morphology with smaller cells and limited stratification. This phenotype is a consequence of increased expression of desmosomal proteins and increased number of desmosomes following depletion of RhoE.

CHAPTER 5 RHOE DEPLETION PROTECTS KERATINOCYTES FROM BOTH THE INTRINSIC AND EXTRINSIC APOPTOSIS PATHWAYS

5.1 Introduction

Apoptosis is a highly regulated process that is critical for normal epidermal homeostasis (Ziegler et al. 1994). Apoptosis can be initiated via two major pathways: the intrinsic pathway involving subcellular organelles or the extrinsic pathway, which involves the activation of death receptors in response to ligand binding (Servais et al. 2008). In this study, cisplatin treatment was used to induce the intrinsic pathway (Fulda et al. 2006). Cisplatin mediated DNA damage induces p53 up-regulation (Wei et al. 2007), which leads to the activation of Bax and MOMP resulting in cytochrome c release and the initiation of the caspase cascade, through caspase 9 activation, resulting in cell death (Servais et al. 2008). The extrinsic apoptosis pathway was induced using TRAIL treatment (Walczak et al. 2000). TRAIL binds to its death receptors inducing receptor trimerisation and recruitment of FADD and caspase 8 to the death domain, resulting in caspase 8 activation (Walczak et al. 2000). Active caspase 8 cleaves Bid, which in turn activates Bax resulting in MOMP and the initiation of the caspase cascade resulting in cell death (Yamada et al. 1999). In each case both pathways converge to a final common pathway involving the activation of the caspase cascade (Ghobrial et al. 2005).

This chapter focuses on the role of RhoE in keratinocyte apoptosis. RhoE knock-down keratinocyte cell lines were used to study the effect of RhoE depletion on apoptosis induced via

the intrinsic and extrinsic pathways. RhoE depletion was shown to protect keratinocytes from apoptosis induced by both pathways and two possible explanations of how RhoE depletion protects from apoptosis have been identified: altered translocation of Bax and a possible role for the desmosomal protein plakoglobin.

5.2 Results

5.2.1 Prolonged Y-27632 treatment protects keratinocytes from apoptosis induced by cisplatin

The pharmacological inhibitor Y-27632 inhibits ROCK I/II activity and has been used to study the function of these kinases (Ishizaki et al. 2000). As part of an analysis of ROCK function in apoptosis, HaCaT cells were incubated in the presence or absence of 5 μM Y-27632 for up to 96 hours before cisplatin was added to induce apoptosis via the intrinsic pathway. Cells were also grown on cover slips and treated with Y-27632 for up to 96 hours before being fixed and stained with Phalloidin, to visualise F-actin. At each time point 24-96 hours Y-27632 treated HaCaTs showed a loss of actin stress fibres (Figure 38A) reminiscent of Y-27632 being an inhibitor of ROCK I/II (Ishizaki et al. 2000). At 0, 24, 48, 72 and 96 hours whole cell lysates were prepared and analysed by immunoblotting with antibodies against full-length caspase 9 and tubulin. A loss of full-length caspase 9 expression, under apoptotic stimulation, indicates a loss of caspase 9 due to cleavage of the full-length protein during apoptosis (Slee et al. 1999; Green et al. 2005). Caspase 9 auto-cleavage and activation occurs after MOMP and the formation of the apoptosome (Acehan et al. 2002). In the absence of Y-27632 and in early Y-27632 treatment

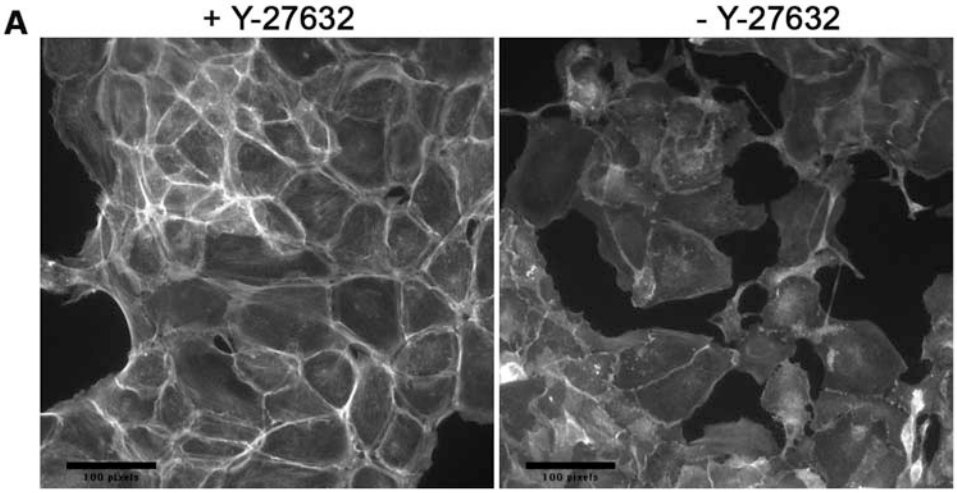
A
+ Y-27632
- Y-27632
100 pixels
100 pixels

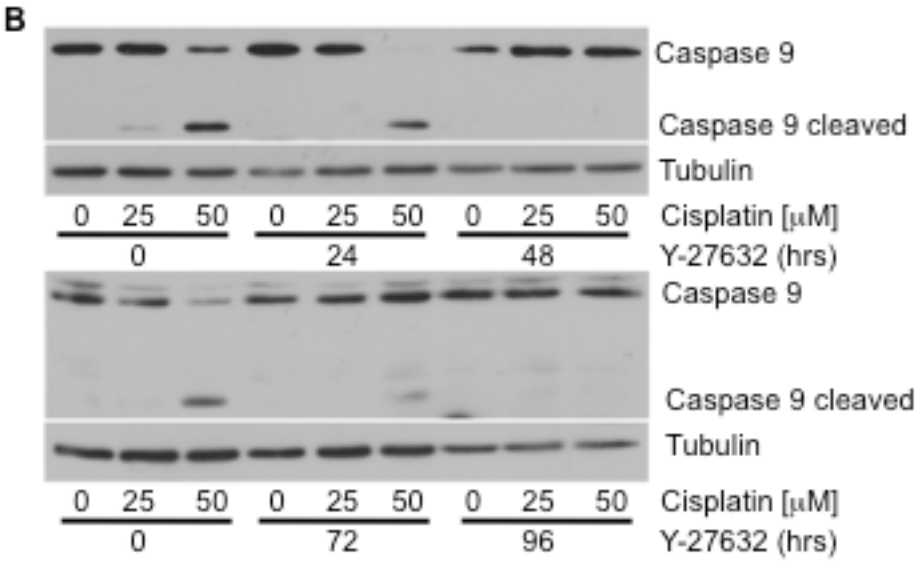
B
Caspase 9
Caspase 9 cleaved
Tubulin
0 25 50 0 25 50 0 25 50
Cisplatin [μM]
0 24 48
Y-27632 (hrs)
Caspase 9
Caspase 9 cleaved
Tubulin
0 25 50 0 25 50 0 25 50
Cisplatin [μM]
0 72 96
Y-27632 (hrs)

Figure 38 Prolonged Y-27632 treatment protects keratinocytes from cisplatin-induced apoptosis.

HaCaT cells were treated with 5 μM of Y-27632 for up to 96 hours with time points every 24 hours. Fresh Y-27632 was added every 12 hours and 24 hours prior to whole cell lysis cisplatin was added to induce apoptosis. Cover slips in each condition were fixed and stained with Phalloidin to visualise F-actin. **A** Data presented are representative immunofluorescent images from three separate experiments, of the actin cytoskeleton in HaCaT cells treated with Y-27632, with the gain and exposure time remaining constant (scale bar 30 μm). In the presence of Y-27632 a loss of actin stress fibres is observed. **B** Whole cell lysates were prepared and analysed by immunoblotting using antibodies against full-length caspase 9 and tubulin (loading control). Data presented are representative immunoblots of three separate experiments.

time points, treatment of HaCaT cells with 50 μM cisplatin resulted in cleavage of caspase 9 indicated by a loss of full-length caspase 9 expression and an increase in the level of the cleaved form. Prolonged treatment (>48 hours) with Y-27632 resulted in protection from cisplatin-induced caspase 9 cleavage (Figure 38B).

5.2.2 Prolonged Y-27632 treatment decreased RhoE expression in keratinocytes

As RhoE is a known ROCK I binding partner (Riento et al. 2003) and has been implicated in having a role in apoptosis (Bektic et al. 2005; Ongusaha et al. 2006; Boswell et al. 2007; Poch et al. 2007) RhoE expression was analysed in cells treated with Y-27632. HaCaT cells were incubated in the presence or absence of 5μM Y-27632 for up to 96 hours. Lysates were prepared every 24 hours and RhoE expression was analysed using immunoblotting (Figure 39). After 24 hours of Y-27632 treatment a decrease in RhoE expression was detected compared to the untreated cells. The expression of RhoE was further decreased at 48 hours and maintained at this level at later time points.

At the concentration Y-27632 was used at (5μM) during these experiments it is known to inhibit ROCK I/II and PRK-2 (Darenfed et al. 2007). ROCK I, but not ROCK II, has been shown to bind to and phosphorylate RhoE increasing the protein stability of RhoE (Riento et al. 2003; Riento et al. 2005). There is no evidence on whether RhoE and PRK-2 interact so I investigated whether ROCK I depletion would decrease RhoE expression using ROCK II-depleted cells as a control. To deplete expression of ROCK I and ROCK II, HaCaT cells were transiently

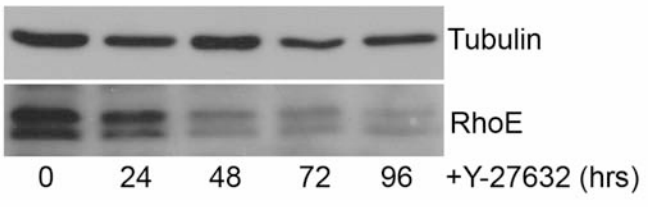

Figure 39 Prolonged Y-27632 treatment decreased RhoE expression in keratinocytes.

HaCaT cells were incubated with 5 μM of Y-27632 for up to 96 hours. Fresh Y-27632 was added every 12 hours and whole cell lysates were prepared every 24 hours. Immunoblotting using antibodies against RhoE and tubulin was used to detect the level of endogenous RhoE or as a loading control. Data presented are representative immunoblots of three separate experiments.

transfected with specific siRNA oligos targeting ROCK I (RI) or ROCK II (RII) or in combination ROCK I/II (RI/II). Expression of these proteins was knocked down for 96 hours prior to whole cell lysis. Immunoblotting was used to detect the expression of endogenous ROCK I, ROCK II and RhoE. Specific depletion of ROCK I and ROCK II expression was confirmed when compared to control lanes. However, no change in RhoE expression was detected (Figure 40).

These data demonstrate that prolonged Y-27632 treatment of HaCaT cells protects from cisplatin-induced apoptosis. Prolonged Y-27632 treatment also decreases RhoE expression. Interestingly, no loss of RhoE expression was detected when either ROCK I or ROCK II was depleted.

5.2.3 RhoE depletion protects keratinocytes from apoptosis induced by cisplatin

Having observed a decrease in RhoE expression when cells were treated with Y-27632 I analysed whether the loss of RhoE played a role in keratinocyte apoptosis. HaCaT cells in which RhoE (shRhoE) expression was stably knocked-down by shRNA were treated with cisplatin for 24 hours prior to lysis. Caspase 9 cleavage was analysed using immunoblotting. In control cells a decrease in the level of full-length caspase 9 was detected in cells treated with 25 μM and 50 μM cisplatin when compared to non-treated cells. However, no change in full-length caspase 9 was detected in RhoE-depleted cells (Figure 41).

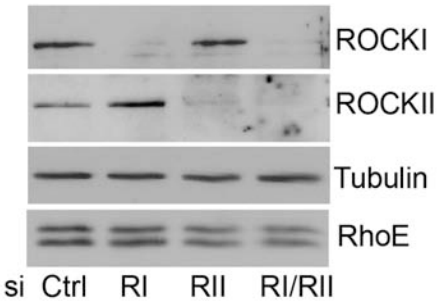

Figure 40 ROCK I, ROCK II and ROCK I/II depletion has no affect on endogenous RhoE expression.

In HaCaT cells expression of ROCK I, ROCK II and ROCK I/II (and in combination) were depleted for 96 hours prior to whole cell lysis by transiently transfecting cells with siRNA oligos. Immunoblotting was used to detect the level of endogenous ROCK I, ROCK II, RhoE and tubulin. Data presented are representative immunoblots of three separate experiments.

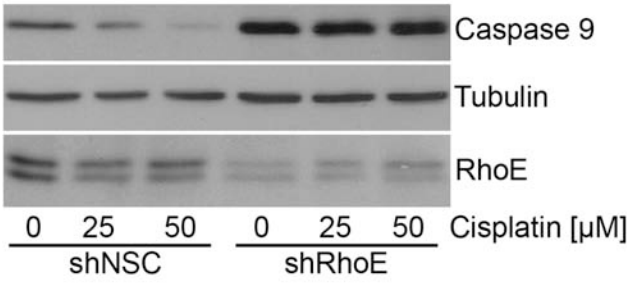

Figure 41 Keratinocytes depleted of RhoE are protected from cisplatin-induced caspase 9 cleavage.

HaCaT cells stably depleted of RhoE (shRhoE) and control cells (shNSC) were treated with cisplatin for 24 hours prior to lysis. Immunoblotting was used to detect the expression of full-length caspase 9, RhoE and tubulin. Data presented are representative immunoblots of three separate experiments.

An alternative method for assessing apoptosis is to analyse the number of condensed nuclei (Nakagawa et al. 2000). Nuclear condensation occurs late in apoptosis after MOMP and caspase 3 activation and is due to the cleavage of DNA by AIF, endonuclease G and caspase 3 targets (Reed 1997; Susin et al. 1999; Li et al. 2001). shRhoE and shNSC cells were seeded onto cover slips for 24 hours before treatment with cisplatin for 24 hours prior to fixation. Cover slips were then stained with Hoechst 33342 to visualise the nuclei and the percentage of condensed nuclei was analysed. With increasing concentrations of cisplatin the percentage of cells with condensed nuclei is significantly higher in control (shNSC) cells compared to RhoE-depleted (shRhoE) cells (Figure 42). The percentage of cells with condensed nuclei rises from ~5% at 0 μM to 25% at 25 μM and to ~75% at 50 μM cisplatin in control cells whereas no appreciable increase in the percentage of cells with condensed nuclei was observed in RhoE-depleted cells (~5% at 0 μM to ~10% at 50 μM cisplatin). Indicating that the level of nuclear condensation is occurring at a frequency close to the basal rate in shRhoE cells, in the presence of cisplatin. Taken together these data suggest that RhoE-depletion protects keratinocytes from apoptosis induced by cisplatin.

Dimethylformamide (DMF) was used as a solvent for cisplatin. To analyse whether DMF had any effect on shRhoE and shNSC cells, these cells were treated with DMF for 24 hours prior to lysis. DMF concentrations were the same as cells were exposed to during the cisplatin-induced apoptotic studies. Immunoblotting was used to detect the levels of caspase 9, RhoE and tubulin. No change in the level of full-length caspase 9 was detected in shNSC or shRhoE cells with increasing concentration of DMF (Figure 43). The percentage of condensed nuclei was also

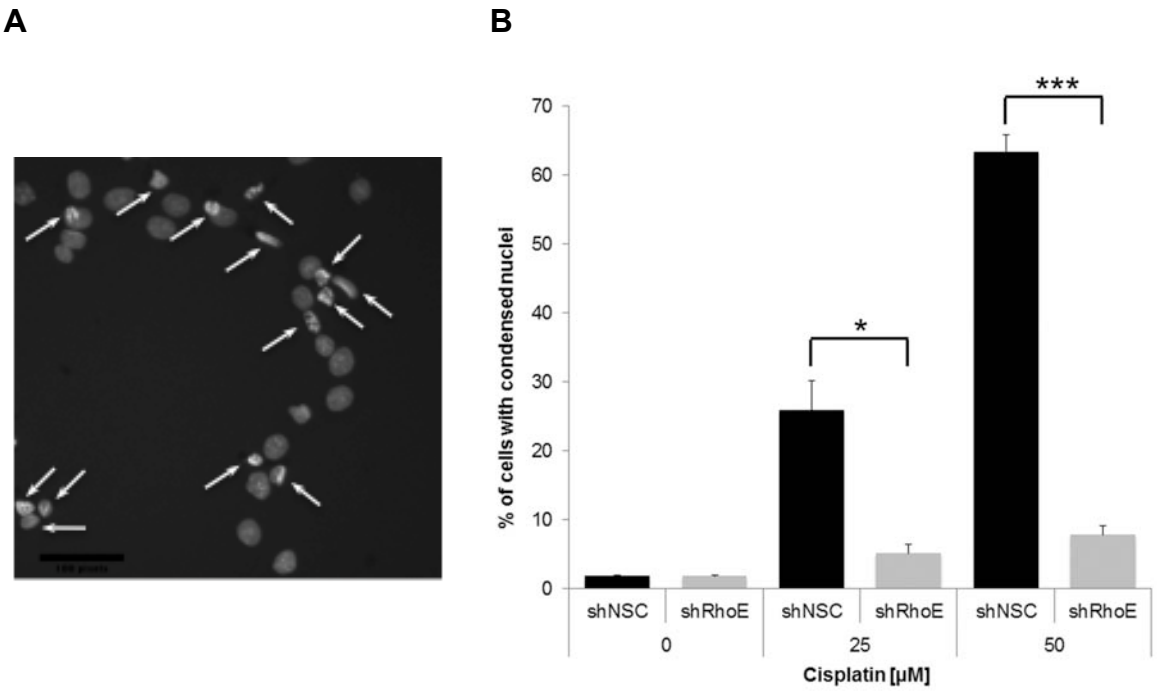

Figure 42 Keratinocytes depleted of RhoE are protected from cisplatin-induced nuclear condensation.

A Examples of condense nuclei in HaCaT cells treated with 50 μM cisplatin for 24 hours fixed and stained with Hoechst 33342. **B** HaCaT cells stably depleted of RhoE (shRhoE) and control (shNSC) cells were seeded onto cover slips and treated with cisplatin for 24 hours prior to fixation. Cover slips were then stained with Hoechst 33342 to visualise the nuclei. Both the total number of nuclei and condensed nuclei were counted with approximately 500 cells counted per condition. The percentage of cells with condensed nuclei was analysed and the data presented are the mean, standard error and t-tests of three separate experiments (* $P<0.05$ and *** $P<0.001$).

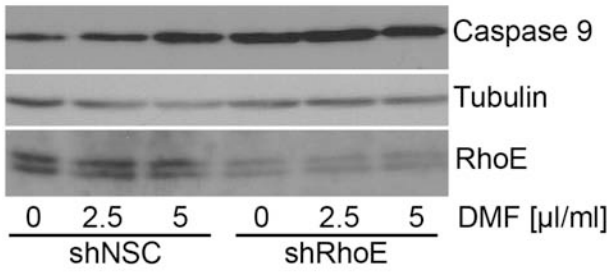

Figure 43 Caspase 9 cleavage was not induced by DMF treatment.

HaCaT cells stably depleted of RhoE (shRhoE) and control (shNSC) cells were incubated with DMF for 24 hours prior to lysis. Immunoblotting was used to detect the level of full-length caspase 9 cleavage, RhoE and tubulin. Data presented are representative immunoblots of three separate experiments.

analysed in these cells. No increase in the percentage of cells with condensed nuclei was detected in either shRhoE or shNSC cells with increasing concentrations of DMF, with the percentage of condensed nuclei remaining at ~5% (Figure 44). At the concentrations used in these experiments DMF was not inducing apoptosis in HaCaT cells.

5.2.4 Transient knock-down of RhoE expression protects keratinocytes from cisplatin-induced apoptosis

Previous data (Section 3.2.3) revealed differences in cell cycle progression data generated using stable RhoE-depleted (shRhoE) and transient RhoE-depleted (siRhoE) cell lines. To verify data on apoptosis generated using the stably RhoE-depleted cell lines, siRNA was also used to deplete RhoE expression in HaCaT cells. HaCaT cells were transiently transfected with siRNA oligos targeting RhoE (siRhoE) and a non-silencing control (siCtrl). siRhoE cells were depleted of RhoE for 144 hours before being treated with cisplatin for 24 hours prior to lysis. Immunoblotting was used to detect the level of full-length caspase 9 and RhoE expression. A decrease in the level of full-length caspase 9 was detected in control siCtrl cells treated with 50 μM cisplatin. However, no change in the level of full-length caspase 9 was detected in siRhoE cells in the presence of cisplatin (Figure 45), indicating that siRhoE cells were not undergoing caspase 9 cleavage in the presence of cisplatin. The percentage of cells with condensed nuclei was also analysed in these cells. With increasing concentrations of cisplatin the percentage of cells with condensed nuclei was significantly higher in control (siCtrl) cells compared to RhoE-depleted (siRhoE) cells (Figure 46). The percentage of cells with condensed nuclei rose from

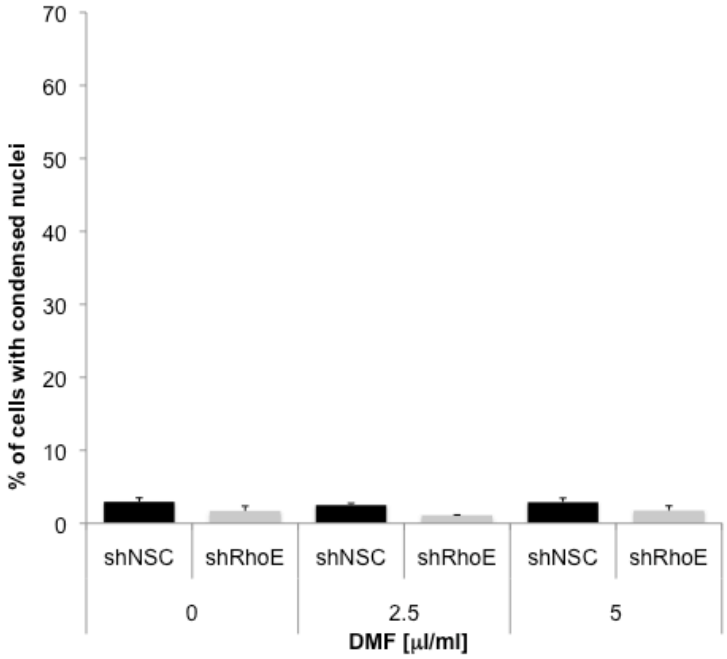

Figure 44 Nuclear condensation was not induced by DMF treatment.

HaCaT cells stably depleted of RhoE (shRhoE) and control (shNSC) cells were seeded onto cover slips and incubated with DMF for 24 hours prior to fixation. Cover slips were then stained with Hoechst 33342 to visualise the nuclei. Both the total number of nuclei and condensed nuclei were counted, with approximately 500 cells counted per condition. The percentage of cells with condensed nuclei was analysed and the data presented are the mean and standard error of three separate experiments.

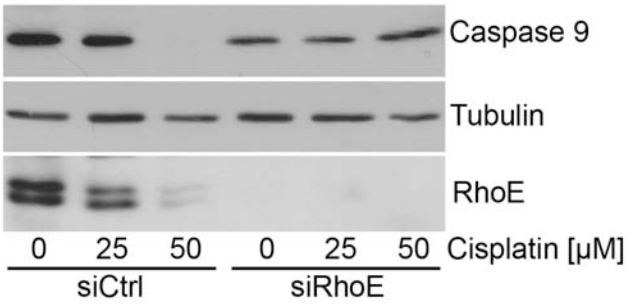

Figure 45 Transient RhoE depletion protects keratinocytes from cisplatin-induced caspase 9 cleavage.

HaCaT cells transiently transfected with siRNA oligo A to depleted RhoE (siRhoE) and control (siCtrl) cells were treated with cisplatin for 24 hours prior to lysis. Immunoblotting was used to detect the expression of full-length caspase 9, RhoE and tubulin. Data presented are representative immunoblots of three separate experiments.

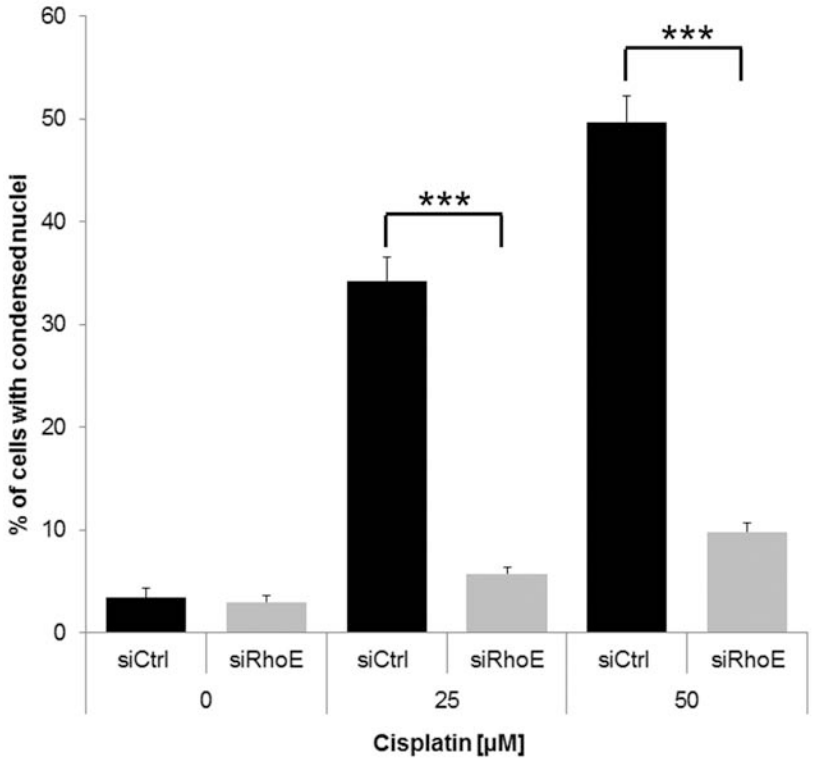

Figure 46 Transient RhoE depletion protects keratinocytes from cisplatin-induced nuclear condensation.

HaCaT cells transiently transfected with siRNA oligo A to depleted RhoE (siRhoE) and control (siCtrl) cells were seeded onto cover slips and treated with cisplatin for 24 hours prior to fixation. Cover slips were then stained with Hoechst 33342 to visualise the nuclei. Both the total number of nuclei and condensed nuclei were counted, with approximately 500 cells counted per condition. The percentage of cells with condensed nuclei was analysed and the data presented are the mean, standard error and t-tests of three separate experiments (*** $P<0.001$).

~5% at 0 μM to ~35% at 25 μM then to ~50% at 50 μM cisplatin whereas no appreciable increase in the percentage of cells with condensed nuclei was observed in RhoE-depleted cells (~5% at 0 μM to ~10% at 50 μM cisplatin). These data verify data generated from the stably RhoE-depleted cell line.

Cisplatin induces apoptosis in control cells, indicated by a loss of full-length caspase 9 as well as an increase in the percentage of cells with condensed nuclei. In contrast, keratinocytes depleted of RhoE were protected from cisplatin-induced apoptosis as no loss of full-length caspase 9 was detected and the percentage of cells with condensed nuclei remained close to basal levels during treatment with cisplatin.

5.2.5 Keratinocytes depleted of RhoE are protected from apoptosis induced by TRAIL

The above data indicate that RhoE depletion protects keratinocytes from cisplatin–induced apoptosis. Cisplatin induces the intrinsic-apoptosis pathway, so I was interested to see whether RhoE depletion could protect keratinocytes from the extrinsic-apoptosis pathway. To induce this pathway cells were treated with the tumour necrosis factor (TNF) related apoptosis-inducing ligand (TRAIL) (Walczak et al. 2000). HaCaT cells stably depleted of RhoE (shRhoE) and control (shNSC) cells were seeded onto cover slips and treated with 25 ng/ml TRAIL for up to 6 hours prior to fixation, with time points taken every 2 hours. In shNSC cells the percentage of cells with condensed nuclei increased with increased exposure to TRAIL from ~10% at 0 hours to ~20%, ~45% and ~55% at 2 hours, 4 hours and 6 hours of TRAIL treatment. However, the

percentage of shRhoE cells with condensed nuclei remained at ~10% throughout the 6 hours of TRAIL treatment (Figure 47). This indicates that the level of nuclear condensation was occurring at a basal rate in shRhoE cells whereas apoptosis was occurring in control cells in the presence of TRAIL.

shRhoE and shNSC cells were also treated with higher concentrations of TRAIL for 6 hours and apoptosis was analysed using immunoblotting and the percentage of cells with condensed nuclei. In shNSC cells a decrease in the level of full-length caspase 9 was detected at both 25 ng/ml and 50 ng/ml TRAIL when compared to controls. No change in the level of full-length caspase 9 was detected in shRhoE cells (Figure 48). With increasing concentrations of TRAIL the percentage of cells with condensed nuclei was significantly higher in control (shNSC) cells compared to RhoE-depleted (shRhoE) cells (Figure 49). In control cells the percentage of cells with condensed nuclei rose from ~10% at 0 ng/ml to ~60% at 25 ng/ml then to ~80% at 50 ng/ml TRAIL. However, no appreciable increase in the percentage of condensed nuclei was observed in RhoE-depleted cells (~10% at 0 ng/ml to ~20% at 50 ng/ml TRAIL).

RhoE-depleted cells were protected from TRAIL-induced apoptosis after 6 hours exposure. The effect of 24 hours of TRAIL exposure at 25ng/ml and 50ng/ml was also analysed in shRhoE and shNSC cells. Apoptosis was analysed using immunoblotting and the percentage of cells with condensed nuclei. In shNSC cells a decrease in the level of full-length caspase 9 was detected in the presence of TRAIL whereas no change in the level of full-length caspase 9 was detected in

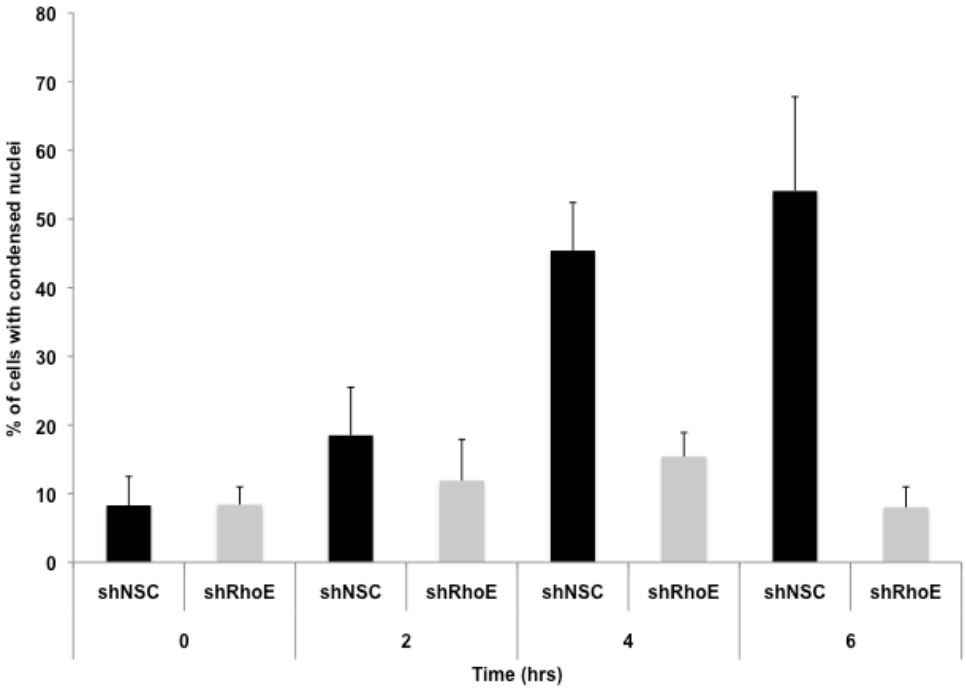

Figure 47 TRAIL-induced apoptosis time course in RhoE-depleted and control keratinocytes.

HaCaT cells stably depleted of RhoE (shRhoE) and control (shNSC) cells were seeded onto cover slips and treated with 25 ng/ml TRAIL for up to 6 hours prior to fixation, with time points taken every 2 hours. Cover slips were then stained with Hoechst 33342 to visualise the nuclei. Both the total number of nuclei and condensed nuclei were counted, with approximately 500 cells counted per condition. The percentage of cells with condensed nuclei was analysed and the data presented are the mean and standard deviation of one experiment.

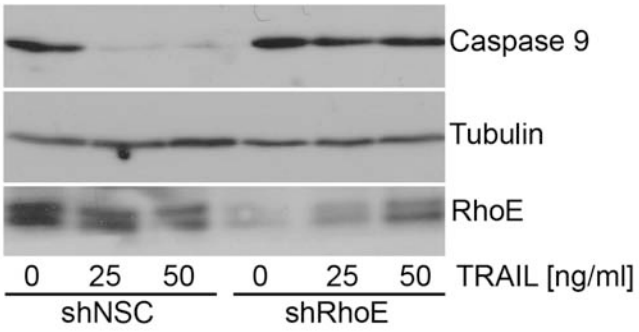

Figure 48 Keratinocytes depleted of RhoE are protected from TRAIL-induced caspase 9 cleavage.

HaCaT cells stably depleted of RhoE (shRhoE) and control (shNSC) cells were treated with TRAIL for 6 hours prior to lysis. Immunoblotting was used to detect the level of full-length caspase 9, RhoE and tubulin. Data presented are representative immunoblots of three separate experiments.

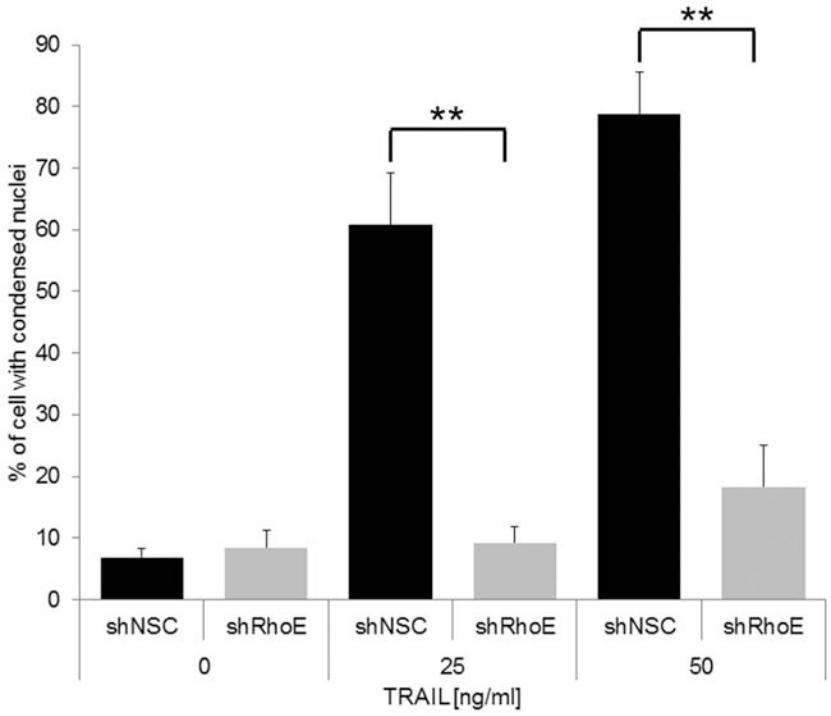

Figure 49 Keratinocytes depleted of RhoE are protected from TRAIL-induced nuclear condensation.

HaCaT cells stably depleted of RhoE (shRhoE) and control (shNSC) cells were seeded onto cover slips and treated with TRAIL for 6 hours prior to fixation. Cover slips were then stained with Hoechst 33342 to visualise the nuclei. Both the total number of nuclei and condensed nuclei were counted with approximately 500 cells counted per condition. The percentage of cells with condensed nuclei was analysed and the data presented are the mean, standard error and t-tests of three separate experiments (** $P<0.01$).

shRhoE cells (Figure 50). With increasing concentrations of TRAIL the percentage of cells with condensed nuclei was significantly higher in control (shNSC) cells compared to RhoE-depleted (shRhoE) cells (Figure 51). In shNSC cells the percentage of cells with condensed nuclei increased from ~5% at 0 ng/ml to ~50% at 25 ng/ml then to ~75% at 50ng/ml TRAIL. However, no appreciable increase in the percentage of cell with condensed nuclei was observed in RhoE-depleted cells (~5% at 0 ng/ml to ~15% at 50 ng/ml TRAIL). These data indicate that RhoE-depletion protects keratinocytes from apoptosis induced by TRAIL.

5.2.6 Transient knock-down of RhoE expression protects keratinocytes from TRAIL-induced apoptosis

To verify data on TRAIL-induced apoptosis generated using the shRhoE stably depleted cell lines, siRNA was used to deplete RhoE expression in HaCaT cells. Transiently RhoE-depleted (siRhoE) and control (siCtrl) HaCaT cells were treated with TRAIL for 24 hours prior to lysis. Immunoblotting was used to detect the level of full-length caspase 9 and RhoE. In siCtrl cells a decrease in the level of full-length caspase 9 was detected in the presence of TRAIL. However, no change in the level of full-length caspase 9 was detected in siRhoE cells (Figure 52). The percentage of cells with condensed nuclei was also analysed in these cells. With increasing concentrations of TRAIL the percentage of condensed nuclei was significantly higher in control (siCtrl) cells compared to RhoE-depleted (siRhoE) cells (Figure 53). In siCtrl cells the percentage of cells with condensed nuclei increased from ~5% at 0 ng/ml to ~45% at 50 ng/ml TRAIL. However, no appreciable increase in the percentage of cells with condensed nuclei was

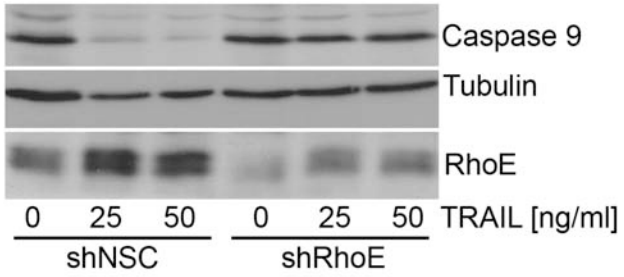

Figure 50 Keratinocytes depleted of RhoE are protected from TRAIL-induced caspase 9 cleavage.

HaCaT cells stably depleted of RhoE (shRhoE) and control (shNSC) cells were treated with TRAIL for 24 hours prior to lysis. Immunoblotting was used to detect the level of full-length caspase 9, RhoE and tubulin. Data presented are representative immunoblots of three separate experiments.

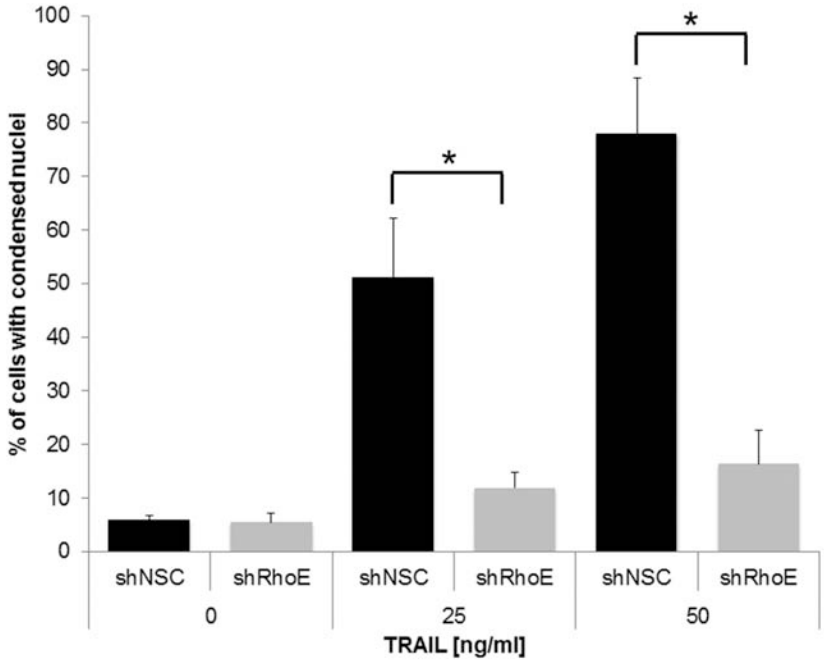

Figure 51 Keratinocytes depleted of RhoE are protected from TRAIL-induced nuclear condensation.

HaCaT cells stably depleted of RhoE (shRhoE) and control (shNSC) cells were seeded onto cover slips and treated with TRAIL for 24 hours prior to fixation. Cover slips were then stained with Hoechst 33342 to visualise the nuclei. Both the total number of nuclei and condensed nuclei were counted with approximately 500 cells counted per condition. The percentage of cells with condensed nuclei was analysed and the data presented are the mean, standard error and t-tests of three separate experiments (* $P<0.05$).

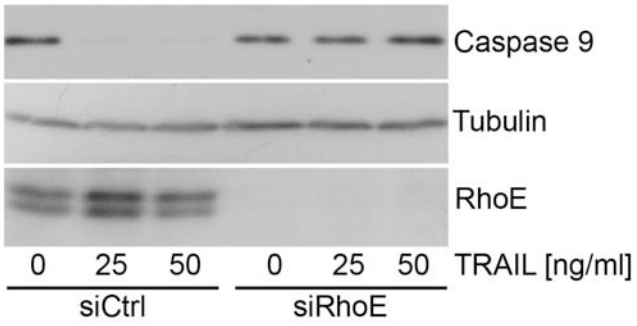

Figure 52 Keratinocytes transiently depleted of RhoE are protected from TRAIL-induced caspase 9 cleavage.

HaCaT cells transiently depleted of RhoE (siRhoE) and control (siCtrl) cells were treated with TRAIL for 24 hours prior to lysis. Immunoblotting was used to detect the level of full-length caspase 9, RhoE and tubulin. Data presented are representative immunoblots of three separate experiments.

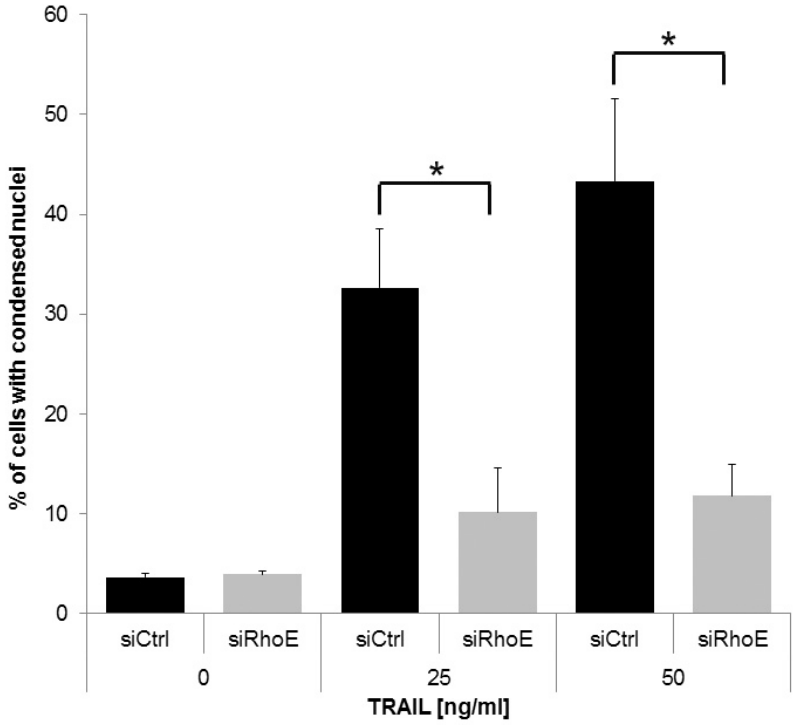

Figure 53 Keratinocytes transiently depleted of RhoE are protected from TRAIL-induced nuclear condensation.

HaCaT cells transiently depleted of RhoE (siRhoE) and control (siCtrl) cells were seeded onto cover slips and treated with TRAIL for 24 hours prior to fixation. Cover slips were then stained with Hoechst 33342 to visualise the nuclei. Both the total number of nuclei and condensed nuclei were counted with approximately 500 cells counted per condition. The percentage of cells with condensed nuclei was analysed and the data presented are the mean, standard error and t-tests of three separate experiments (* $P<0.05$).

observed in RhoE-depleted cells (~5% at 0 ng/ml to ~15% at 50 ng/ml TRAIL). These data verify the data generated from the stably RhoE-depleted cell line.

TRAIL induces apoptosis in control cells, indicated by a loss of full-length caspase 9 as well as an increase in the percentage of cells with condensed nuclei. In contrast, keratinocytes depleted of RhoE are protected from TRAIL-induced apoptosis as no loss of caspase 9 was detected and the percentage of cells with condensed nuclei remained close to basal levels during treatment with TRAIL.

5.2.7 Re-expression of RhoE restores sensitivity to both cisplatin- and TRAIL-induced apoptosis in keratinocytes

Another method for verifying the apoptosis data generated using RhoE-depleted cell lines was to rescue RhoE expression in these cells. To rescue expression of RhoE in the shRhoE cell line, cells were transiently transfected with pCVM5FlagRhoE, containing cDNA encoding wild type mouse RhoE to generate shRhoE:RhoE wt cells. As controls both shRhoE and shNSC cells were transiently transfected with pCMV5FlagEV (empty vector). shRhoE:RhoE wt, shRhoE:EV and shNSC:EV cell lines were treated with cisplatin for 24 hours prior to lysis. Immunoblotting was used to detect the level of full-length caspase 9 and RhoE. Reconstitution of RhoE was detected and is indicated by the arrow on the third panel (Figure 54). In both shNSC:EV cells and shRhoE:RhoE wt cells a decrease in the level of full-length caspase 9 was detected in the presence of cisplatin whereas no change in the level of full-length caspase 9 was observed in

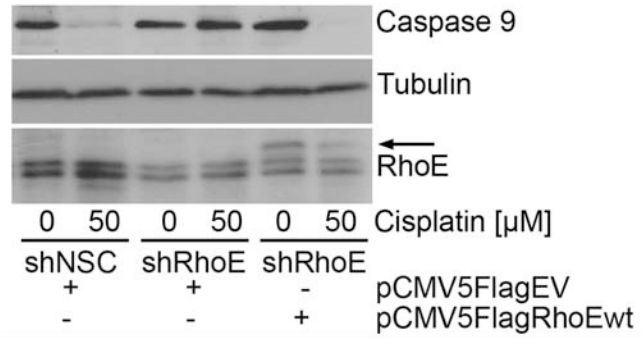

Figure 54 Re-expression of RhoE restores sensitivity to cisplatin-induced caspase 9 cleavage.

Stably RhoE-depleted (shRhoE) and control (shNSC) HaCaT cells were transiently transfected with pCMV5 FlagRhoE wild type (RhoE wt) or pCMV5 empty vector for 48 hours. The shRhoE:RhoE wt, shRhoE:EV and shNSC:EV cell lines were treated with cisplatin for 24 hours prior to lysis. Immunoblotting was used to detect the level of full-length caspase 9, RhoE and tubulin. Data presented are representative immunoblots from three separate experiments. Expression of exogenous murine RhoE is indicated by the arrow on the third panel.

shRhoE:EV cells. The percentage of condensed nuclei was also analysed in these cells. In the presence of cisplatin the percentage of cells with condensed nuclei increased significantly in the shNSC:EV cells and shRhoE:RhoE wt cells compared to shRhoE:EV cells (Figure 55). The percentage of cells with condensed nuclei in shNSC:EV cells and shRhoE:RhoE wt increased from ~10% at 0 μM to ~55% at 50 μM cisplatin. However, no appreciable increase in the percentage of cells with condensed nuclei was detected in shRhoE:EV cells with cisplatin treatment (from ~10% to ~15% with treatment). Cisplatin failed to induce apoptosis in shRhoE:EV cells, indicated by no loss of full-length caspase 9 and close to basal rate of condensed nuclei. However, apoptosis was induced by cisplatin in both shNSC:EV and shRhoE:RhoE cell lines, indicated by a loss of full-length caspase 9 and increased frequency of condensed nuclei. These data indicate that reconstitution of RhoE expression restores sensitivity to cisplatin-induced apoptosis in keratinocytes.

The effect of RhoE re-expression was also analysed following TRAIL treatment. shRhoE:RhoE wt, shRhoE:EV and shNSC:EV cell lines were treated with TRAIL for 24 hours prior to lysis. Immunoblotting was used to detect the level of full-length caspase 9 and RhoE. Reconstitution of RhoE was detected and is indicated by the arrow on the third panel (Figure 56). In both shNSC:EV and shRhoE:RhoE wt cells a decrease in the level of full-length caspase 9 was detected in the presence of TRAIL whereas no change in the level of full-length caspase 9 was detected in shRhoE:EV cells. The percentage of condensed nuclei was also analysed in these cells. In the presence of TRAIL the percentage of cells with condensed nuclei increased significantly in the shNSC:EV and shRhoE:RhoE wt cells compared to shRhoE:EV cells

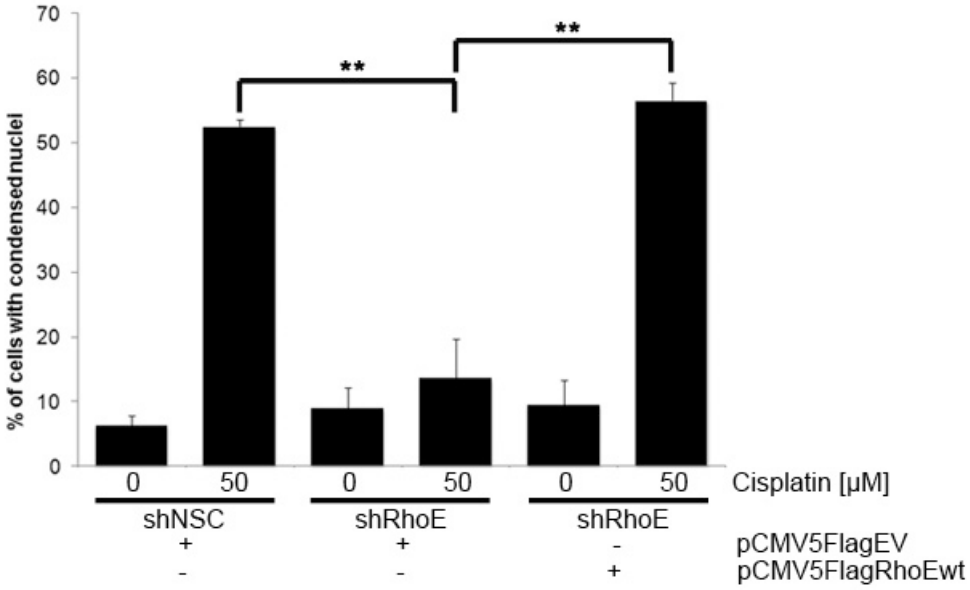

Figure 55 Re-expression of RhoE restores sensitivity to cisplatin-induced nuclear condensation.

Stably RhoE-depleted (shRhoE) and control (shNSC) HaCaT cells were transiently transfected with pCMV5FlagRhoE wild type (RhoE wt) or pCMV5 empty vector. The shRhoE:RhoE wt, shRhoE:EV and shNSC:EV cell lines were seeded onto cover slips and treated with cisplatin for 24 hours prior to fixation. Cover slips were then stained with Hoechst 33342 to visualise the nuclei. Both the total number of nuclei and condensed nuclei were counted with approximately 400 cells counted per condition. The percentage of cells with condensed nuclei was analysed and the data presented are the mean, standard error and t-tests of three separate experiments (**P<0.01).

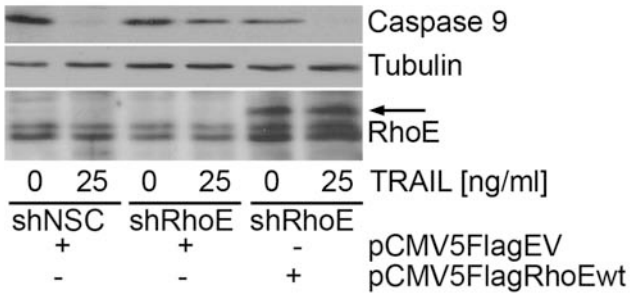

Figure 56 Re-expression of RhoE restores sensitivity to TRAIL-induced caspase 9 cleavage.

Stably RhoE-depleted (shRhoE) and control (shNSC) HaCaT cells were transiently transfected with pCMV5 FlagRhoE wild type (RhoE wt) or pCMV5 empty vector. The shRhoE:RhoE wt, shRhoE:EV and shNSC:EV cell lines were treated with TRAIL for 24 hours prior to lysis. Immunoblotting was used to detect the level of full-length caspase 9, RhoE and tubulin. Data presented are representative immunoblots from three separate experiments. Expression of exogenous murine RhoE is indicated by the arrow on the third panel.

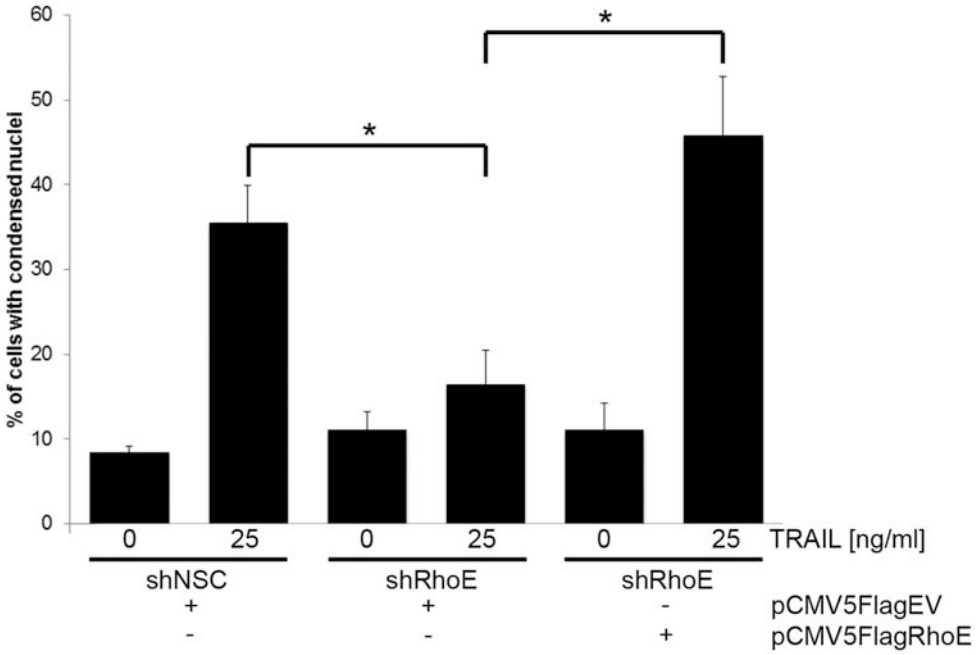

Figure 57 Re-expression of RhoE restores sensitivity to TRAIL-induced nuclear condensation.

Stably RhoE-depleted (shRhoE) and control (shNSC) HaCaT cells were transiently transfected with pCMV5 FlagRhoE wild type (RhoE wt) or pCMV5 empty vector. The shRhoE:RhoE wt, shRhoE:EV and shNSC:EV cell lines were seeded onto cover slips and treated with TRAIL for 24 hours prior to fixation. Cover slips were then stained with Hoechst 33342 to visualise the nuclei. Both the total number of nuclei and condensed nuclei were counted with approximately 400 cells counted per condition. The percentage of cells with condensed nuclei was analysed and the data presented are the mean, standard error and t-tests of three separate experiments (* $P<0.05$).

(Figure 57). The percentage of condensed nuclei in shNSC:EV and shRhoE:RhoE wt cells increased from ~10% at 0 ng/ml to ~35% and ~45% at 25 ng/ml TRAIL. However, no appreciable increase in the percentage of cells with condensed nuclei was detected in shRhoE:EV cells with TRAIL treatment (from ~10% to ~15% with treatment). TRAIL failed to induce apoptosis in shRhoE:EV cells, indicated by no loss of full-length caspase 9 and close to basal rate of condensed nuclei. However, apoptosis was induced by TRAIL in both shNSC:EV and shRhoE:RhoE wt cell lines, indicated by a loss of full-length caspase 9 and increased frequency of condensed nuclei. These data indicate that reconstitution of RhoE expression restores sensitivity to TRAIL-induced apoptosis in keratinocytes.

Taken together these data imply that re-expression of RhoE restores keratinocyte sensitivity to both cisplatin- and TRAIL-induced apoptosis.

5.2.8 Bax translocation is altered in RhoE depleted cells

Both the intrinsic and extrinsic pathways, induced by cisplatin and TRAIL, converge to a final common pathway involving the activation of Bax, which leads to MOMP and the initiation of the caspase cascade (Yamada et al. 1999; Ghobrial et al. 2005; Servais et al. 2008). RhoE has been implicated in the regulation of Bax expression, with the over-expression of RhoE suppressing Bax expression (Li et al. 2009). Endogenous Bax expression was analysed in both stably depleted RhoE (shRhoE) and transiently depleted RhoE (siRhoE) cell lines using immunoblotting. No differences in Bax expression was detected between RhoE depleted and

control HaCaT cells (Figure 58A & B). I then analysed whether the induction of apoptosis altered Bax expression and if there were any differences between RhoE depleted and control cells. shRhoE and shNSC HaCaT cells were treated with cisplatin for 24 hours prior to lysis. Immunoblotting was used to detect the expression of full-length caspase 9, Bax, RhoE and tubulin (Figure 59). A decrease in the level of full-length caspase 9 was detected in the presence of cisplatin in shNSC cells whereas no change in the level of full-length caspase 9 was detected in shRhoE cells. No changes in Bax expression were detected in either shRhoE or shNSC cells in response to cisplatin treatment. Although apoptosis was induced in shNSC cells and prevented in shRhoE cells treated with cisplatin, indicated by caspase 9 cleavage, no change in Bax expression was detected in either cell line.

During apoptosis activated Bax is translocated from the cytoplasm to the mitochondrial membrane and mediates MOMP by inserting into the outer mitochondrial membrane forming pore-like structures (Korsmeyer et al. 2000; Basanez et al. 2002). The change from cytoplasmic to mitochondrial localised Bax can be seen using immunofluorescent microscopy as diffuse to punctate Bax staining localised to the mitochondria (Wolter et al. 1997) (Figure 60A). This method was used to analyse Bax translocation in RhoE depleted cells treated with TRAIL. shRhoE and shNSC HaCaT cells were seeded onto cover slips and treated with TRAIL for 6 hours. To visualise the mitochondria the cells were incubated with MitoTracker Red for 45 minutes prior to fixation. Cover slips were then stained with Bax and Hoechst 33342 to visualise Bax localisation and nuclei. To illustrate Bax translocation, epifluorescent images were taken of shNSC cells after TRAIL treatment. In most cells Bax staining was diffuse but in cells that were

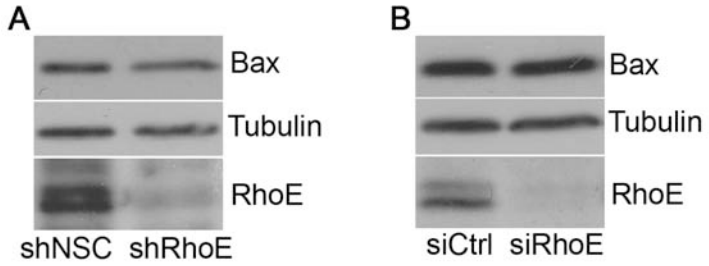

Figure 58 Bax expression is unchanged in RhoE depleted keratinocytes.

Whole cell lysates were prepared from HaCaT cell lines depleted of RhoE by **A** shRNA and **B** siRNA. Bax, RhoE and tubulin expression was analysed by immunoblotting. Data presented are representative immunoblots of three separate experiments.

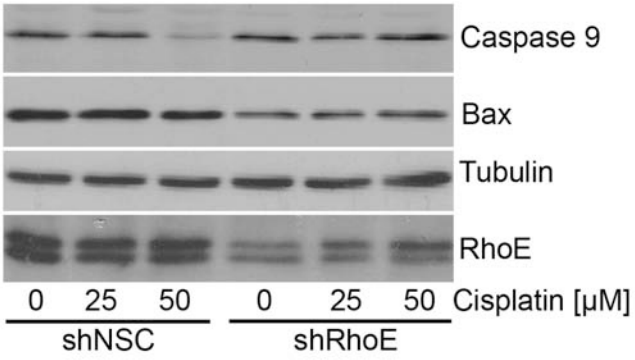

Figure 59 Bax expression is unchanged in RhoE-depleted and control keratinocytes treated with cisplatin.

Stably RhoE-depleted (shRhoE) and control (shNSC) cells were treated with cisplatin for 24 hours prior to lysis. Caspase 9 cleavage and the expression level of Bax, RhoE and tubulin were analysed using immunoblotting. Data presented are representative immunoblots from two separate experiments.

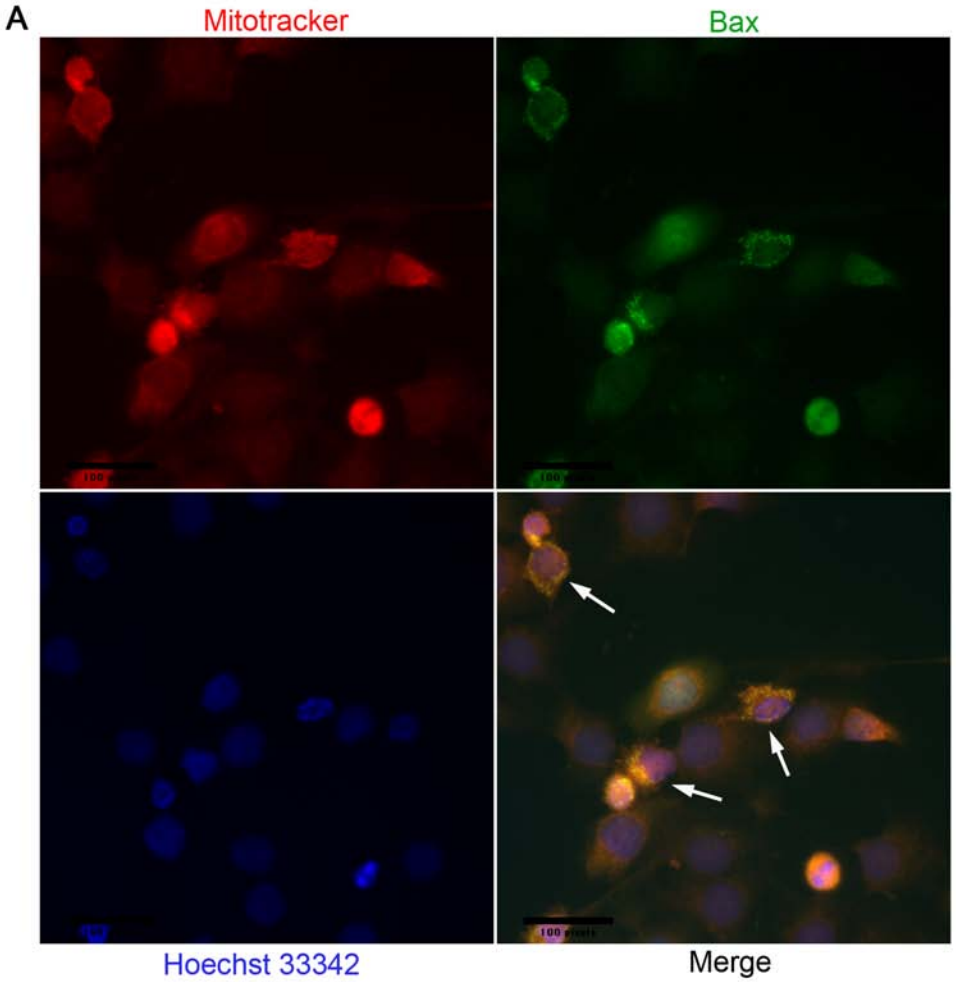
A
Mitotracker
Bax
Hoechst 33342
Merge
B
% cells with punctate Bax
30
25
20
15
10
5
0
shNSC
shRhoE
shNSC
shRhoE
0
6
Time (hrs)

Figure 60 The percentage of cells with punctate Bax staining following TRAIL treatment is decreased in RhoE-depleted cells.

Stably RhoE-depleted (shRhoE) and control (shNSC) HaCaT cells were seeded onto cover slips and treated with 25 ng/ml TRAIL for 6 hours. To visualise the mitochondria the cells were incubated with 250 ng/ml MitoTracker Red for 45 minutes prior to fixation. Cover slips were then stained with Bax and Hoechst 33342 to visualise Bax localisation and the nuclei. **A** Epifluorescent images were taken, using a 40x lens, of shNSC cells after 6 hours of TRAIL treatment to illustrate punctate Bax staining co-localising with mitochondria. Bax green, mitochondria red, merge yellow and nuclei blue. Cells scored as having punctate Bax staining are indicated with arrows (scale bar 30 μm). **B** The total number of nuclei and cells with punctate Bax staining were counted, with approximately 200 cells counted per condition. Data presented are the mean and standard error of two separate experiments.

undergoing Bax translocation, Bax staining was punctate (Green). Mitochodria staining (Red) co-localised with punctate Bax staining (Merge) (Figure 60A). To analyse the percentage of cells with punctate Bax staining the total number of nuclei and cells with punctate Bax staining and were counted. The condition of the cells and nuclei were also taken into account. If a cell had become rounded or if the nucleus was fragmented the cell was not included in the count contributing to punctate Bax staining. Examples of cells included in counts are indicated with arrows in Figure 60A. The percentage of cells with punctate Bax staining in both shNSC and shRhoE cells in the absences of TRAIL treatment was ~2% (Figure 60B). With TRAIL treatment this was increased to ~22% in shNSC cells and ~6% in shRhoE cells, suggesting the translocation of Bax was disrupted in RhoE-depleted keratinocytes.

5.2.9 Relocalised plackoglobin protects keratinocytes depleted of RhoE from apoptosis

Previous data (Section 4.2.1) revealed that RhoE depletion altered keratinocyte colony morphology from a 2D spread monolayer phenotype in control cells, to a 3D compacted stratified phenotype. The altered colony morphology was induced by RhoE depletion increasing the expression of desmosomal proteins and number of desmosomes (Section 4.2.3 & 4.2.4). In low calcium conditions both adherens junctions and desomsomes are disrupted (Chitaev et al. 1997; Jamora et al. 2002), resulting in the loss of cell-cell adhesion in both control and RhoE-depleted cells and reverting the RhoE-depleted colony morphology back to a control phenotype (Section 4.2.5). The effects of RhoE depletion on keratinocyte apoptosis in low calcium conditions were analysed to investigate whether cell-cell adhesion was playing a role in

protecting keratinocytes from apoptosis. Transiently RhoE-depleted (siRhoE) and control (siCtrl) HaCaT cells were incubated in normal or low calcium medium for 24 hours prior to and then during treatment with cisplatin for 24 hours prior to lysis. Immunoblotting was used to detect the level of caspase 9 cleavage and RhoE expression (Figure 61). In normal conditions a decrease in the level of full-length caspase 9 was detected in siCtrl cells in the presence of cisplatin whereas no loss of full-length caspase 9 was detected in siRhoE cells. In low calcium conditions a decrease in the level of full-length caspase 9 in the presence of cisplatin was detected in both siCtrl and siRhoE cell lines.

Previous data (Section 4.2.6) revealed by depleting desmoplakin I/II or plakoglobin in RhoE-depleted cells colony morphology reverted back to a more normal phenotype (Figure 37). The effects of individual and combined depletion of desmoplakin (Dsp), plakoglobin (Diepgen et al.) and RhoE (siRhoE) on keratinocyte apoptosis were analysed. HaCaT cells were transiently transfected with siRNA oligos to deplete proteins of interest and were treated with cisplatin for 24 hours prior to lysis. Caspase 9 cleavage and the expression of desmoplakin, plakoglobin, RhoE and tubulin were analysed using immunoblotting. Specific depletion of desmoplakin, plakoglobin and RhoE expression was detected when compared to control lanes (Figure 62A). In the presence of cisplatin a decrease in the level of full-length caspase 9 was detected in siCtrl, siDsp, siPG and siRhoE:PG cells. However, no change in the level of full-length caspase 9 was detected in siRhoE or siRhoE:Dsp cells (Figure 62B). A decrease in total caspase 9 was observed in cells depleted of desmoplakin I/II (Figure 62B). The percentage of cells with condensed nuclei was also analysed in these cells (Figure 63). In the presence of cisplatin the

percentage of cells with condensed nuclei is higher in siCtrl, siDP, siPG and siRhoE:PG cells compared to siRhoE and siRhoE:DP cells. Taken together these data indicate that sensitivity to cisplatin-induced apoptosis is restored in RhoE-depleted keratinocytes when plakoglobin is also depleted in these cells.

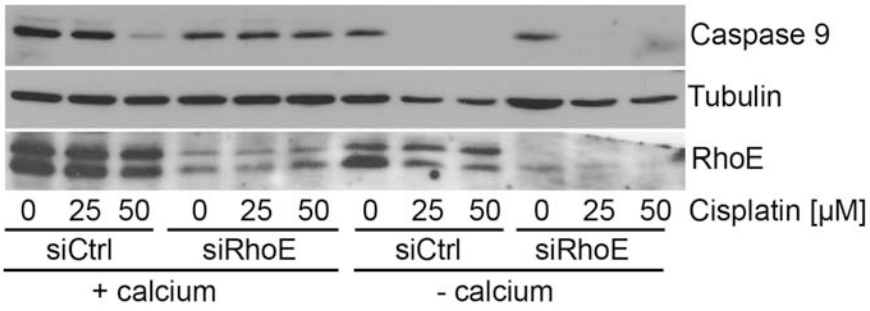

Figure 61 Keratinocytes depleted of RhoE are protected from cisplatin-induced apoptosis in normal growth conditions but not in low calcium conditions.

HaCaT cells transiently depleted of RhoE (siRhoE) and control (siCtrl) cells where incubated in normal or low calcium media for 24 hour prior to and then during treatment with cisplatin for 24 hours prior to lysis. Immunoblotting was used to detect the level of caspase 9 cleavage, RhoE and tubulin. Data presented are representative immunoblots of three separate experiments.

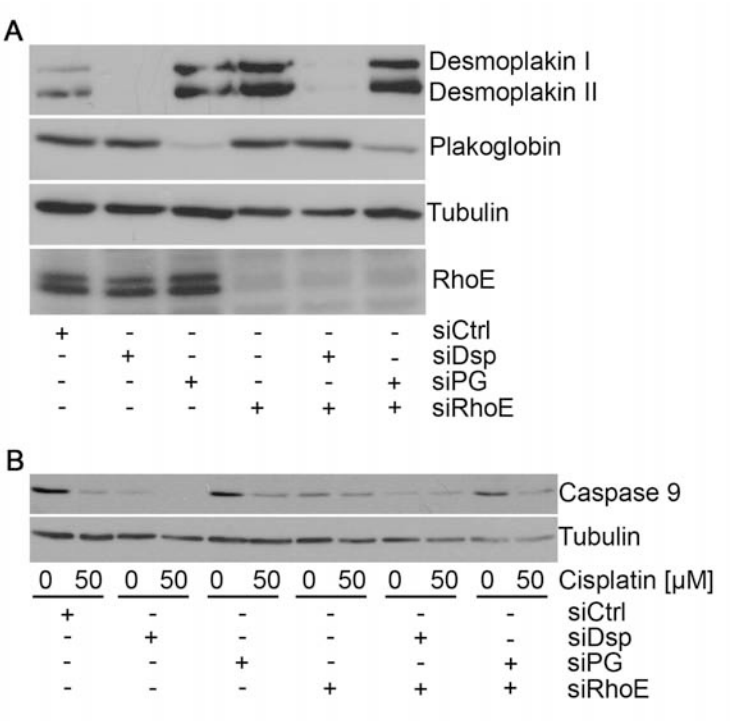

Figure 62 Depletion of plakoglobin in RhoE-depleted keratinocytes restores sensitivity to cisplatin-induced caspase 9 cleavage.

A HaCaT cells were transiently transfected with siRNA oligos to depleted desmoplakin I/II (Dsp), plakoglobin (Diepgen et al.) and RhoE expression individually and in combination. **B** siCtrl, siDsp, siPG, siRhoE, siRhoE:Dsp and siRhoE:PG cells were treated with cisplatin for 24 hours prior to lysis. Immunoblotting was used to detect the expression of full-length caspase 9, RhoE, desmoplakin, plakoglobin and tubulin. Data presented are representative immunoblots of three separate experiments.

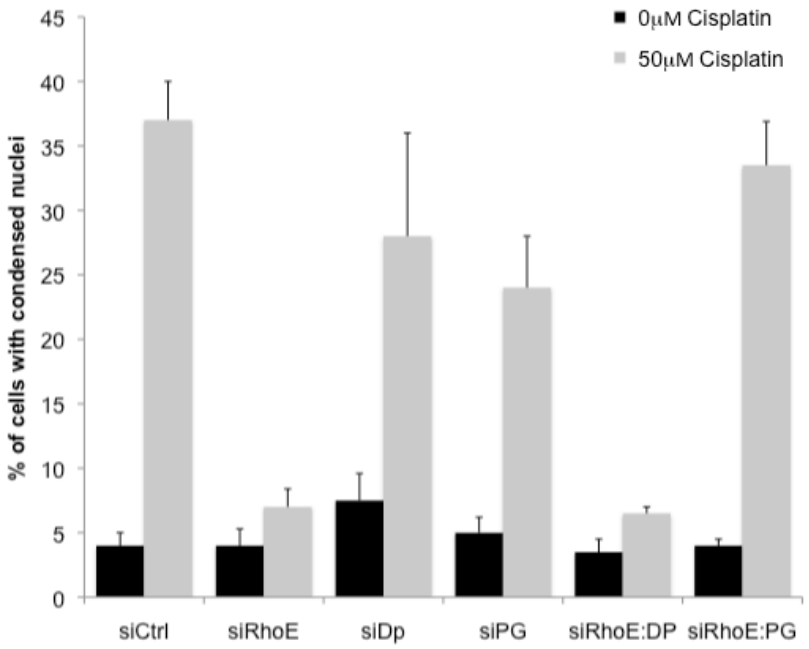

Figure 63 Depletion of plakoglobin in RhoE-depleted keratinocytes restores sensitivity to cisplatin-induced nuclear condensation.

HaCaT cells were transiently transfected with siRNA oligos to deplete desmoplakin I/II (Dsp), plakoglobin (Diepgen et al.) and RhoE expression individually and in combination. siCtrl, siDsp, siPG, siRhoE, siRhoE:Dsp and siRhoE:PG cells were seeded onto cover slips and treated with cisplatin for 24 hours prior to fixation. Cover slips were then stained with Hoechst 33342 to visualise the nuclei. Both the total number of nuclei and condensed nuclei were counted, with approximately 400 cells counted per condition. The percentage of cells with condensed nuclei was analysed and the data presented are the mean and standard deviation of one experiment.

5.3 Discussion

5.3.1 ROCK I and apoptosis in RhoE-depleted cells

Prolonged treatment of keratinocytes with Y-27632 to inhibit ROCK I and ROCK II protected keratinocytes from cisplatin-induced apoptosis (Section 5.2.1). Treatment with Y-27632 also protects U2OS cells from camptothecin-induced apoptosis (Ongusaha et al. 2006) and the administration of Y-27632 greatly reduced endotoxin-induced apoptosis in the liver (Thorlacius et al. 2006). During apoptosis, caspase 3-mediated activation of ROCK I induces membrane blebbing, stimulates nuclear fragmentation and packaging of nuclear material into blebs at the cell surface (Coleman et al. 2001; Sebbagh et al. 2001). Treatment with Y-27632 prevents ROCK I-induced membrane blebbing in cells undergoing apoptosis (Coleman et al. 2001; Cocca et al. 2002).

RhoE has been implicated in apoptosis (Bektic et al. 2005; Ongusaha et al. 2006; Boswell et al. 2007; Poch et al. 2007). To investigate how Y-27632 might be protecting keratinocytes I analysed the expression of RhoE, which inhibits ROCK I activity (Riento et al. 2003). In keratinocytes treated with Y-27632, a decrease in RhoE expression was observed. The temporal decrease in RhoE expression also correlated with Y-27632 treatment protecting the cells from apoptosis induced by cisplatin (Figure 38B & 39).

ROCK I, but not ROCK II, binds to and phosphorylates RhoE, increasing RhoE protein stability (Riento et al. 2003; Riento et al. 2005). To investigate whether the inhibition of ROCK activity

was responsible for the loss of RhoE expression in Y-27632 treated cells siRNA oligos were used to deplete keratinocytes of ROCK I. Prolonged depletion of ROCK I did not alter the expression levels of RhoE in keratinocytes (Figure 40). This was surprising as ROCK I is known to phosphorylate RhoE, increasing its protein stability (Riento et al. 2005). Combined depletion of ROCK I and ROCK II expression also had no effect on RhoE expression (Figure 40). Taken together these data indicate that whilst treatment with Y-27632 affected RhoE expression this is not a function of ROCK I in keratinocytes. Possible explanations to explain how Y-27632 treatment might decrease RhoE expression independently of ROCK I include, kinase independent effects or the inhibition of other kinases by Y-27632. The concentration of Y-27632 required to inhibit ROCK I and ROCK II also inhibits PRK-2 (Darenfed et al. 2007). PRK-2 is an effector of both Rho and Rac GTPases and regulates the actin cytoskeleton and cell-cell adhesions (Vincent et al. 1997; Calautti et al. 2002). A recent report correlating Y-27632 treatment with specific knock-downs of ROCK I, ROCK II and PRK-2 revealed significant differences in phenotype (Darenfed et al. 2007). One possibility which has not been explored here is that RhoE might also interact with PRK-2 as well as ROCK I. Further experiments in which keratinocytes are depleted of PRK-2 and combined depletion of ROCK I, ROCK II and PRK-2 would be required to clarify this issue.

Several studies have implicated RhoE in apoptosis (Bektic et al. 2005; Ongusaha et al. 2006; Boswell et al. 2007; Poch et al. 2007). Both stably and transiently transfected keratinocytes were used to analyse the effect of RhoE-depletion on the intrinsic apoptosis pathway induced by cisplatin. Keratinocytes stably and transiently depleted of RhoE were protected from apoptosis

induced by the intrinsic pathway, arguing against off-target effects from either system (Section 5.2 4 & 5.2.5). In addition, reconstitution of RhoE expression in the RhoE-depleted cell line rescued sensitivity to cisplatin-induced apoptosis resulting in cell death (Section 5.2.7). Taken together these data show that depletion of RhoE protects keratinocytes from apoptosis induced by the intrinsic pathway.

A number of studies have reported increased RhoE expression following treatment with various apoptosis-inducing stimuli (Murakami et al. 2001; Villalonga et al. 2004; Ongusaha et al. 2006; Boswell et al. 2007). Two studies, which used siRNA to inhibit RhoE induction following apoptotic stimuli, reported an increase in apoptosis (Ongusaha et al. 2006; Boswell et al. 2007). These studies imply RhoE expression protects cells from apoptosis (Ongusaha et al. 2006; Boswell et al. 2007). Conversely, other studies have shown RhoE over-expression increases the basal rate of apoptosis (Bektic et al. 2005; Poch et al. 2007). These studies use fundamentally different approaches to studying the role of RhoE in apoptosis including: different cell types, different apoptosis-inducing agents and different expression systems. Unlike other studies I have depleted RhoE expression in keratinocytes and in this system I observed protection from apoptosis induced via the intrinsic and extrinsic pathways.

Cisplatin induces apoptosis through the intrinsic pathway by up-regulating the tumour suppressor gene p53, which induces expression of PIDD protein and PUMA, promoting apoptosis (Wei et al. 2007). RhoE is also a transcriptional target of p53 and has been reported to

be induced in response to DNA damage (Jeffers et al. 2003; Ongusaha et al. 2006). Treatment with cisplatin has also been reported to increase RhoE expression in fibroblasts (Villalonga et al. 2004). However, no increase in RhoE expression was observed in HaCaT cells following treatment with cisplatin (Figure 41). The HaCaT cell line behaves phenotypically like normal keratinocytes with regard to patterns of growth and differentiation (Boukamp et al. 1988). However, HaCaT cells have three mutations in both alleles of their p53 gene, resulting in p53 having an extended half-life (Lehman et al. 1993). This results in p53 being highly expressed in HaCaT cells when compared to normal human keratinocytes (Bowen et al. 2003). UVB irradiation also induces the intrinsic apoptosis pathway through the up-regulation of p53 (Ziegler et al. 1994). UVB irradiation has been shown to increase the expression of p53 and induce nuclear fragmentation in HaCaT cells as well as up-regulating RhoE (Henseleit et al. 1997; Boswell et al. 2007). Thus, whilst p53 is highly expressed in HaCaT cells, expression can be further induced following DNA damage. However, the up-regulation of RhoE observed after UVB irradiation in HaCaT cells was shown to be independent of p53 (Boswell et al. 2007). These data show that although HaCaT cells have a mutated p53, p53 still up-regulated in these cells and that RhoE up-regulation is not solely dependent on p53. The explanation for RhoE up-regulation in response to cisplatin in fibroblasts but not HaCaT cells could be cell type specific and not because RhoE is unable to be up-regulated.

Most studies investigating the role of RhoE in apoptosis have focused on the intrinsic apoptosis pathway induced by a variety of different apoptotic stimuli. However, UVB irradiation, which induces the intrinsic pathway through DNA damage and p53 up-regulation, can also induce the

extrinsic pathway through the activation of the death receptor CD95 (Kulms et al. 2000). UVB-irradiated HaCaT cells prevented from inducing RhoE expression by siRNA demonstrated an increase in apoptosis (Boswell et al. 2007). Depletion of RhoE in HaCaT cells protected cells from apoptosis induced via the intrinsic pathway, so I investigated whether RhoE-depletion would protect keratinocytes from apoptosis mediated via the extrinsic pathway. To do this I used the death ligand TRAIL (Section 1.2.3.1). I observed that keratinocytes depleted of RhoE were protected from apoptosis induced by TRAIL. This was confirmed using both stably and transiently RhoE-depleted cell lines along with reconstitution of RhoE expression (Sections 5.2.5-5.2.7). Taken together these data show that RhoE-depletion protects keratinocytes from apoptosis induced via both the intrinsic and extrinsic pathways.

Both the intrinsic and the extrinsic pathways converge at the level of Bax activation (Sprick et al. 2004; Ott et al. 2007) (Section 1.2.1 Figure 5 & 7). Upon activation, Bax translocates from the cytoplasm to the mitochondria and alters the integrity of the mitochondrial membrane, resulting in cytochrome c release, which leads to the activation of the caspase cascade (Ott et al. 2007). RhoE over-expression (in a gastric adenocarinoma cell line) was reported to suppress the expression of Bax at a post-transcriptional level, resulting in resistance to multiple anti-tumour drugs (Li et al. 2009). No change in Bax expression was observed in RhoE-depleted cells in the presence or absence of cisplatin treatment (Figure 58 & 59). Once activated, Bax translocates to the mitochondria where it mediates MOMP by inserting into the outer mitochondrial membrane forming pore-like structures (Korsmeyer et al. 2000; Basanez et al. 2002) (Figure 5A). Bax translocation was analysed in RhoE-depleted cells treated with TRAIL and a decrease in the

percentage of cells containing punctate Bax staining was observed in RhoE-depleted cells (Figure 60B). These data suggest that whilst Bax expression is unaffected by RhoE-depletion, Bax translocation is inhibited, which could be responsible for the protection seen in RhoE-depleted cells (Figure 64).

During apoptosis, caspase 3 cleaves and activates ROCK I, which induces membrane blebbing and aids in the apoptotic process (Coleman et al. 2001; Sebbagh et al. 2001). Consistent with this, over-expression of the ROCK I 130kDa fragment produced by caspase 3 cleavage induces apoptosis but expression of full-length ROCK I does not (Ongusaha et al. 2006). Loss of ROCK I expression, using siRNA, resulted in decreased apoptosis induced by camptothecin (Ongusaha et al. 2006). Also, Y-27632 treatment prevents ROCK I-induced membrane blebbing in cells undergoing apoptosis (Coleman et al. 2001; Cocca et al. 2002). Treatment with Y-27632 also protects other cell types from apoptosis (Ongusaha et al. 2006) and the administration of Y-27632 reduces endotoxin-induced apoptosis in the liver (Thorlacius et al. 2006). Thus there is clear evidence linking ROCK I to the apoptotic pathway. Therefore one argument could be that the protection from apoptosis seen in RhoE-depleted cells is a ROCK I-dependent process. This would be consistent with a report where cells prevented from inducing RhoE expression show an increase in ROCK I activity during campothecin-induced apoptosis (Ongusaha et al. 2006). However, I observed that Y-27632 treatment, which inhibits ROCK I kinase activity (as well as ROCK II and PRK-2), protected HaCaT cells from cisplatin-induced apoptosis (Figure 38) and that this protection correlated with a decrease in RhoE expression (Figure 39). In keratinocytes depleted of RhoE, an increase in stellate actin stress fibres was observed indicating increased

ROCK activity in these cells (Section 3.2.1). However, apoptosis is still inhibited suggesting a ROCK I independent process. This is consistent with Boswell el al. (2007) who also reported that the prevention of RhoE induction during UVB irradiation was also independent of ROCK I activity (Boswell et al. 2007). These data suggest that it is RhoE depletion that is important for protection against apoptosis in keratinocytes and that the protection is independent of ROCK I activity.

5.3.2 Desmosomes and apoptosis in RhoE-depleted cells

RhoE-depleted keratinocytes show clear changes in colony morphology (Section 4.2.1). This is a consequence of RhoE-depletion inducing expression of desmosomal proteins and increasing the number of desmosomes (Figure 28 & 29). I analysed whether the increase in desmosomal proteins or desmosomes played a role in protecting these cells from apoptosis induced by the intrinsic pathway. In low calcium conditions, in which both adherens junctions and desomsomes are disrupted (Chitaev et al. 1997; Jamora et al. 2002) I observed that RhoE colony morphology reverted to a normal phenotype and that the expression of desmosomal proteins was lost (Section 4.2.5). Under these conditions induction of the intrinsic apoptosis pathway resulted in similar levels of apoptosis in both RhoE-depleted and control cells (Section 5.2.9 Figure 61). This indicates that disruption of desmosomal adhesion or loss of desmosomal proteins is involved in the protection observed in RhoE-depleted cells.

Depletion of desmoplakin I/II or plakoglobin disrupts desmosomes and reverses the stratified phenotype in RhoE-depleted cells (Section 4.2.6). I analysed whether depletion of these desmosomal proteins affected the response to cisplatin-induced apoptosis. In control keratinocytes depleted of either desmoplakin I/II or plakoglobin, apoptosis was observed following treatment with cisplatin (Figure 62 & 63). In cells depleted of both RhoE and desmoplakin I/II protection from apoptosis was observed (Figure 62 & 63), even though desmosomes had been disrupted (Figure 37). However, in cells depleted of both RhoE and plakoglobin sensitivity to cisplatin was restored (Figure 62 & 63). The protection from cisplatin-induced apoptosis generated by RhoE depletion in keratinocytes was lost when cells were cultured either in low calcium conditions or when plakoglobin was depleted in these cells. In low calcium medium I saw a loss of desmosomal proteins (Figure 35) and although plakoglobin expression was not analysed it is possible that it too was decreased or relocalised in these conditions. It has also been reported that depletion of desmoplakin I/II disrupts desmosomes but does not alter plakoglobin expression (Wan et al. 2007). Taken together, these data suggest that the protection from cisplatin-induced apoptosis seen in RhoE-depleted keratinocytes is not dependent on desmosomes but on the desmosomal protein plakoglobin.

Plakoglobin is closely related to β-catenin, which functions as a structural protein and as a transcriptional activator mediating Wnt signaling (Zhurinsky et al. 2000; Moon et al. 2002). Plakoglobin can affect Wnt signaling through binding the transcription factors Tcf/Lcf (Ben-Ze'ev et al. 1998; Klymkowsky et al. 1999; Zhurinsky et al. 2000). Activation of Wnt signaling blocks apoptosis in a variety of cells whilst suppression of Wnt signaling induces apoptosis

(Longo et al. 2002). Suppression of desmoplakin I/II expression results in the relocalisation of plakoglobin to the nucleus where its accumulation suppresses Wnt signaling (Garcia-Gras et al. 2006). RhoE has been implicated in the translocation of β-catenin to adherens junctions (Rubenstein et al. 2005). Thus it is possible RhoE may also have a role in the translocation of plakoglobin. Thus RhoE-depletion may prevent plakoglobin from localising to the nucleus following desmosomal disruption (Figure 64).

Plakoglobin has also been reported to regulate members of the Bcl-2 family (Hakimelahi et al. 2000; Dusek et al. 2007). The Bcl-2 family proteins mediate MOMP and consist of both anti-apoptotic members that act as repressors of apoptosis by blocking the release of cytochrome c, and pro-apoptotic members that act as promoters of apoptosis (Green et al. 2004). Over-expression of plakoglobin in keratinocytes has been reported to induce the expression of the anti-apoptotic protein Bcl-2, protecting the cells from apoptosis (Hakimelahi et al. 2000). In contrast, keratinocytes derived from plakoglobin-null mice showed increased expression of the anti-apoptotic protein Bcl-x_L and reduced susceptibility to apoptosis (Dusek et al. 2007). Taken together these data suggest the level of plakoglobin expression is important for the expression of different Bcl-2 family members. RhoE expression has also been reported in the regulation of the Bcl-2 family member Bax (Li et al. 2009).

In summary, depletion of RhoE expression protects keratinocytes from apoptosis induced via the intrinsic and extrinsic apoptosis pathways. The protection generated by RhoE depletion is probably independent of ROCK I activity. I suggest two possible explanations for the protection

observed following depletion of RhoE expression, firstly I observed significant decrease in Bax translocation and secondly depletion of the desmosomal protein plakoglobin restored sensitivity to apoptosis (Figure 64).

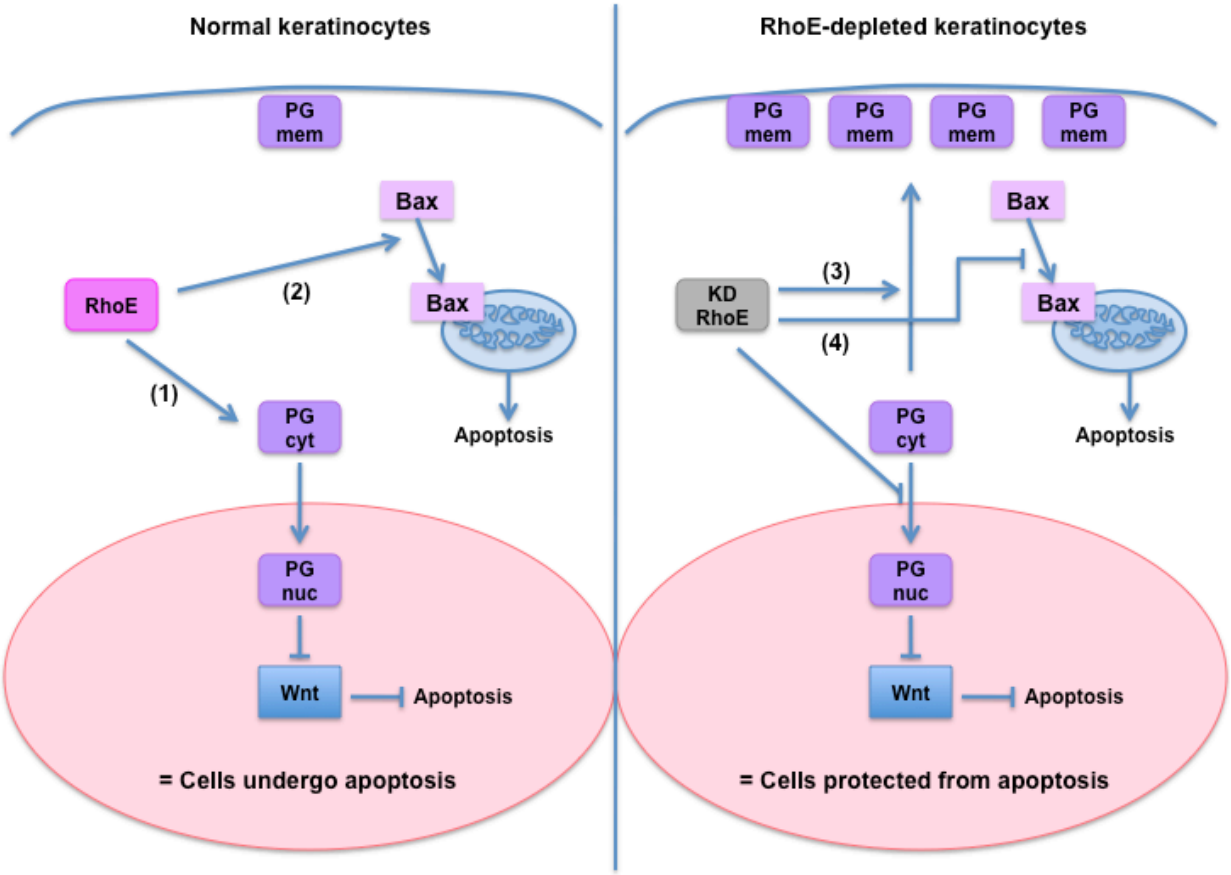

Figure 64 Mechanism of how RhoE depletion protects keratinocytes from apoptosis.

In normal keratinocytes RhoE may play a role in the translacation of plakoglobin to the cytoplasm (PG cyt) and nucleus (PG nuc). Once in the nucleus plakoglobin can suppress Wnt signaling leading to apoptosis (1). RhoE may also have a role in translocating Bax to the mitochondrial membrane enabling the cell to undergo apoptosis (2). In RhoE depleted keratinocytes plakoglobin accumulates at the plasma membrane (PG mem) coupled with a decrease in nuclear plakoglobin levels. In this situation Wnt signaling is not suppressed and apoptosis is not induced (3). Bax translocation to the mitochondrial membrane in RhoE-depleted keratinocytes is inhibited protecting the cells from apoptosis (4).

CHAPTER 6 CONCLUDING REMARKS AND FUTURE DIRECTIONS

6.1 Regulation of the cell cycle by RhoE induced desmosomal proteins

Loss of RhoE expression in keratinocytes resulted in a G1 phase cell cycle arrest and a decrease in the level of active ERK and cyclin D1 expression. I have also shown that RhoE-depletion increased the expression of the desmosomal proteins desmoglein 3 and desmoplakin I/II. Keratinocytes expressing low levels of desmoglein 3 have increased colony forming efficiency as well as increased proliferation compared to keratinocytes expressing high levels of desmoglein 3 (Wan et al. 2003). In HaCaT cells depleted of desmoplakin I/II cell proliferation was increased with an enhanced G1 to S phase transition (Wan et al. 2007). This was also associated with increased ERK and Akt activation (Wan et al. 2007). These data support my findings and suggest that RhoE may regulate cell cycle progression in keratinocytes through the regulation of desmosomal proteins. Further work is required to confirm this.

6.2 Regulation of desmosomal assembly by RhoE

Desmosomes are cell-cell adhesion complexes important for maintaining the structural integrity of many tissues including the skin and heart (Garrod et al. 2008). Cell-cell adhesion in the skin is vital for epidermal differentiation and maintaining architecture of the epidermis (Braga 2002; Fuchs 2007). Desmosomes also have roles in tissue morphogenesis, proliferation and differentiation (Yin et al. 2004; Muller et al. 2008). Desmosomes are disrupted in several human diseases including the autoimmune disease pemphigus vulgaris and the hereditary disease

arrhythmogenic right ventricular dysplasia/cardiomyopathy (Garcia-Gras et al. 2006; Waschke 2008).

My work shows that depletion of RhoE in keratinocytes results in the up-regulation of desmosomal proteins and increased numbers of desmosomes. How RhoE regulates these events is not known. Unlike desmosomal protein-protein interactions, which are fairly well documented, little is known about how desmosomal proteins are regulated (Green et al. 2007). Desmosomes are relatively stable structures with not much evidence for recycling (Windoffer et al. 2002; Thomason et al. 2010), thus it is likely that the increase in desmosomes in RhoE-depleted keratinocytes is a consequence of new desmosomes being formed. RhoA activity has been implicated in regulating desmoplakin I/II translocation to maturing desmosomes and RhoE has been reported to regulate RhoA activity (Wennerberg et al. 2003; Godsel et al. 2010; Goh et al. 2010). The actin cytoskeleton is also required for desmosomal assembly (Pasdar et al. 1993; Godsel et al. 2005) and RhoE is involved in the regulation of the actin cytoskeleton (Katoh et al. 2002; Riento et al. 2003; Komander et al. 2008). Further analysis of the role of RhoE in desmosomal assembly may help understand how these structures are disrupted in human diseases.

6.3 Regulation of Bax by RhoE during apoptosis

Keratinocytes depleted of RhoE were protected from apoptosis induced by the intrinsic and extrinsic pathways. Both the intrinsic and the extrinsic pathways converge at the level of Bax activation (Sprick et al. 2004; Ott et al. 2007). Upon activation, Bax translocates to the mitochondria where it mediates MOMP initiating the caspase cascade (Korsmeyer et al. 2000;

Basanez et al. 2002). RhoE has also been implicated in the regulation of Bax expression (Li et al. 2009). Here I report Bax expression in RhoE-depleted cells was not changed. However, the translocation of Bax to the mitochondria was disrupted in RhoE-depleted cells. Establishing how RhoE regulates Bax translocation would give further insight into how apoptosis is regulated and how the intrinsic and extrinsic pathways converge.

6.4 RhoE, plakoglobin and apoptosis

The protection from cisplatin-induced apoptosis observed in RhoE-depleted cells was lost following plakoglobin depletion, implicating plakoglobin in the regulation of apoptosis. Plakoglobin can translocate to the nucleus were it can alter transcription. Numerous studies have implicated plakoglobin in the regulation of Wnt signaling via Tcf/Lef transcription (Ben-Ze'ev et al. 1998; Klymkowsky et al. 1999; Zhurinsky et al. 2000; Garcia-Gras et al. 2006). Wnt signaling is known to regulate apoptosis (Longo et al. 2002; Garcia-Gras et al. 2006). Activation of Wnt signaling blocks apoptosis in a variety of cells whereas suppression of Wnt signaling induces apoptosis (Longo et al. 2002). Depletion of RhoE has no effect on plakoglobin expression but relocalisation of plakoglobin was observed in RhoE-depleted cells. Plakoglobin has also been implicated in the regulation of Bcl-2 family protein expression (Hakimelahi et al. 2000; Dusek et al. 2007). Furthermore, RhoE expression has been reported to regulate the expression of the Bcl-2 family member Bax (Li et al. 2009). An understanding of how RhoE regulates plakoglobin and how plakoglobin regulates apoptosis are clearly key areas for research.

LIST OF REFERENCES

Abbas, T. and A. Dutta (2009). "p21 in cancer: intricate networks and multiple activities." Nat Rev Cancer **9**(6): 400-414.

Acehan, D., X. Jiang, D. G. Morgan, J. E. Heuser, X. Wang and C. W. Akey (2002). "Three-dimensional structure of the apoptosome: implications for assembly, procaspase-9 binding, and activation." Mol Cell **9**(2): 423-432.

Acehan, D., C. Petzold, I. Gumper, D. D. Sabatini, E. J. Muller, P. Cowin and D. L. Stokes (2008). "Plakoglobin is required for effective intermediate filament anchorage to desmosomes." Journal of Investigative Dermatology **128**(11): 2665-2675.

Adams, J. C. and F. M. Watt (1989). "Fibronectin inhibits the terminal differentiation of human keratinocytes." Nature **340**(6231): 307-309.

Adrain, C., E. A. Slee, M. T. Harte and S. J. Martin (1999). "Regulation of apoptotic protease activating factor-1 oligomerization and apoptosis by the WD-40 repeat region." Journal of Biological Chemistry **274**(30): 20855-20860.

Akhtar, N., K. R. Hudson and N. A. Hotchin (2000). "Co-localization of Rac1 and E-cadherin in human epidermal keratinocytes." Cell Adhes Commun **7**(6): 465-476.

Albers, K. M., F. Greif, R. W. Setzer and L. B. Taichman (1987). "Cell-cycle withdrawal in cultured keratinocytes." Differentiation **34**(3): 236-240.

Amano, M., K. Chihara, N. Nakamura, T. Kaneko, Y. Matsuura and K. Kaibuchi (1999). "The COOH terminus of Rho-kinase negatively regulates rho-kinase activity." Journal of Biological Chemistry **274**(45): 32418-32424.

Amano, M., H. Mukai, Y. Ono, K. Chihara, T. Matsui, Y. Hamajima, K. Okawa, A. Iwamatsu and K. Kaibuchi (1996). "Identification of a putative target for Rho as the serine-threonine kinase protein kinase N." Science **271**(5249): 648-650.

Arnemann, J., K. H. Sullivan, A. I. Magee, I. A. King and R. S. Buxton (1993). "Stratification-related expression of isoforms of the desmosomal cadherins in human epidermis." J Cell Sci **104 (Pt 3)**: 741-750.

Ashkenazi, A. (2002). "Targeting death and decoy receptors of the tumour-necrosis factor superfamily." Nat Rev Cancer **2**(6): 420-430.

Assoian, R. K. and E. A. Klein (2008). "Growth control by intracellular tension and extracellular stiffness." Trends Cell Biol **18**(7): 347-352.

Assoian, R. K. and M. A. Schwartz (2001). "Coordinate signaling by integrins and receptor tyrosine kinases in the regulation of G1 phase cell-cycle progression." Curr Opin Genet Dev **11**(1): 48-53.

Bao, Q., S. J. Riedl and Y. Shi (2005). "Structure of Apaf-1 in the auto-inhibited form: a critical role for ADP." Cell Cycle **4**(8): 1001-1003.

Basanez, G., J. C. Sharpe, J. Galanis, T. B. Brandt, J. M. Hardwick and J. Zimmerberg (2002). "Bax-type apoptotic proteins porate pure lipid bilayers through a mechanism sensitive to intrinsic monolayer curvature." Journal of Biological Chemistry **277**(51): 49360-49365.

Bass-Zubek, A. E., R. P. Hobbs, E. V. Amargo, N. J. Garcia, S. N. Hsieh, X. Chen, J. K. Wahl, 3rd, M. F. Denning and K. J. Green (2008). "Plakophilin 2: a critical scaffold for PKC alpha that regulates intercellular junction assembly." J Cell Biol **181**(4): 605-613.

Bata-Csorgo, Z., C. Hammerberg, J. J. Voorhees and K. D. Cooper (1995). "Kinetics and regulation of human keratinocyte stem cell growth in short-term primary ex vivo culture. Cooperative growth factors from psoriatic lesional T lymphocytes stimulate proliferation among psoriatic uninvolved, but not normal, stem keratinocytes." J Clin Invest **95**(1): 317-327.

Bazzi, H., A. Getz, M. G. Mahoney, A. Ishida-Yamamoto, L. Langbein, J. K. Wahl, 3rd and A. M. Christiano (2006). "Desmoglein 4 is expressed in highly differentiated keratinocytes and trichocytes in human epidermis and hair follicle." Differentiation **74**(2-3): 129-140.

Bektic, J., K. Pfeil, A. P. Berger, R. Ramoner, A. Pelzer, G. Schafer, K. Kofler, G. Bartsch and H. Klocker (2005). "Small G-protein RhoE is underexpressed in prostate cancer and induces cell cycle arrest and apoptosis." Prostate **64**(4): 332-340.

Ben-Ze'ev, A. and B. Geiger (1998). "Differential molecular interactions of beta-catenin and plakoglobin in adhesion, signaling and cancer." Curr Opin Cell Biol **10**(5): 629-639.

Berckmans, B. and L. De Veylder (2009). "Transcriptional control of the cell cycle." Curr Opin Plant Biol **12**(5): 599-605.

Bernards, A. (2003). "GAPs galore! A survey of putative Ras superfamily GTPase activating proteins in man and Drosophila." Biochim Biophys Acta **1603**(2): 47-82.

Bierkamp, C., H. Schwarz, O. Huber and R. Kemler (1999). "Desmosomal localization of beta-catenin in the skin of plakoglobin null-mutant mice." Development **126**(2): 371-381.

Blanpain, C., W. E. Lowry, A. Geoghegan, L. Polak and E. Fuchs (2004). "Self-renewal, multipotency, and the existence of two cell populations within an epithelial stem cell niche." Cell **118**(5): 635-648.

Borradori, L. and A. Sonnenberg (1999). "Structure and function of hemidesmosomes: more than simple adhesion complexes." Journal of Investigative Dermatology **112**(4): 411-418.

Boswell, S. A., P. P. Ongusaha, P. Nghiem and S. W. Lee (2007). "The protective role of a small GTPase RhoE against UVB-induced DNA damage in keratinocytes." Journal of Biological Chemistry **282**(7): 4850-4858.

Boukamp, P., R. T. Petrussevska, D. Breitkreutz, J. Hornung, A. Markham and N. E. Fusenig (1988). "Normal keratinization in a spontaneously immortalized aneuploid human keratinocyte cell line." J Cell Biol **106**(3): 761-771.

Bourne, H. R., D. A. Sanders and F. McCormick (1991). "The GTPase superfamily: conserved structure and molecular mechanism." Nature **349**(6305): 117-127.

Bowen, A. R., A. N. Hanks, S. M. Allen, A. Alexander, M. J. Diedrich and D. Grossman (2003). "Apoptosis regulators and responses in human melanocytic and keratinocytic cells." Journal of Investigative Dermatology **120**(1): 48-55.

Braga, V. M. (2002). "Cell-cell adhesion and signalling." Curr Opin Cell Biol **14**(5): 546-556.

Braga, V. M., L. M. Machesky, A. Hall and N. A. Hotchin (1997). "The small GTPases Rho and Rac are required for the establishment of cadherin-dependent cell-cell contacts." J Cell Biol **137**(6): 1421-1431.

Brandner, J. M., S. Kief, C. Grund, M. Rendl, P. Houdek, C. Kuhn, E. Tschachler, W. W. Franke and I. Moll (2002). "Organization and formation of the tight junction system in human epidermis and cultured keratinocytes." Eur J Cell Biol **81**(5): 253-263.

Brennan, D., Y. Hu, S. Joubeh, Y. W. Choi, D. Whitaker-Menezes, T. O'Brien, J. Uitto, U. Rodeck and M. G. Mahoney (2007). "Suprabasal Dsg2 expression in transgenic mouse skin confers a hyperproliferative and apoptosis-resistant phenotype to keratinocytes." J Cell Sci **120**(Pt 5): 758-771.

Bustelo, X. R., V. Sauzeau and I. M. Berenjeno (2007). "GTP-binding proteins of the Rho/Rac family: regulation, effectors and functions in vivo." Bioessays **29**(4): 356-370.

Calautti, E., M. Grossi, C. Mammucari, Y. Aoyama, M. Pirro, Y. Ono, J. Li and G. P. Dotto (2002). "Fyn tyrosine kinase is a downstream mediator of Rho/PRK2 function in keratinocyte cell-cell adhesion." J Cell Biol **156**(1): 137-148.

Chang, J., M. Xie, V. R. Shah, M. D. Schneider, M. L. Entman, L. Wei and R. J. Schwartz (2006). "Activation of Rho-associated coiled-coil protein kinase 1 (ROCK-1) by caspase-3 cleavage plays an essential role in cardiac myocyte apoptosis." Proc Natl Acad Sci U S A **103**(39): 14495-14500.

Chapman, S. J. and A. Walsh (1990). "Desmosomes, corneosomes and desquamation. An ultrastructural study of adult pig epidermis." Arch Dermatol Res **282**(5): 304-310.

Chipuk, J. E., T. Kuwana, L. Bouchier-Hayes, N. M. Droin, D. D. Newmeyer, M. Schuler and D. R. Green (2004). "Direct activation of Bax by p53 mediates mitochondrial membrane permeabilization and apoptosis." Science **303**(5660): 1010-1014.

Chitaev, N. A. and S. M. Troyanovsky (1997). "Direct Ca2+-dependent heterophilic interaction between desmosomal cadherins, desmoglein and desmocollin, contributes to cell-cell adhesion." J Cell Biol **138**(1): 193-201.

Cocca, B. A., A. M. Cline and M. Z. Radic (2002). "Blebs and apoptotic bodies are B cell autoantigens." J Immunol **169**(1): 159-166.

Cohen, S. N., A. C. Chang and L. Hsu (1972). "Nonchromosomal antibiotic resistance in bacteria: genetic transformation of Escherichia coli by R-factor DNA." Proc Natl Acad Sci U S A **69**(8): 2110-2114.

Coleman, M. L., E. A. Sahai, M. Yeo, M. Bosch, A. Dewar and M. F. Olson (2001). "Membrane blebbing during apoptosis results from caspase-mediated activation of ROCK I." Nature Cell Biology **3**(4): 339-345.

Darenfed, H., B. Dayanandan, T. Zhang, S. H. Hsieh, A. E. Fournier and C. A. Mandato (2007). "Molecular characterization of the effects of Y-27632." Cell Motil Cytoskeleton **64**(2): 97-109.

Daugas, E., S. A. Susin, N. Zamzami, K. F. Ferri, T. Irinopoulou, N. Larochette, M. C. Prevost, B. Leber, D. Andrews, J. Penninger and G. Kroemer (2000). "Mitochondrio-nuclear translocation of AIF in apoptosis and necrosis." FASEB J **14**(5): 729-739.

Davies, S. P., H. Reddy, M. Caivano and P. Cohen (2000). "Specificity and mechanism of action of some commonly used protein kinase inhibitors." Biochemical Journal **351**(Pt 1): 95-105.

Diehl, J. A. (2002). "Cycling to cancer with cyclin D1." Cancer Biology & Therapy **1**(3): 226-231.

Diepgen, T. L. and V. Mahler (2002). "The epidemiology of skin cancer." Br J Dermatol **146 Suppl 61**: 1-6.

Diessenbacher, P., M. Hupe, M. R. Sprick, A. Kerstan, P. Geserick, T. L. Haas, T. Wachter, M. Neumann, H. Walczak, J. Silke and M. Leverkus (2008). "NF-kappaB inhibition reveals differential mechanisms of TNF versus TRAIL-induced apoptosis upstream or at the level of caspase-8 activation independent of cIAP2." Journal of Investigative Dermatology **128**(5): 1134-1147.

Du, C., M. Fang, Y. Li, L. Li and X. Wang (2000). "Smac, a mitochondrial protein that promotes cytochrome c-dependent caspase activation by eliminating IAP inhibition." Cell **102**(1): 33-42.

Dusek, R. L., L. M. Godsel, F. Chen, A. M. Strohecker, S. Getsios, R. Harmon, E. J. Muller, R. Caldelari, V. L. Cryns and K. J. Green (2007). "Plakoglobin deficiency protects keratinocytes from apoptosis." Journal of Investigative Dermatology **127**(4): 792-801.

Dusek, R. L., L. M. Godsel and K. J. Green (2007). "Discriminating roles of desmosomal cadherins: beyond desmosomal adhesion." J Dermatol Sci **45**(1): 7-21.

Edinger, A. L. and C. B. Thompson (2004). "Death by design: apoptosis, necrosis and autophagy." Curr Opin Cell Biol **16**(6): 663-669.

Etienne-Manneville, S. and A. Hall (2002). "Rho GTPases in cell biology." Nature **420**(6916): 629-635.

Fehon, R. G., A. I. McClatchey and A. Bretscher (2010). "Organizing the cell cortex: the role of ERM proteins." Nat Rev Mol Cell Biol **11**(4): 276-287.

Feng, J., M. Ito, Y. Kureishi, K. Ichikawa, M. Amano, N. Isaka, K. Okawa, A. Iwamatsu, K. Kaibuchi, D. J. Hartshorne and T. Nakano (1999). "Rho-associated kinase of chicken gizzard smooth muscle." Journal of Biological Chemistry **274**(6): 3744-3752.

Fleckman, P., B. A. Dale and K. A. Holbrook (1985). "Profilaggrin, a high-molecular-weight precursor of filaggrin in human epidermis and cultured keratinocytes." Journal of Investigative Dermatology **85**(6): 507-512.

Foster, R., K. Q. Hu, Y. Lu, K. M. Nolan, J. Thissen and J. Settleman (1996). "Identification of a novel human Rho protein with unusual properties: GTPase deficiency and in vivo farnesylation." Molecular and Cellular Biology **16**(6): 2689-2699.

Frisch, S. M. and E. Ruoslahti (1997). "Integrins and anoikis." Curr Opin Cell Biol **9**(5): 701-706.

Fuchs, E. (1990). "Epidermal differentiation: the bare essentials." J Cell Biol **111**(6 Pt 2): 2807-2814.

Fuchs, E. (2007). "Scratching the surface of skin development." Nature **445**(7130): 834-842.

Fuchs, E. and H. Green (1980). "Changes in keratin gene expression during terminal differentiation of the keratinocyte." Cell **19**(4): 1033-1042.

Fujisawa, K., P. Madaule, T. Ishizaki, G. Watanabe, H. Bito, Y. Saito, A. Hall and S. Narumiya (1998). "Different regions of Rho determine Rho-selective binding of different

classes of Rho target molecules." Journal of Biological Chemistry **273**(30): 18943-18949.
Fulda, S. and K. M. Debatin (2006). "Extrinsic versus intrinsic apoptosis pathways in anticancer chemotherapy." Oncogene **25**(34): 4798-4811.
Fulda, S., E. Meyer and K. M. Debatin (2002). "Inhibition of TRAIL-induced apoptosis by Bcl-2 overexpression." Oncogene **21**(15): 2283-2294.
Gallicano, G. I., P. Kouklis, C. Bauer, M. Yin, V. Vasioukhin, L. Degenstein and E. Fuchs (1998). "Desmoplakin is required early in development for assembly of desmosomes and cytoskeletal linkage." J Cell Biol **143**(7): 2009-2022.
Gandarillas, A. (2000). "Epidermal differentiation, apoptosis, and senescence: common pathways?" Exp Gerontol **35**(1): 53-62.
Gandarillas, A., L. A. Goldsmith, S. Gschmeissner, I. M. Leigh and F. M. Watt (1999). "Evidence that apoptosis and terminal differentiation of epidermal keratinocytes are distinct processes." Exp Dermatol **8**(1): 71-79.
Garcia-Gras, E., R. Lombardi, M. J. Giocondo, J. T. Willerson, M. D. Schneider, D. S. Khoury and A. J. Marian (2006). "Suppression of canonical Wnt/beta-catenin signaling by nuclear plakoglobin recapitulates phenotype of arrhythmogenic right ventricular cardiomyopathy." J Clin Invest **116**(7): 2012-2021.
Garg, R., K. Riento, N. Keep, J. D. Morris and A. J. Ridley (2008). "N-terminus-mediated dimerization of ROCK-I is required for RhoE binding and actin reorganization." Biochemical Journal **411**(2): 407-414.
Garrod, D. and M. Chidgey (2008). "Desmosome structure, composition and function." Biochim Biophys Acta **1778**(3): 572-587.
Garrod, D. R., A. J. Merritt and Z. Nie (2002). "Desmosomal cadherins." Curr Opin Cell Biol **14**(5): 537-545.
Ghobrial, I. M., T. E. Witzig and A. A. Adjei (2005). "Targeting apoptosis pathways in cancer therapy." CA Cancer J Clin **55**(3): 178-194.
Gniadecki, R. (1998). "Regulation of keratinocyte proliferation." Gen Pharmacol **30**(5): 619-622.
Godsel, L. M., A. D. Dubash, A. E. Bass-Zubek, E. V. Amargo, J. L. Klessner, R. P. Hobbs, X. Chen and K. J. Green (2010). "Plakophilin 2 couples actomyosin remodeling to desmosomal plaque assembly via RhoA." Molecular Biology of the Cell **21**(16): 2844-2859.
Godsel, L. M., S. N. Hsieh, E. V. Amargo, A. E. Bass, L. T. Pascoe-McGillicuddy, A. C. Huen, M. E. Thorne, C. A. Gaudry, J. K. Park, K. Myung, R. D. Goldman, T. L. Chew and K. J. Green (2005). "Desmoplakin assembly dynamics in four dimensions: multiple phases differentially regulated by intermediate filaments and actin." J Cell Biol **171**(6): 1045-1059.
Goh, L. L. and E. Manser (2010). "The RhoA GEF Syx Is a Target of Rnd3 and Regulated via a Raf1-Like Ubiquitin-Related Domain." PLoS One **5**(8).
Green, D. R. and G. Kroemer (2004). "The pathophysiology of mitochondrial cell death." Science **305**(5684): 626-629.
Green, D. R. and G. Kroemer (2005). "Pharmacological manipulation of cell death: clinical applications in sight?" J Clin Invest **115**(10): 2610-2617.

Green, H. (1977). "Terminal differentiation of cultured human epidermal cells." Cell **11**(2): 405-416.

Green, K. J. and C. L. Simpson (2007). "Desmosomes: new perspectives on a classic." Journal of Investigative Dermatology **127**(11): 2499-2515.

Grossi, M., A. Hiou-Feige, A. Tommasi Di Vignano, E. Calautti, P. Ostano, S. Lee, G. Chiorino and G. P. Dotto (2005). "Negative control of keratinocyte differentiation by Rho/CRIK signaling coupled with up-regulation of KyoT1/2 (FHL1) expression." Proc Natl Acad Sci U S A **102**(32): 11313-11318.

Guasch, R. M., A. M. Blanco, A. Perez-Arago, R. Minambres, R. Talens-Visconti, B. Peris and C. Guerri (2007). "RhoE participates in the stimulation of the inflammatory response induced by ethanol in astrocytes." Experimental Cell Research **313**(17): 3779-3788.

Guasch, R. M., P. Scambler, G. E. Jones and A. J. Ridley (1998). "RhoE regulates actin cytoskeleton organization and cell migration." Molecular and Cellular Biology **18**(8): 4761-4771.

Haake, A. R. and R. R. Polakowska (1993). "Cell death by apoptosis in epidermal biology." Journal of Investigative Dermatology **101**(2): 107-112.

Hakimelahi, S., H. R. Parker, A. J. Gilchrist, M. Barry, Z. Li, R. C. Bleackley and M. Pasdar (2000). "Plakoglobin regulates the expression of the anti-apoptotic protein BCL-2." Journal of Biological Chemistry **275**(15): 10905-10911.

Hansen, S. H., M. M. Zegers, M. Woodrow, P. Rodriguez-Viciana, P. Chardin, K. E. Mostov and M. McMahon (2000). "Induced expression of Rnd3 is associated with transformation of polarized epithelial cells by the Raf-MEK-extracellular signal-regulated kinase pathway." Molecular and Cellular Biology **20**(24): 9364-9375.

Hardman, M. J., K. Liu, A. A. Avilion, A. Merritt, K. Brennan, D. R. Garrod and C. Byrne (2005). "Desmosomal cadherin misexpression alters beta-catenin stability and epidermal differentiation." Molecular and Cellular Biology **25**(3): 969-978.

Harper, N., M. Hughes, M. MacFarlane and G. M. Cohen (2003). "Fas-associated death domain protein and caspase-8 are not recruited to the tumor necrosis factor receptor 1 signaling complex during tumor necrosis factor-induced apoptosis." Journal of Biological Chemistry **278**(28): 25534-25541.

Hatzfeld, M. (1999). "The armadillo family of structural proteins." Int Rev Cytol **186**: 179-224.

Hatzfeld, M. (2007). "Plakophilins: Multifunctional proteins or just regulators of desmosomal adhesion?" Biochim Biophys Acta **1773**(1): 69-77.

Henseleit, U., J. Zhang, R. Wanner, I. Haase, G. Kolde and T. Rosenbach (1997). "Role of p53 in UVB-induced apoptosis in human HaCaT keratinocytes." Journal of Investigative Dermatology **109**(6): 722-727.

Hu, P., P. Berkowitz, E. J. O'Keefe and D. S. Rubenstein (2003). "Keratinocyte adherens junctions initiate nuclear signaling by translocation of plakoglobin from the membrane to the nucleus." Journal of Investigative Dermatology **121**(2): 242-251.

Huber, O. (2003). "Structure and function of desmosomal proteins and their role in development and disease." Cell Mol Life Sci **60**(9): 1872-1890.

Ilkovitch, D. (2010). "Role of immune-regulatory cells in skin pathology." J Leukoc Biol.

Ishizaki, T., M. Maekawa, K. Fujisawa, K. Okawa, A. Iwamatsu, A. Fujita, N. Watanabe, Y. Saito, A. Kakizuka, N. Morii and S. Narumiya (1996). "The small GTP-binding protein Rho binds to and activates a 160 kDa Ser/Thr protein kinase homologous to myotonic dystrophy kinase." Embo Journal **15**(8): 1885-1893.

Ishizaki, T., M. Naito, K. Fujisawa, M. Maekawa, N. Watanabe, Y. Saito and S. Narumiya (1997). "p160ROCK, a Rho-associated coiled-coil forming protein kinase, works downstream of Rho and induces focal adhesions." Febs Letters **404**(2-3): 118-124.

Ishizaki, T., M. Uehata, I. Tamechika, J. Keel, K. Nonomura, M. Maekawa and S. Narumiya (2000). "Pharmacological properties of Y-27632, a specific inhibitor of rho-associated kinases." Mol Pharmacol **57**(5): 976-983.

Jaffe, A. B. and A. Hall (2005). "Rho GTPases: biochemistry and biology." Annu Rev Cell Dev Biol **21**: 247-269.

Jamora, C. and E. Fuchs (2002). "Intercellular adhesion, signalling and the cytoskeleton." Nature Cell Biology **4**(4): E101-108.

Jeffers, J. R., E. Parganas, Y. Lee, C. Yang, J. Wang, J. Brennan, K. H. MacLean, J. Han, T. Chittenden, J. N. Ihle, P. J. McKinnon, J. L. Cleveland and G. P. Zambetti (2003). "Puma is an essential mediator of p53-dependent and -independent apoptotic pathways." Cancer Cell **4**(4): 321-328.

Jiang, M., Q. Wei, J. Wang, Q. Du, J. Yu, L. Zhang and Z. Dong (2006). "Regulation of PUMA-alpha by p53 in cisplatin-induced renal cell apoptosis." Oncogene **25**(29): 4056-4066.

Jones, P. H. and F. M. Watt (1993). "Separation of human epidermal stem cells from transit amplifying cells on the basis of differences in integrin function and expression." Cell **73**(4): 713-724.

Jonkman, M. F., A. M. Pasmooij, S. G. Pasmans, M. P. van den Berg, H. J. Ter Horst, A. Timmer and H. H. Pas (2005). "Loss of desmoplakin tail causes lethal acantholytic epidermolysis bullosa." Am J Hum Genet **77**(4): 653-660.

Kalden, J. (2004). "Apoptosis in systemic autoimmunity." Autoimmun Rev **3 Suppl 1**: S9-10.

Karin, M. and A. Lin (2002). "NF-kappaB at the crossroads of life and death." Nat Immunol **3**(3): 221-227.

Katoh, H., A. Harada, K. Mori and M. Negishi (2002). "Socius is a novel Rnd GTPase-interacting protein involved in disassembly of actin stress fibers." Molecular and Cellular Biology **22**(9): 2952-2964.

Katoh, K., Y. Kano, M. Amano, H. Onishi, K. Kaibuchi and K. Fujiwara (2001). "Rho-kinase--mediated contraction of isolated stress fibers." J Cell Biol **153**(3): 569-584.

Kerr, J. F., A. H. Wyllie and A. R. Currie (1972). "Apoptosis: a basic biological phenomenon with wide-ranging implications in tissue kinetics." Br J Cancer **26**(4): 239-257.

Kim, S. H., K. Kim, J. G. Kwagh, D. T. Dicker, M. Herlyn, A. K. Rustgi, Y. Chen and W. S. El-Deiry (2004). "Death induction by recombinant native TRAIL and its prevention by a caspase 9 inhibitor in primary human esophageal epithelial cells." Journal of Biological Chemistry **279**(38): 40044-40052.

Kimura, K., M. Ito, M. Amano, K. Chihara, Y. Fukata, M. Nakafuku, B. Yamamori, J. Feng, T. Nakano, K. Okawa, A. Iwamatsu and K. Kaibuchi (1996). "Regulation of myosin

phosphatase by Rho and Rho-associated kinase (Rho-kinase)." Science **273**(5272): 245-248.

Kischkel, F. C., S. Hellbardt, I. Behrmann, M. Germer, M. Pawlita, P. H. Krammer and M. E. Peter (1995). "Cytotoxicity-dependent APO-1 (Fas/CD95)-associated proteins form a death-inducing signaling complex (DISC) with the receptor." Embo Journal **14**(22): 5579-5588.

Klein, E. A. and R. K. Assoian (2008). "Transcriptional regulation of the cyclin D1 gene at a glance." J Cell Sci **121**(Pt 23): 3853-3857.

Klein, R. M. and A. E. Aplin (2009). "Rnd3 regulation of the actin cytoskeleton promotes melanoma migration and invasive outgrowth in three dimensions." Cancer Res **69**(6): 2224-2233.

Klein, R. M., L. S. Spofford, E. V. Abel, A. Ortiz and A. E. Aplin (2008). "B-RAF regulation of Rnd3 participates in actin cytoskeletal and focal adhesion organization." Molecular Biology of the Cell **19**(2): 498-508.

Klein-Szanto, A. J. (1977). "Stereologic baseline data of normal human epidermis." Journal of Investigative Dermatology **68**(2): 73-78.

Klymkowsky, M. W., B. O. Williams, G. D. Barish, H. E. Varmus and Y. E. Vourgourakis (1999). "Membrane-anchored plakoglobins have multiple mechanisms of action in Wnt signaling." Molecular Biology of the Cell **10**(10): 3151-3169.

Komander, D., R. Garg, P. T. Wan, A. J. Ridley and D. Barford (2008). "Mechanism of multi-site phosphorylation from a ROCK-I:RhoE complex structure." Embo Journal **27**(23): 3175-3185.

Korsmeyer, S. J., M. C. Wei, M. Saito, S. Weiler, K. J. Oh and P. H. Schlesinger (2000). "Pro-apoptotic cascade activates BID, which oligomerizes BAK or BAX into pores that result in the release of cytochrome c." Cell Death and Differentiation **7**(12): 1166-1173.

Koster, M. I. and D. R. Roop (2007). "Mechanisms regulating epithelial stratification." Annu Rev Cell Dev Biol **23**: 93-113.

Kowalczyk, A. P., E. A. Bornslaeger, J. E. Borgwardt, H. L. Palka, A. S. Dhaliwal, C. M. Corcoran, M. F. Denning and K. J. Green (1997). "The amino-terminal domain of desmoplakin binds to plakoglobin and clusters desmosomal cadherin-plakoglobin complexes." J Cell Biol **139**(3): 773-784.

Krueger, A., S. Baumann, P. H. Krammer and S. Kirchhoff (2001). "FLICE-inhibitory proteins: regulators of death receptor-mediated apoptosis." Molecular and Cellular Biology **21**(24): 8247-8254.

Kuhnel, F., L. Zender, Y. Paul, M. K. Tietze, C. Trautwein, M. Manns and S. Kubicka (2000). "NFkappaB mediates apoptosis through transcriptional activation of Fas (CD95) in adenoviral hepatitis." Journal of Biological Chemistry **275**(9): 6421-6427.

Kulms, D. and T. Schwarz (2000). "Molecular mechanisms of UV-induced apoptosis." Photodermatol Photoimmunol Photomed **16**(5): 195-201.

Kuwana, T., L. Bouchier-Hayes, J. E. Chipuk, C. Bonzon, B. A. Sullivan, D. R. Green and D. D. Newmeyer (2005). "BH3 domains of BH3-only proteins differentially regulate Bax-mediated mitochondrial membrane permeabilization both directly and indirectly." Mol Cell **17**(4): 525-535.

Kuwana, T. and D. D. Newmeyer (2003). "Bcl-2-family proteins and the role of mitochondria in apoptosis." Curr Opin Cell Biol **15**(6): 691-699.

Laemmli, U. K. (1970). "Cleavage of structural proteins during the assembly of the head of bacteriophage T4." Nature **227**(5259): 680-685.

Lang, P., F. Gesbert, M. Delespine-Carmagnat, R. Stancou, M. Pouchelet and J. Bertoglio (1996). "Protein kinase A phosphorylation of RhoA mediates the morphological and functional effects of cyclic AMP in cytotoxic lymphocytes." Embo Journal **15**(3): 510-519.

Lansbury, L., J. Leonardi-Bee, W. Perkins, T. Goodacre, J. A. Tweed and F. J. Bath-Hextall (2010). "Interventions for non-metastatic squamous cell carcinoma of the skin." Cochrane Database Syst Rev **4**: CD007869.

LeBlanc, H. N. and A. Ashkenazi (2003). "Apo2L/TRAIL and its death and decoy receptors." Cell Death and Differentiation **10**(1): 66-75.

Legan, P. K., K. K. Yue, M. A. Chidgey, J. L. Holton, R. W. Wilkinson and D. R. Garrod (1994). "The bovine desmocollin family: a new gene and expression patterns reflecting epithelial cell proliferation and differentiation." J Cell Biol **126**(2): 507-518.

Lehman, T. A., R. Modali, P. Boukamp, J. Stanek, W. P. Bennett, J. A. Welsh, R. A. Metcalf, M. R. Stampfer, N. Fusenig, E. M. Rogan and et al. (1993). "p53 mutations in human immortalized epithelial cell lines." Carcinogenesis **14**(5): 833-839.

Leigh, I., E. B. Lane and M. Watt Fiona (1994). The keratinocyte handbook. Cambridge England ; New York, NY, USA, Cambridge University Press.

Leigh, I. and F. M. Watt (1994). Keratinocyte methods. Cambridge ; New York, Cambridge University Press.

Letai, A., M. C. Bassik, L. D. Walensky, M. D. Sorcinelli, S. Weiler and S. J. Korsmeyer (2002). "Distinct BH3 domains either sensitize or activate mitochondrial apoptosis, serving as prototype cancer therapeutics." Cancer Cell **2**(3): 183-192.

Leu, J. I., P. Dumont, M. Hafey, M. E. Murphy and D. L. George (2004). "Mitochondrial p53 activates Bak and causes disruption of a Bak-Mcl1 complex." Nature Cell Biology **6**(5): 443-450.

Leung, T., X. Q. Chen, E. Manser and L. Lim (1996). "The p160 RhoA-binding kinase ROK alpha is a member of a kinase family and is involved in the reorganization of the cytoskeleton." Molecular and Cellular Biology **16**(10): 5313-5327.

Leung, T., E. Manser, L. Tan and L. Lim (1995). "A novel serine/threonine kinase binding the Ras-related RhoA GTPase which translocates the kinase to peripheral membranes." Journal of Biological Chemistry **270**(49): 29051-29054.

Leverkus, M., M. Neumann, T. Mengling, C. T. Rauch, E. B. Brocker, P. H. Krammer and H. Walczak (2000). "Regulation of tumor necrosis factor-related apoptosis-inducing ligand sensitivity in primary and transformed human keratinocytes." Cancer Res **60**(3): 553-559.

Leverkus, M., M. R. Sprick, T. Wachter, A. Denk, E. B. Brocker, H. Walczak and M. Neumann (2003). "TRAIL-induced apoptosis and gene induction in HaCaT keratinocytes: differential contribution of TRAIL receptors 1 and 2." Journal of Investigative Dermatology **121**(1): 149-155.

Li, K., Y. Lu, J. Liang, G. Luo, G. Ren, X. Wang and D. Fan (2009). "RhoE enhances multidrug resistance of gastric cancer cells by suppressing Bax." Biochem Biophys Res Commun **379**(2): 212-216.

Li, L. Y., X. Luo and X. Wang (2001). "Endonuclease G is an apoptotic DNase when released from mitochondria." Nature **412**(6842): 95-99.

Li, P., D. Nijhawan, I. Budihardjo, S. M. Srinivasula, M. Ahmad, E. S. Alnemri and X. Wang (1997). "Cytochrome c and dATP-dependent formation of Apaf-1/caspase-9 complex initiates an apoptotic protease cascade." Cell **91**(4): 479-489.

Liebig, T., J. Erasmus, R. Kalaji, D. Davies, G. Loirand, A. Ridley and V. M. Braga (2009). "RhoE Is required for keratinocyte differentiation and stratification." Molecular Biology of the Cell **20**(1): 452-463.

Lippens, S., E. Hoste, P. Vandenabeele, P. Agostinis and W. Declercq (2009). "Cell death in the skin." Apoptosis **14**(4): 549-569.

Lippens, S., M. Kockx, M. Knaapen, L. Mortier, R. Polakowska, A. Verheyen, M. Garmyn, A. Zwijsen, P. Formstecher, D. Huylebroeck, P. Vandenabeele and W. Declercq (2000). "Epidermal differentiation does not involve the pro-apoptotic executioner caspases, but is associated with caspase-14 induction and processing." Cell Death and Differentiation **7**(12): 1218-1224.

Litjens, S. H., J. M. de Pereda and A. Sonnenberg (2006). "Current insights into the formation and breakdown of hemidesmosomes." Trends Cell Biol **16**(7): 376-383.

Lock, F. E. and N. A. Hotchin (2009). "Distinct roles for ROCK1 and ROCK2 in the regulation of keratinocyte differentiation." PLoS One **4**(12): e8190.

Longley, D. B., T. R. Wilson, M. McEwan, W. L. Allen, U. McDermott, L. Galligan and P. G. Johnston (2006). "c-FLIP inhibits chemotherapy-induced colorectal cancer cell death." Oncogene **25**(6): 838-848.

Longo, K. A., J. A. Kennell, M. J. Ochocinska, S. E. Ross, W. S. Wright and O. A. MacDougald (2002). "Wnt signaling protects 3T3-L1 preadipocytes from apoptosis through induction of insulin-like growth factors." Journal of Biological Chemistry **277**(41): 38239-38244.

Madaule, P., T. Furuyashiki, M. Eda, H. Bito, T. Ishizaki and S. Narumiya (2000). "Citron, a Rho target that affects contractility during cytokinesis." Microsc Res Tech **49**(2): 123-126.

Madigan, J. P., B. O. Bodemann, D. C. Brady, B. J. Dewar, P. J. Keller, M. Leitges, M. R. Philips, A. J. Ridley, C. J. Der and A. D. Cox (2009). "Regulation of Rnd3 localization and function by protein kinase C alpha-mediated phosphorylation." Biochemical Journal **424**(1): 153-161.

Maekawa, M., T. Ishizaki, S. Boku, N. Watanabe, A. Fujita, A. Iwamatsu, T. Obinata, K. Ohashi, K. Mizuno and S. Narumiya (1999). "Signaling from Rho to the actin cytoskeleton through protein kinases ROCK and LIM-kinase." Science **285**(5429): 895-898.

Maiuri, M. C., E. Zalckvar, A. Kimchi and G. Kroemer (2007). "Self-eating and self-killing: crosstalk between autophagy and apoptosis." Nat Rev Mol Cell Biol **8**(9): 741-752.

Maldonado, V., J. Melendez-Zajgla and A. Ortega (1997). "Modulation of NF-kappa B, and Bcl-2 in apoptosis induced by cisplatin in HeLa cells." Mutat Res **381**(1): 67-75.

Marinkovich, M. P., D. R. Keene, C. S. Rimberg and R. E. Burgeson (1993). "Cellular origin of the dermal-epidermal basement membrane." Dev Dyn **197**(4): 255-267.

McMullan, R., S. Lax, V. H. Robertson, D. J. Radford, S. Broad, F. M. Watt, A. Rowles, D. R. Croft, M. F. Olson and N. A. Hotchin (2003). "Keratinocyte differentiation is regulated by the Rho and ROCK signaling pathway." Current Biology **13**(24): 2185-2189.

Mejlvang, J., M. Kriajevska, C. Vandewalle, T. Chernova, A. E. Sayan, G. Berx, J. K. Mellon and E. Tulchinsky (2007). "Direct repression of cyclin D1 by SIP1 attenuates cell cycle progression in cells undergoing an epithelial mesenchymal transition." Molecular Biology of the Cell **18**(11): 4615-4624.

Merritt, A. J., M. Y. Berika, W. Zhai, S. E. Kirk, B. Ji, M. J. Hardman and D. R. Garrod (2002). "Suprabasal desmoglein 3 expression in the epidermis of transgenic mice results in hyperproliferation and abnormal differentiation." Molecular and Cellular Biology **22**(16): 5846-5858.

Micheau, O. and J. Tschopp (2003). "Induction of TNF receptor I-mediated apoptosis via two sequential signaling complexes." Cell **114**(2): 181-190.

Mills, J. C., N. L. Stone, J. Erhardt and R. N. Pittman (1998). "Apoptotic membrane blebbing is regulated by myosin light chain phosphorylation." J Cell Biol **140**(3): 627-636.

Moon, R. T., B. Bowerman, M. Boutros and N. Perrimon (2002). "The promise and perils of Wnt signaling through beta-catenin." Science **296**(5573): 1644-1646.

Motley, R., P. Kersey and C. Lawrence (2002). "Multiprofessional guidelines for the management of the patient with primary cutaneous squamous cell carcinoma." Br J Dermatol **146**(1): 18-25.

Muller, E. J., L. Williamson, C. Kolly and M. M. Suter (2008). "Outside-in signaling through integrins and cadherins: a central mechanism to control epidermal growth and differentiation?" Journal of Investigative Dermatology **128**(3): 501-516.

Murakami, T., M. Fujimoto, M. Ohtsuki and H. Nakagawa (2001). "Expression profiling of cancer-related genes in human keratinocytes following non-lethal ultraviolet B irradiation." J Dermatol Sci **27**(2): 121-129.

Nadiminty, N., S. Dutt, C. Tepper and A. C. Gao (2010). "Microarray analysis reveals potential target genes of NF-kappaB2/p52 in LNCaP prostate cancer cells." Prostate **70**(3): 276-287.

Nakagawa, O., K. Fujisawa, T. Ishizaki, Y. Saito, K. Nakao and S. Narumiya (1996). "ROCK-I and ROCK-II, two isoforms of Rho-associated coiled-coil forming protein serine/threonine kinase in mice." Febs Letters **392**(2): 189-193.

Nakagawa, T., H. Zhu, N. Morishima, E. Li, J. Xu, B. A. Yankner and J. Yuan (2000). "Caspase-12 mediates endoplasmic-reticulum-specific apoptosis and cytotoxicity by amyloid-beta." Nature **403**(6765): 98-103.

Nemes, Z. and P. M. Steinert (1999). "Bricks and mortar of the epidermal barrier." Exp Mol Med **31**(1): 5-19.

Niessen, C. M. (2007). "Tight junctions/adherens junctions: basic structure and function." Journal of Investigative Dermatology **127**(11): 2525-2532.

Nobes, C. D., I. Lauritzen, M. G. Mattei, S. Paris, A. Hall and P. Chardin (1998). "A new member of the Rho family, Rnd1, promotes disassembly of actin filament structures and loss of cell adhesion." J Cell Biol **141**(1): 187-197.

Noren, N. K., C. M. Niessen, B. M. Gumbiner and K. Burridge (2001). "Cadherin engagement regulates Rho family GTPases." Journal of Biological Chemistry **276**(36): 33305-33308.

North, A. J., M. A. Chidgey, J. P. Clarke, W. G. Bardsley and D. R. Garrod (1996). "Distinct desmocollin isoforms occur in the same desmosomes and show reciprocally graded distributions in bovine nasal epidermis." Proc Natl Acad Sci U S A **93**(15): 7701-7705.

Nuber, U. A., S. Schafer, A. Schmidt, P. J. Koch and W. W. Franke (1995). "The widespread human desmocollin Dsc2 and tissue-specific patterns of synthesis of various desmocollin subtypes." Eur J Cell Biol **66**(1): 69-74.

O'Keefe, E. J., R. A. Briggaman and B. Herman (1987). "Calcium-induced assembly of adherens junctions in keratinocytes." J Cell Biol **105**(2): 807-817.

Olofsson, B. (1999). "Rho guanine dissociation inhibitors: pivotal molecules in cellular signalling." Cell Signal **11**(8): 545-554.

Olson, M. F., A. Ashworth and A. Hall (1995). "An essential role for Rho, Rac, and Cdc42 GTPases in cell cycle progression through G1." Science **269**(5228): 1270-1272.

Olson, M. F., H. F. Paterson and C. J. Marshall (1998). "Signals from Ras and Rho GTPases interact to regulate expression of p21Waf1/Cip1." Nature **394**(6690): 295-299.

Oltersdorf, T., S. W. Elmore, A. R. Shoemaker, R. C. Armstrong, D. J. Augeri, B. A. Belli, M. Bruncko, T. L. Deckwerth, J. Dinges, P. J. Hajduk, M. K. Joseph, S. Kitada, S. J. Korsmeyer, A. R. Kunzer, A. Letai, C. Li, M. J. Mitten, D. G. Nettesheim, S. Ng, P. M. Nimmer, J. M. O'Connor, A. Oleksijew, A. M. Petros, J. C. Reed, W. Shen, S. K. Tahir, C. B. Thompson, K. J. Tomaselli, B. Wang, M. D. Wendt, H. Zhang, S. W. Fesik and S. H. Rosenberg (2005). "An inhibitor of Bcl-2 family proteins induces regression of solid tumours." Nature **435**(7042): 677-681.

Ongusaha, P. P., H. G. Kim, S. A. Boswell, A. J. Ridley, C. J. Der, G. P. Dotto, Y. B. Kim, S. A. Aaronson and S. W. Lee (2006). "RhoE is a pro-survival p53 target gene that inhibits ROCK I-mediated apoptosis in response to genotoxic stress." Current Biology **16**(24): 2466-2472.

Ott, M., E. Norberg, K. M. Walter, P. Schreiner, C. Kemper, D. Rapaport, B. Zhivotovsky and S. Orrenius (2007). "The mitochondrial TOM complex is required for tBid/Bax-induced cytochrome c release." Journal of Biological Chemistry **282**(38): 27633-27639.

Pasdar, M. and Z. Li (1993). "Disorganization of microfilaments and intermediate filaments interferes with the assembly and stability of desmosomes in MDCK epithelial cells." Cell Motil Cytoskeleton **26**(2): 163-180.

Pellegrin, S. and H. Mellor (2007). "Actin stress fibres." J Cell Sci **120**(Pt 20): 3491-3499.

Perrais, M., X. Chen, M. Perez-Moreno and B. M. Gumbiner (2007). "E-cadherin homophilic ligation inhibits cell growth and epidermal growth factor receptor signaling independently of other cell interactions." Molecular Biology of the Cell **18**(6): 2013-2025.

Petit, V. and J. P. Thiery (2000). "Focal adhesions: structure and dynamics." Biol Cell **92**(7): 477-494.

Poch, E., R. Minambres, E. Mocholi, C. Ivorra, A. Perez-Arago, C. Guerri, I. Perez-Roger and R. M. Guasch (2007). "RhoE interferes with Rb inactivation and regulates the proliferation and survival of the U87 human glioblastoma cell line." Experimental Cell Research **313**(4): 719-731.

Potten, C. S. (1981). "Cell replacement in epidermis (keratopoiesis) via discrete units of proliferation." Int Rev Cytol **69**: 271-318.

Poznic, M. (2009). "Retinoblastoma protein: a central processing unit." J Biosci **34**(2): 305-312.

Reed, J. C. (1994). "Bcl-2 and the regulation of programmed cell death." J Cell Biol **124**(1-2): 1-6.

Reed, J. C. (1997). "Bcl-2 family proteins: regulators of apoptosis and chemoresistance in hematologic malignancies." Semin Hematol **34**(4 Suppl 5): 9-19.

Rheinwald, J. G. and H. Green (1975). "Serial cultivation of strains of human epidermal keratinocytes: the formation of keratinizing colonies from single cells." Cell **6**(3): 331-343.

Rice, R. H. and H. Green (1979). "Presence in human epidermal cells of a soluble protein precursor of the cross-linked envelope: activation of the cross-linking by calcium ions." Cell **18**(3): 681-694.

Riento, K., R. M. Guasch, R. Garg, B. Jin and A. J. Ridley (2003). "RhoE binds to ROCK I and inhibits downstream signaling." Molecular and Cellular Biology **23**(12): 4219-4229.

Riento, K. and A. J. Ridley (2003). "Rocks: multifunctional kinases in cell behaviour." Nat Rev Mol Cell Biol **4**(6): 446-456.

Riento, K., N. Totty, P. Villalonga, R. Garg, R. Guasch and A. J. Ridley (2005). "RhoE function is regulated by ROCK I-mediated phosphorylation." Embo Journal **24**(6): 1170-1180.

Ries, F. and J. Klastersky (1986). "Nephrotoxicity induced by cancer chemotherapy with special emphasis on cisplatin toxicity." Am J Kidney Dis **8**(5): 368-379.

Robles, A. I., F. Larcher, R. B. Whalin, R. Murillas, E. Richie, I. B. Gimenez-Conti, J. L. Jorcano and C. J. Conti (1996). "Expression of cyclin D1 in epithelial tissues of transgenic mice results in epidermal hyperproliferation and severe thymic hyperplasia." Proc Natl Acad Sci U S A **93**(15): 7634-7638.

Robles, A. I., M. L. Rodriguez-Puebla, A. B. Glick, C. Trempus, L. Hansen, P. Sicinski, R. W. Tennant, R. A. Weinberg, S. H. Yuspa and C. J. Conti (1998). "Reduced skin tumor development in cyclin D1-deficient mice highlights the oncogenic ras pathway in vivo." Genes Dev **12**(16): 2469-2474.

Rossman, K. L., C. J. Der and J. Sondek (2005). "GEF means go: turning on RHO GTPases with guanine nucleotide-exchange factors." Nat Rev Mol Cell Biol **6**(2): 167-180.

Rothe, M., M. G. Pan, W. J. Henzel, T. M. Ayres and D. V. Goeddel (1995). "The TNFR2-TRAF signaling complex contains two novel proteins related to baculoviral inhibitor of apoptosis proteins." Cell **83**(7): 1243-1252.

Rovere-Querini, P., A. A. Manfredi and M. G. Sabbadini (2005). "Environmental adjuvants, apoptosis and the censorship over autoimmunity." Autoimmun Rev **4**(8): 555-560.

Rubenstein, N. M., J. F. Chan, J. Y. Kim, S. H. Hansen and G. L. Firestone (2005). "Rnd3/RhoE induces tight junction formation in mammary epithelial tumor cells." Experimental Cell Research **305**(1): 74-82.

Rubin, A. I., E. H. Chen and D. Ratner (2005). "Basal-cell carcinoma." N Engl J Med **353**(21): 2262-2269.

Runswick, S. K., M. J. O'Hare, L. Jones, C. H. Streuli and D. R. Garrod (2001). "Desmosomal adhesion regulates epithelial morphogenesis and cell positioning." Nature Cell Biology **3**(9): 823-830.

Saelens, X., N. Festjens, L. Vande Walle, M. van Gurp, G. van Loo and P. Vandenabeele (2004). "Toxic proteins released from mitochondria in cell death." Oncogene **23**(16): 2861-2874.

Sardet, C., M. Vidal, D. Cobrinik, Y. Geng, C. Onufryk, A. Chen and R. A. Weinberg (1995). "E2F-4 and E2F-5, two members of the E2F family, are expressed in the early phases of the cell cycle." Proc Natl Acad Sci U S A **92**(6): 2403-2407.

Scaffidi, C., S. Fulda, A. Srinivasan, C. Friesen, F. Li, K. J. Tomaselli, K. M. Debatin, P. H. Krammer and M. E. Peter (1998). "Two CD95 (APO-1/Fas) signaling pathways." Embo Journal **17**(6): 1675-1687.

Scaffidi, C., I. Schmitz, P. H. Krammer and M. E. Peter (1999). "The role of c-FLIP in modulation of CD95-induced apoptosis." Journal of Biological Chemistry **274**(3): 1541-1548.

Schafer, S., S. Stumpp and W. W. Franke (1996). "Immunological identification and characterization of the desmosomal cadherin Dsg2 in coupled and uncoupled epithelial cells and in human tissues." Differentiation **60**(2): 99-108.

Schmidt, A. and A. Hall (2002). "Guanine nucleotide exchange factors for Rho GTPases: turning on the switch." Genes Dev **16**(13): 1587-1609.

Schmidt, A. and S. Jager (2005). "Plakophilins--hard work in the desmosome, recreation in the nucleus?" Eur J Cell Biol **84**(2-3): 189-204.

Schwartz, M. (2004). "Rho signalling at a glance." J Cell Sci **117**(Pt 23): 5457-5458.

Scorrano, L. and S. J. Korsmeyer (2003). "Mechanisms of cytochrome c release by proapoptotic BCL-2 family members." Biochem Biophys Res Commun **304**(3): 437-444.

Scott, R. W. and M. F. Olson (2007). "LIM kinases: function, regulation and association with human disease." J Mol Med **85**(6): 555-568.

Sebbagh, M., C. Renvoize, J. Hamelin, N. Riche, J. Bertoglio and J. Breard (2001). "Caspase-3-mediated cleavage of ROCK I induces MLC phosphorylation and apoptotic membrane blebbing." Nature Cell Biology **3**(4): 346-352.

Servais, H., A. Ortiz, O. Devuyst, S. Denamur, P. M. Tulkens and M. P. Mingeot-Leclercq (2008). "Renal cell apoptosis induced by nephrotoxic drugs: cellular and molecular mechanisms and potential approaches to modulation." Apoptosis **13**(1): 11-32.

Seth, R., C. Yang, V. Kaushal, S. V. Shah and G. P. Kaushal (2005). "p53-dependent caspase-2 activation in mitochondrial release of apoptosis-inducing factor and its role in renal tubular epithelial cell injury." Journal of Biological Chemistry **280**(35): 31230-31239.

Sherr, C. J. (1993). "Mammalian G1 cyclins." Cell **73**(6): 1059-1065.

Shi, J. and L. Wei (2007). "Rho kinase in the regulation of cell death and survival." Arch Immunol Ther Exp (Warsz) **55**(2): 61-75.

Shurin, G. V., I. L. Tourkova and M. R. Shurin (2008). "Low-dose chemotherapeutic agents regulate small Rho GTPase activity in dendritic cells." J Immunother **31**(5): 491-499.

Siddik, Z. H. (2003). "Cisplatin: mode of cytotoxic action and molecular basis of resistance." Oncogene **22**(47): 7265-7279.

Skerrow, C. J., D. G. Clelland and D. Skerrow (1989). "Changes to desmosomal antigens and lectin-binding sites during differentiation in normal human epidermis: a quantitative ultrastructural study." J Cell Sci **92 (Pt 4)**: 667-677.

Slee, E. A., C. Adrain and S. J. Martin (1999). "Serial killers: ordering caspase activation events in apoptosis." Cell Death and Differentiation **6**(11): 1067-1074.

Slee, E. A., C. Adrain and S. J. Martin (2001). "Executioner caspase-3, -6, and -7 perform distinct, non-redundant roles during the demolition phase of apoptosis." Journal of Biological Chemistry **276**(10): 7320-7326.

Slee, E. A., M. T. Harte, R. M. Kluck, B. B. Wolf, C. A. Casiano, D. D. Newmeyer, H. G. Wang, J. C. Reed, D. W. Nicholson, E. S. Alnemri, D. R. Green and S. J. Martin (1999). "Ordering the cytochrome c-initiated caspase cascade: hierarchical activation of caspases-2, -3, -6, -7, -8, and -10 in a caspase-9-dependent manner." J Cell Biol **144**(2): 281-292.

Sprick, M. R. and H. Walczak (2004). "The interplay between the Bcl-2 family and death receptor-mediated apoptosis." Biochim Biophys Acta **1644**(2-3): 125-132.

Steinberg, M. S. and P. M. McNutt (1999). "Cadherins and their connections: adhesion junctions have broader functions." Curr Opin Cell Biol **11**(5): 554-560.

Susin, S. A., H. K. Lorenzo, N. Zamzami, I. Marzo, B. E. Snow, G. M. Brothers, J. Mangion, E. Jacotot, P. Costantini, M. Loeffler, N. Larochette, D. R. Goodlett, R. Aebersold, D. P. Siderovski, J. M. Penninger and G. Kroemer (1999). "Molecular characterization of mitochondrial apoptosis-inducing factor." Nature **397**(6718): 441-446.

Swartzendruber, D. C., P. W. Wertz, D. J. Kitko, K. C. Madison and D. T. Downing (1989). "Molecular models of the intercellular lipid lamellae in mammalian stratum corneum." Journal of Investigative Dermatology **92**(2): 251-257.

Takai, Y., T. Sasaki and T. Matozaki (2001). "Small GTP-binding proteins." Physiol Rev **81**(1): 153-208.

Tanimura, S., K. Nomura, K. Ozaki, M. Tsujimoto, T. Kondo and M. Kohno (2002). "Prolonged nuclear retention of activated extracellular signal-regulated kinase 1/2 is required for hepatocyte growth factor-induced cell motility." Journal of Biological Chemistry **277**(31): 28256-28264.

Thomason, H. A., A. Scothern, S. McHarg and D. R. Garrod (2010). "Desmosomes: adhesive strength and signalling in health and disease." Biochemical Journal **429**(3): 419-433.

Thorlacius, K., J. E. Slotta, M. W. Laschke, Y. Wang, M. D. Menger, B. Jeppsson and H. Thorlacius (2006). "Protective effect of fasudil, a Rho-kinase inhibitor, on chemokine expression, leukocyte recruitment, and hepatocellular apoptosis in septic liver injury." J Leukoc Biol **79**(5): 923-931.

Totsukawa, G., Y. Yamakita, S. Yamashiro, D. J. Hartshorne, Y. Sasaki and F. Matsumura (2000). "Distinct roles of ROCK (Rho-kinase) and MLCK in spatial regulation of MLC phosphorylation for assembly of stress fibers and focal adhesions in 3T3 fibroblasts." J Cell Biol **150**(4): 797-806.

Towbin, H., T. Staehelin and J. Gordon (1979). "Electrophoretic transfer of proteins from polyacrylamide gels to nitrocellulose sheets: procedure and some applications." Proc Natl Acad Sci U S A **76**(9): 4350-4354.

Uehata, M., T. Ishizaki, H. Satoh, T. Ono, T. Kawahara, T. Morishita, H. Tamakawa, K. Yamagami, J. Inui, M. Maekawa and S. Narumiya (1997). "Calcium sensitization of smooth muscle mediated by a Rho-associated protein kinase in hypertension." Nature **389**(6654): 990-994.

Vasioukhin, V., E. Bowers, C. Bauer, L. Degenstein and E. Fuchs (2001). "Desmoplakin is essential in epidermal sheet formation." Nature Cell Biology **3**(12): 1076-1085.

Verhagen, A. M., P. G. Ekert, M. Pakusch, J. Silke, L. M. Connolly, G. E. Reid, R. L. Moritz, R. J. Simpson and D. L. Vaux (2000). "Identification of DIABLO, a mammalian protein that promotes apoptosis by binding to and antagonizing IAP proteins." Cell **102**(1): 43-53.

Vetter, I. R. and A. Wittinghofer (2001). "The guanine nucleotide-binding switch in three dimensions." Science **294**(5545): 1299-1304.

Villalonga, P., R. M. Guasch, K. Riento and A. J. Ridley (2004). "RhoE inhibits cell cycle progression and Ras-induced transformation." Molecular and Cellular Biology **24**(18): 7829-7840.

Vincent, S. and J. Settleman (1997). "The PRK2 kinase is a potential effector target of both Rho and Rac GTPases and regulates actin cytoskeletal organization." Molecular and Cellular Biology **17**(4): 2247-2256.

Wagner, A. D., W. Grothe, J. Haerting, G. Kleber, A. Grothey and W. E. Fleig (2006). "Chemotherapy in advanced gastric cancer: a systematic review and meta-analysis based on aggregate data." J Clin Oncol **24**(18): 2903-2909.

Walczak, H. and P. H. Krammer (2000). "The CD95 (APO-1/Fas) and the TRAIL (APO-2L) apoptosis systems." Experimental Cell Research **256**(1): 58-66.

Walczak, H., R. E. Miller, K. Ariail, B. Gliniak, T. S. Griffith, M. Kubin, W. Chin, J. Jones, A. Woodward, T. Le, C. Smith, P. Smolak, R. G. Goodwin, C. T. Rauch, J. C. Schuh and D. H. Lynch (1999). "Tumoricidal activity of tumor necrosis factor-related apoptosis-inducing ligand in vivo." Nat Med **5**(2): 157-163.

Wan, H., A. P. South and I. R. Hart (2007). "Increased keratinocyte proliferation initiated through downregulation of desmoplakin by RNA interference." Experimental Cell Research **313**(11): 2336-2344.

Wan, H., M. G. Stone, C. Simpson, L. E. Reynolds, J. F. Marshall, I. R. Hart, K. M. Hodivala-Dilke and R. A. Eady (2003). "Desmosomal proteins, including desmoglein 3, serve as novel negative markers for epidermal stem cell-containing population of keratinocytes." J Cell Sci **116**(Pt 20): 4239-4248.

Wang, C. Y., M. W. Mayo, R. G. Korneluk, D. V. Goeddel and A. S. Baldwin, Jr. (1998). "NF-kappaB antiapoptosis: induction of TRAF1 and TRAF2 and c-IAP1 and c-IAP2 to suppress caspase-8 activation." Science **281**(5383): 1680-1683.

Wang, G., E. Reed and Q. Q. Li (2004). "Molecular basis of cellular response to cisplatin chemotherapy in non-small cell lung cancer (Review)." Oncol Rep **12**(5): 955-965.

Wang, H. R., Y. Zhang, B. Ozdamar, A. A. Ogunjimi, E. Alexandrova, G. H. Thomsen and J. L. Wrana (2003). "Regulation of cell polarity and protrusion formation by targeting RhoA for degradation." Science **302**(5651): 1775-1779.

Ward, Y., S. F. Yap, V. Ravichandran, F. Matsumura, M. Ito, B. Spinelli and K. Kelly (2002). "The GTP binding proteins Gem and Rad are negative regulators of the Rho-Rho kinase pathway." J Cell Biol **157**(2): 291-302.

Waschke, J. (2008). "The desmosome and pemphigus." Histochem Cell Biol **130**(1): 21-54.

Waschke, J., V. Spindler, P. Bruggeman, D. Zillikens, G. Schmidt and D. Drenckhahn (2006). "Inhibition of Rho A activity causes pemphigus skin blistering." J Cell Biol **175**(5): 721-727.

Watt, F. M. (1983). "Involucrin and other markers of keratinocyte terminal differentiation." Journal of Investigative Dermatology **81**(1 Suppl): 100s-103s.

Watt, F. M. (1988). "Keratinocyte cultures: an experimental model for studying how proliferation and terminal differentiation are co-ordinated in the epidermis." J Cell Sci **90 (Pt 4)**: 525-529.

Watt, F. M., D. L. Mattey and D. R. Garrod (1984). "Calcium-induced reorganization of desmosomal components in cultured human keratinocytes." J Cell Biol **99**(6): 2211-2215.

Wei, Q., G. Dong, T. Yang, J. Megyesi, P. M. Price and Z. Dong (2007). "Activation and involvement of p53 in cisplatin-induced nephrotoxicity." Am J Physiol Renal Physiol **293**(4): F1282-1291.

Welsh, C. F. (2004). "Rho GTPases as key transducers of proliferative signals in g1 cell cycle regulation." Breast Cancer Res Treat **84**(1): 33-42.

Welsh, C. F., K. Roovers, J. Villanueva, Y. Liu, M. A. Schwartz and R. K. Assoian (2001). "Timing of cyclin D1 expression within G1 phase is controlled by Rho." Nature Cell Biology **3**(11): 950-957.

Wennerberg, K., M. A. Forget, S. M. Ellerbroek, W. T. Arthur, K. Burridge, J. Settleman, C. J. Der and S. H. Hansen (2003). "Rnd proteins function as RhoA antagonists by activating p190 RhoGAP." Current Biology **13**(13): 1106-1115.

Wiley, S. R., K. Schooley, P. J. Smolak, W. S. Din, C. P. Huang, J. K. Nicholl, G. R. Sutherland, T. D. Smith, C. Rauch, C. A. Smith and et al. (1995). "Identification and characterization of a new member of the TNF family that induces apoptosis." Immunity **3**(6): 673-682.

Windoffer, R., M. Borchert-Stuhltrager and R. E. Leube (2002). "Desmosomes: interconnected calcium-dependent structures of remarkable stability with significant integral membrane protein turnover." J Cell Sci **115**(Pt 8): 1717-1732.

Wolter, K. G., Y. T. Hsu, C. L. Smith, A. Nechushtan, X. G. Xi and R. J. Youle (1997). "Movement of Bax from the cytosol to mitochondria during apoptosis." J Cell Biol **139**(5): 1281-1292.

Yamada, H., S. Tada-Oikawa, A. Uchida and S. Kawanishi (1999). "TRAIL causes cleavage of bid by caspase-8 and loss of mitochondrial membrane potential resulting in apoptosis in BJAB cells." Biochem Biophys Res Commun **265**(1): 130-133.

Yin, T. and K. J. Green (2004). "Regulation of desmosome assembly and adhesion." Semin Cell Dev Biol **15**(6): 665-677.

Yoneda, A., H. A. Multhaupt and J. R. Couchman (2005). "The Rho kinases I and II regulate different aspects of myosin II activity." J Cell Biol **170**(3): 443-453.

Zhang, S. Q., A. Kovalenko, G. Cantarella and D. Wallach (2000). "Recruitment of the IKK signalosome to the p55 TNF receptor: RIP and A20 bind to NEMO (IKKgamma) upon receptor stimulation." Immunity **12**(3): 301-311.

Zhurinsky, J., M. Shtutman and A. Ben-Ze'ev (2000). "Differential mechanisms of LEF/TCF family-dependent transcriptional activation by beta-catenin and plakoglobin." Molecular and Cellular Biology **20**(12): 4238-4252.

Zhurinsky, J., M. Shtutman and A. Ben-Ze'ev (2000). "Plakoglobin and beta-catenin: protein interactions, regulation and biological roles." J Cell Sci **113 (Pt 18)**: 3127-3139.

Ziegler, A., A. S. Jonason, D. J. Leffell, J. A. Simon, H. W. Sharma, J. Kimmelman, L. Remington, T. Jacks and D. E. Brash (1994). "Sunburn and p53 in the onset of skin cancer." Nature **372**(6508): 773-776.

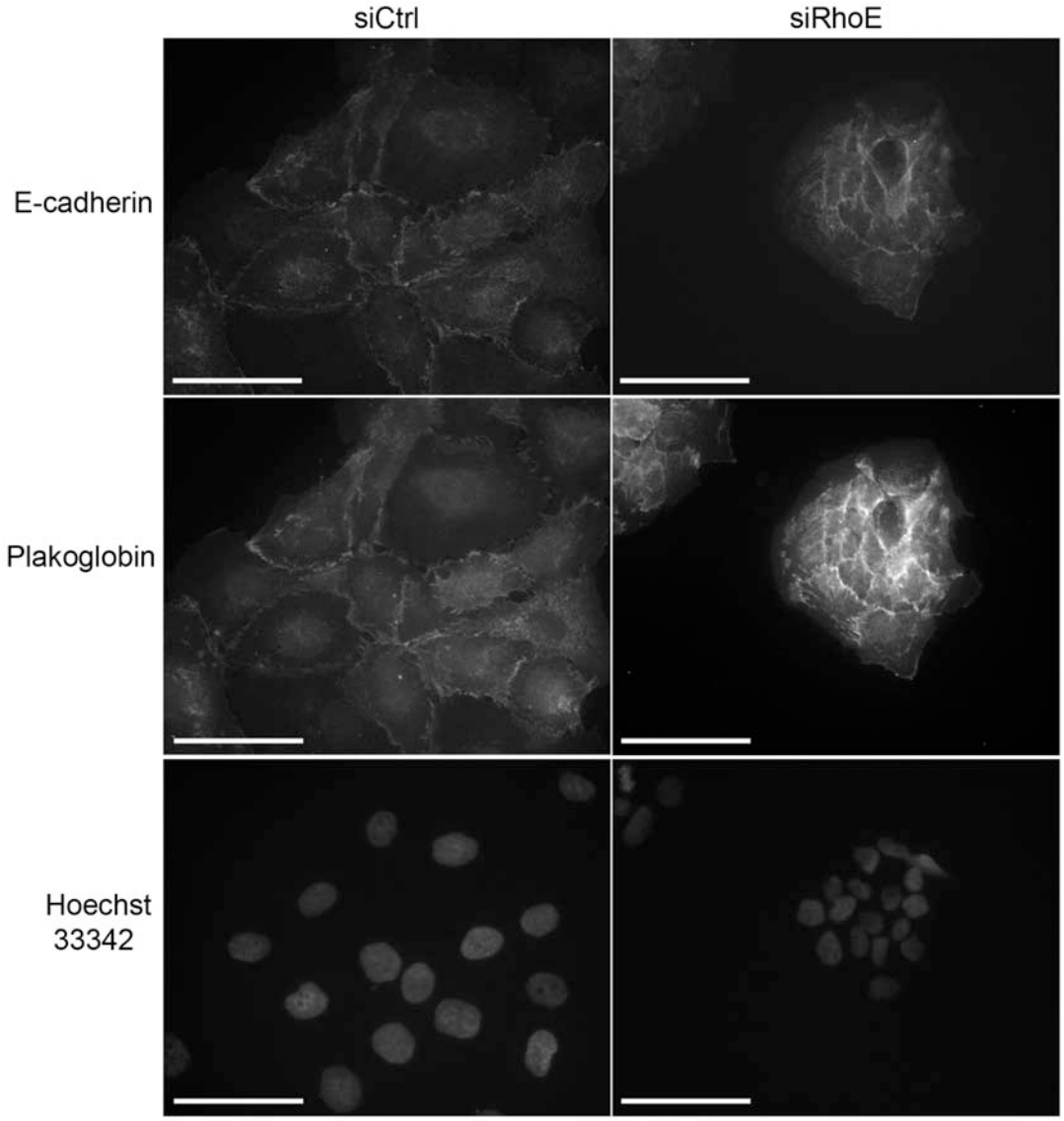
siCtrl
siRhoE
E-cadherin
Plakoglobin
Hoechst
33342

APPENDIX 1 SEQUENCE OF HUMAN RHOE WITH SHRNA AND SIRNA SEQUNCES HIGHLIGHTED

CAGTCGGCTCGGAATTGGACTTGGGAGGCGCGGTGAGGAGTCAGGCTTAAAACTTGTTGGAGGG
GAGTAACCAGCCTGCTCCTCTCGCTCTCCTCCTCGTCTGCGCCGCGTTTCAGAGAGAAAATTCC
TGTTCCAAGAGAAAATAAGGCAACATCAATGAAGGAGAGAAGAGCCAGCCAGAAATTATCCAGC
AAATCTATCATGGATCCTAATCAGAACGTGAAATGCAAGATAGTTGTGGTGGGAGACAGTCAGT
GTGGAAAAACTGCGCTGCTCCATGTCTTCGCCAAGGACTGCTTCCCCGAGAATTACGTTCCTAC
AGTGTTTGAGAATTACACGGCCAGTTTTGAAATCGACACACAAAGAATAGAGTTGAGCCTGTGG
GACACTTCGGGTTCTCCTTACTATGACAATGTCCGCCCCCTCTCTTACCCTGATTCGGATGCTG
TGCTGATTTGCTTTGACATCAGTAGACCAGAGACCCTGGACAGTGTCCTCAAAAAGTGGAAAGG
TGAAATCCAGGAATTTTGTCCAAATACCAAAATGCTCTTGGTCGGCTGCAAGTCTGATCTGCGG
ACAGATGTTAGTACATTAGTAGAGCTCTCCAATCACAGGCAGACGCCAGTGTCCTATGACCAGG
GGGCAAATATGGCCAAACAGATTGGAGCAGCTACTTATATCGAATGCTCAGCTTTACAGTCGGA
AAATAGCGTCAGAGACATTTTTCACGTTGCCACCTTGGCATGTGTAAATAAGACAAATAAAAAC
GTTAAGCGGAACAAATCACAGAGAGCCACAAAGCGGATTTCACACATGCCTAGCAGACCAGAAC
TCTCGGCAGTTGCTACGGACTTACGAAAGGACAAAGCGAAGAGCTGCACTGTGATGTGAATCTT
TCATTATCTTTAATGAAGACAAAGGAATCTAGTGTAAAAAACAACAGCAAACAAAAAGGTGAAG
TCTAAATGAAGTGCACAGCCAAAGTCATGTATACCAGAGGCTTAGGAGGCGTTTGAGAGGATAC
TCATCTTTTTGGAATCCTGACCTTAGGTTCGGCATGTAGACCAAGTGATGAGAAGTGAATACAT
GGAAGAGTTTTTAAGTGTGACTTGAAAAATATGCCAAAAAATGAGAGATACAAATGAGCTAGAG
GAAGATGAGGGGGGATGCGAGTACCTCCAAGAAGAAAAATCACACTCTGAATGGTGCTTGCATT
TTTGGGTTTTTTTTTTTTGTTATAATCTATTCATGGATCTCCACTTTGATTTAATTTTTAAATG
TTTTAATCTCCTTTACAAAAAGTATACGTTAATATACCGTCCTCAAGGGGGAACTGGCACTGTG
ACCTTAGCATTTAGTTTTCTAGAGGATGTGATCTAATTTCTTTCTAGCTCATCATTAAAAAGGA
AATTGTATCAGGACCCATGGGATATATCCAGAGGCAAACTTTATGAGGCTTTGAAATCTTGCCT
TCCTGAAGATAGCTGAGTAGGATGGTTCTAAGGAAAGCCTTTGCAATCTTGCAAGATTTGTAGA
CCAGCACTACAAAGATCGCATAGATCAAATAGGAAAAAAAATGTCGATTTTTATTCAGTCTGAT
GGTTCTGTTCTTCATTGTGATTGTCATTAAAAAGTGGTAAATTGCTCAATGTAATATTTTTGTG
CGCTGTTTAGAAGTTGTGTGATTTTTTGCCATCGTTGATAAAAATGCAAAGTCAAATAAAAGGT

GTCTTGGTTTGATGTCATAGAATGATCCAAGGAGAGAAAAAAGGTAGTTACTGTTTTCACCAGA
AAAGGTAATGAGTGAAGGAAAGAATAGTAGCAGAAAGCACAGTTTGTGAGTAAAGCTGTCTGGA
ATTAAGTTACCAAAAATACAAAGCAAAAGGACTATTATTTTGGGTTGAAGCTCCAAAACTGACA
GCATCTGATAATCTGTTGGTTTATTTCACTTTTCATTAAATGAACATTGATGAGAGAAGATGCC
ACTTACCCAAGCTTTAGAGAATCCCTAGTGGAAGATTATATGATAAACTTTCAGTCCTGACATA
ACACTAGGGCATTTCTAGAGTGTCATTGCTAAAACCTCACTGAACAGATGCAGCCAAGGTCTGT
GTTCAGCACTTGGTCTCTGTTGTTACGTAAAATAATAAGCATTTAAAATAGTTTACAGATATTT
TTGACCAGTTCCTTTTAGAGATTCTTTCAGAGAAGAAACCAGATCTGACCTGTTTATTGTTGGC
GCTTGTTGAAAACGAGCTTTCTTTCCCATGATAGTGCTTCGTTTTTGAAGTGTTGAAGCTGTGC
TCCCCTTAAATCGTGGCAGGAGAGATTAAGGTAATTACAACACTCAGTTCTATGTCTTACAAGC
ACTTTGTCTTGTCTCTGCAAGAAAATTCGATTCCAGTCATTTCCCATAAAATACAGACATTTTA
CCAACATAATATGCTTTGATTGATGCAGCATTATGCTTTGGGCAGTATTACAAAATAGCTGGCG
AGTGCTTTCTGTATTTAAATATTGTAAAAAGAAAATAAGTTATAACTGTTATAAAGCAGAACTT
TTGTTGCATTTTTTAAACTGTTGAAGTCACTGTGTATGTTTGTTTGGTCAATGTTTCCGCAGTA
TTTATTAAAACATACTTTTTTTTTCTTCAAATAAAAAAGTAACCATGTCTTTGTCTAAA

shRNA [TCTGATAATCTGTTGGTTTAT]

Oligo A [TAGTAGAGCTCTCCAATCA]

Oligo B [CAAACAGATTGGAGCAGCT]

shRNAmir pGIPZRhoE construct; green is sense and blue is antisense

TGCTGTTGACAGTGAGCGCTCTGATAATCTGTTGGTTTATTAGTGAAGCCACAGATGTA
ATAAACCAACAGATTATCAGATTGCCTACTGCCTCGGA